Particle acceleration from PWNe and SNRs

Mattia Di Mauro

Fermi Summer School, May 28 2019

CR data

- Satellite experiments as well as Cherenkov telescope arrays are measuring with unprecedented precision and in a wide energy range the spectrum and anisotropy of CRs.
- The interpretation of this rich dataset is one of the main challenge in Astroparticle Physics.
- This is important to study the emission mechanism of Galactic sources and explore new Physics such as dark matter particles.

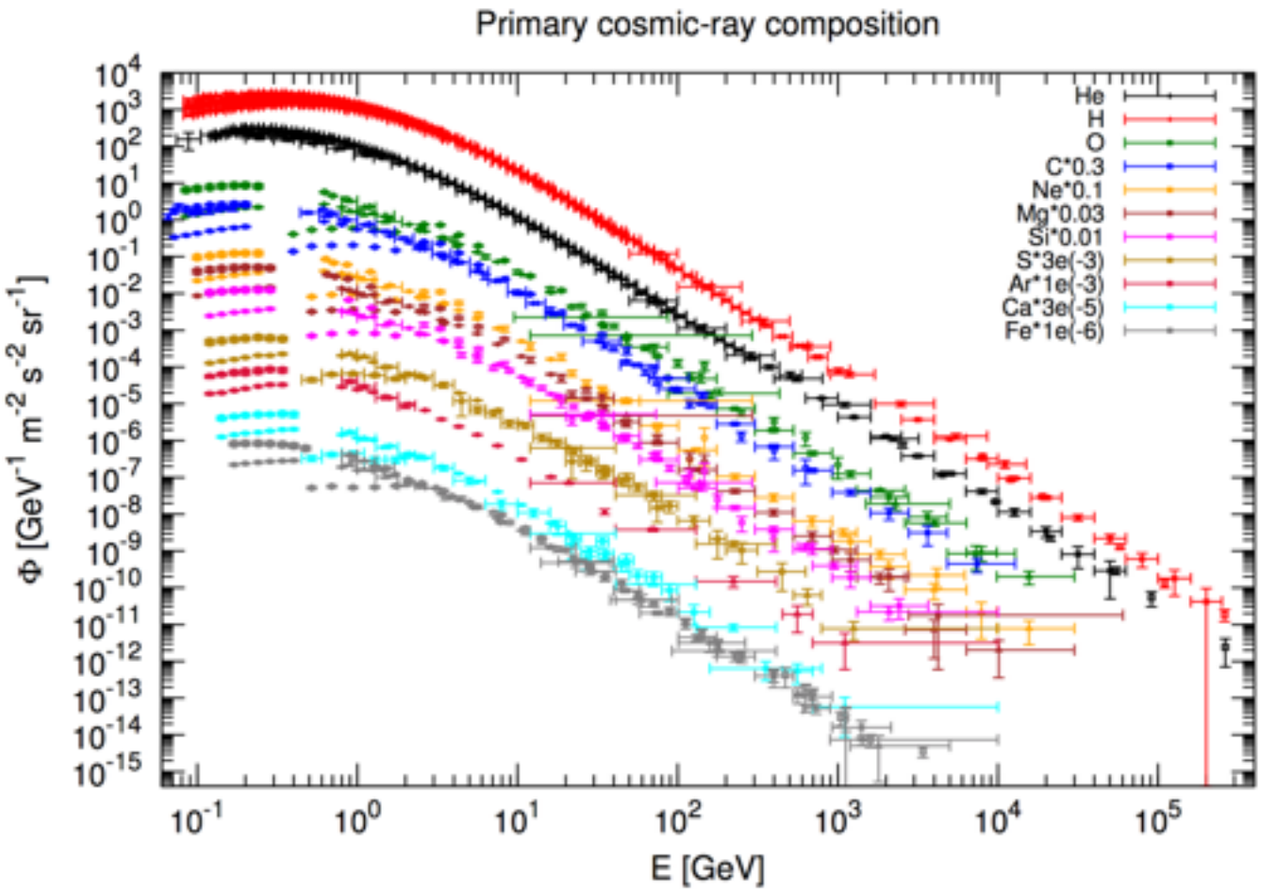

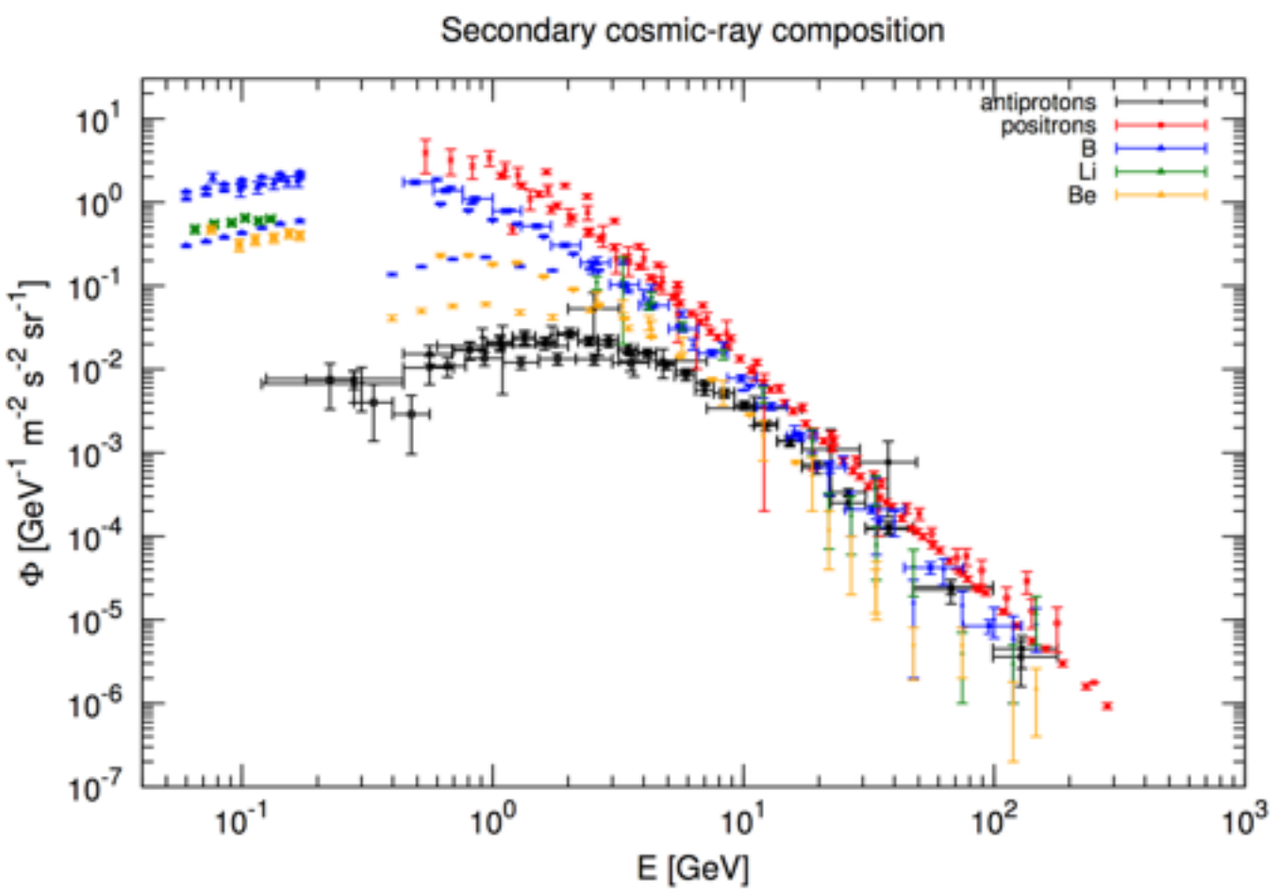

Origin of cosmic rays (CRs)

Primary CRs

- Supernova remnants (SNRs) are believed to be the major accelerators of charged particles up to very high energies, via a first-type Fermi mechanism.
- Pulsar wind nebulae (PWNe), rapidly spinning neutron stars with a strong surface magnetic field, are considered to be among the most powerful sources of electrons and positrons in the Galaxy.

Secondary CRs

- Secondary production: secondary CRs originate from the spallation reactions of primary CR species with the interstellar material.

Crab Nebula pulsar wind nebula optical (HST, NASA/ESA)

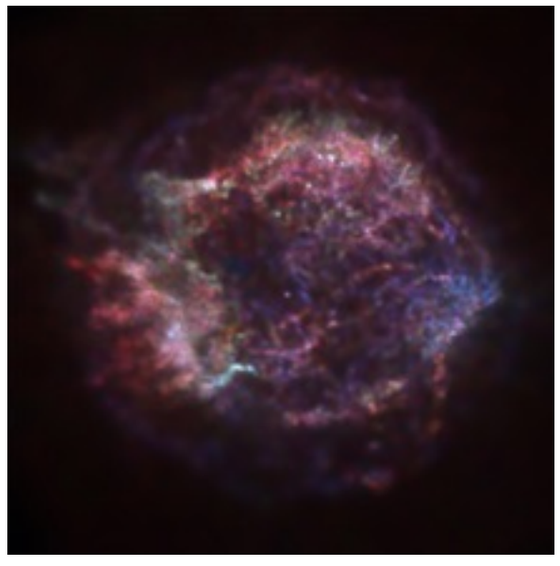

Cassiopea A supernova remnant optical (HST, NASA/ESA)

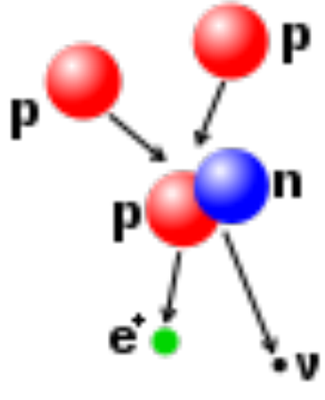

Proton interaction with helium

CR acceleration mechanism in SNRs

- The acceleration of Galactic CRs takes place after the explosion of a supernova (10^{51} erg).
- A supernova (SN) shell is generated right after the explosion and expands in the ISM at 10% of the speed of light.
- CRs are accelerated up to very-high-energy in the SN shell through the Fermi mechanism (known also as diffusive shock acceleration).

Fermi mechanism (diffusive shock acceleration)

https://www.youtube.com/watch?v=C3ue7cEocvI

CR $e^{\pm}$ acceleration in PWNe

- The engine of a PWN is a pulsar, i.e. a rapidly spinning neutral star (NS).
- A NS has huge magnetic fields (10^{9}-10^{12} G) which produce wind of particles extracted from the NS surface.
- This wind shines from radio to gamma rays and after a few kyrs interact with the SNR reverse shock.
- The pulsar proper motion and the interaction with the SNR reverse shock generate a relic PWN and a bow shock components.

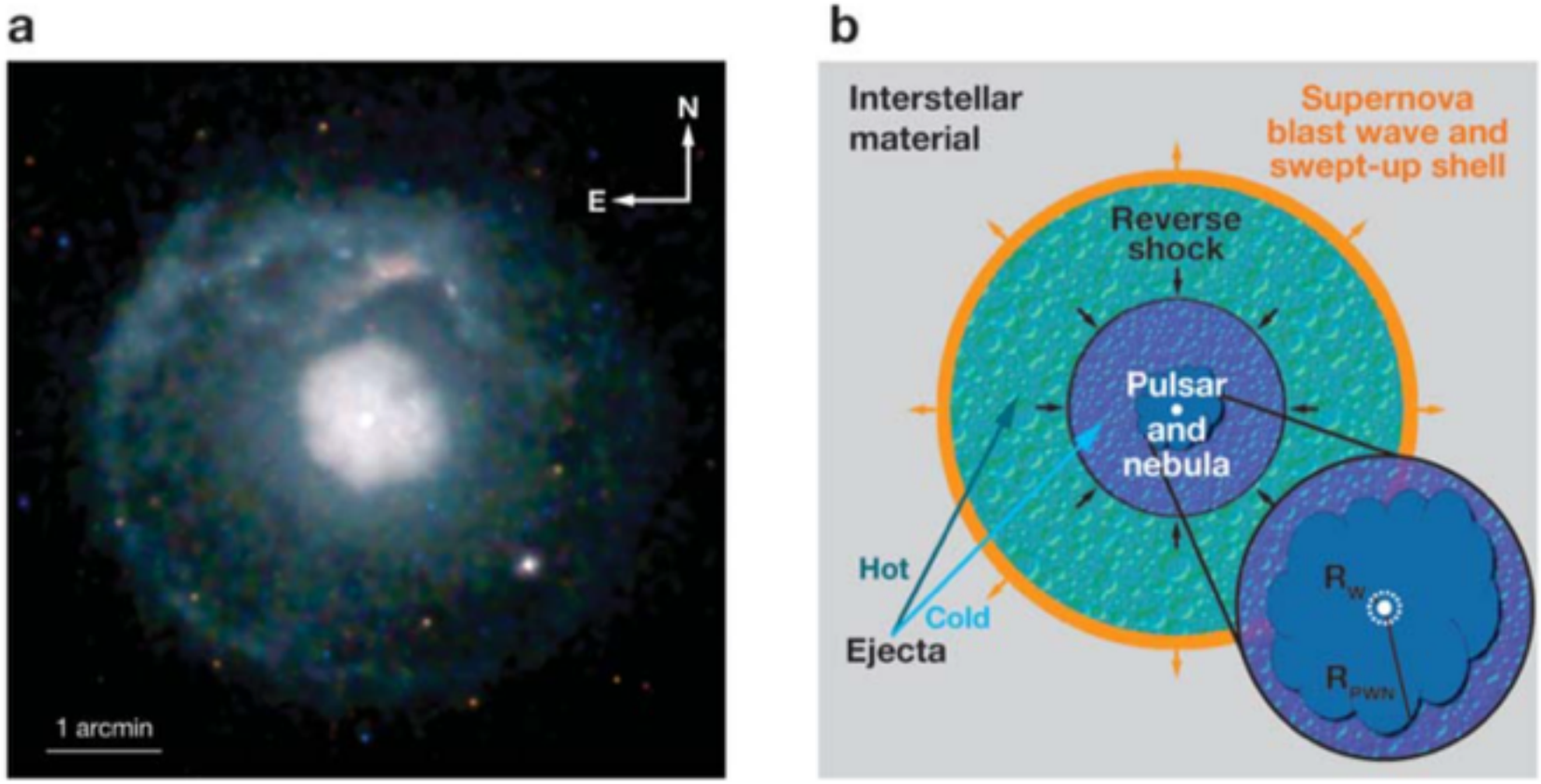

CR $e^{\pm}$ acceleration in PWNe

- The engine of a PWN is a pulsar, i.e. a rapidly spinning neutral star (NS).
- A NS has huge magnetic fields (10^{9}-10^{12} G) which produce wind of particles extracted from the NS surface.
- This wind shines from radio to gamma rays and after a few kyrs interact with the SNR reverse shock.
- The pulsar proper motion and the interaction with the SNR reverse shock generate a relic PWN and a bow shock.

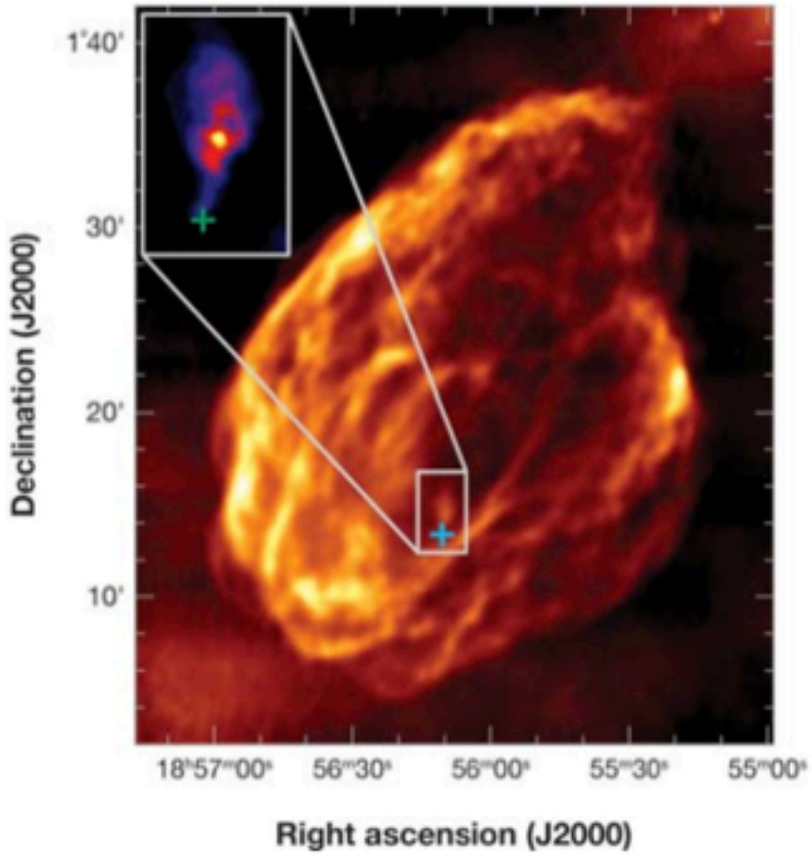

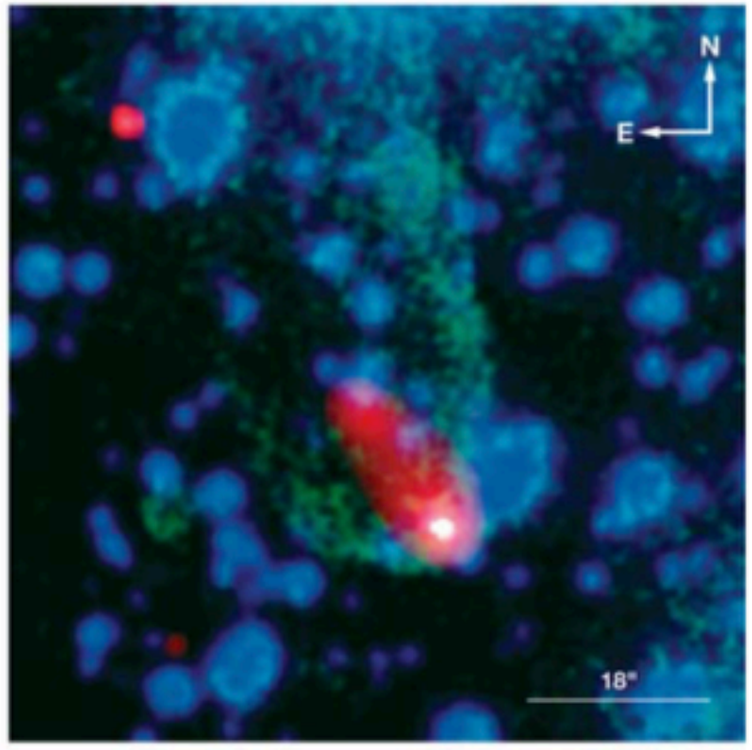

Crab nebula

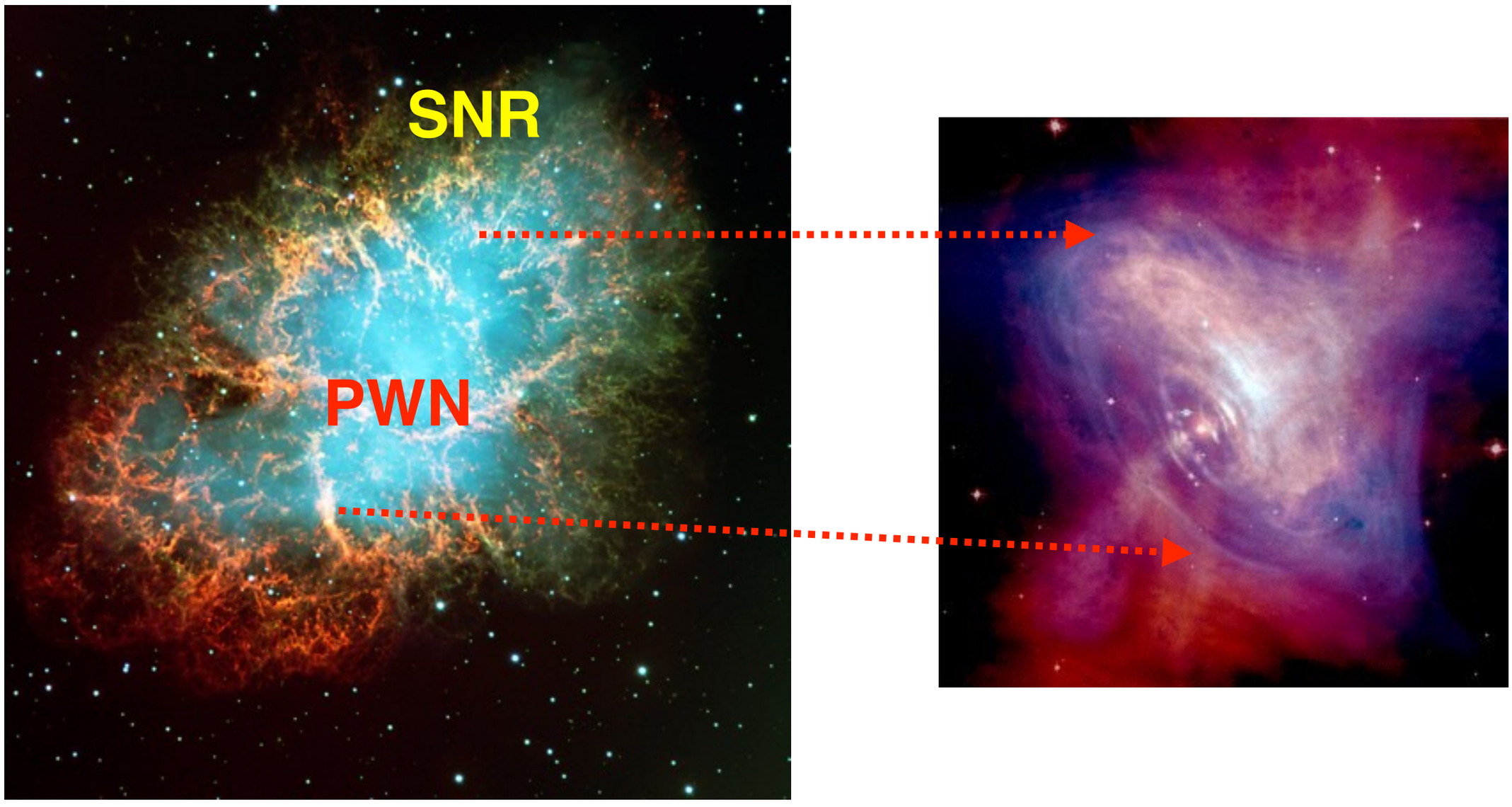

Propagation of CRs in the Galaxy

- After CR particles are accelerated from the source, they travel in the Galaxy and they do what is called propagation.
- CRs lose energy through the interaction with the Galactic magnetic fields and inverse Compton scattering with the ISRF.
- Charged CRs are also deflected by the Galactic magnetic fields (diffusion).

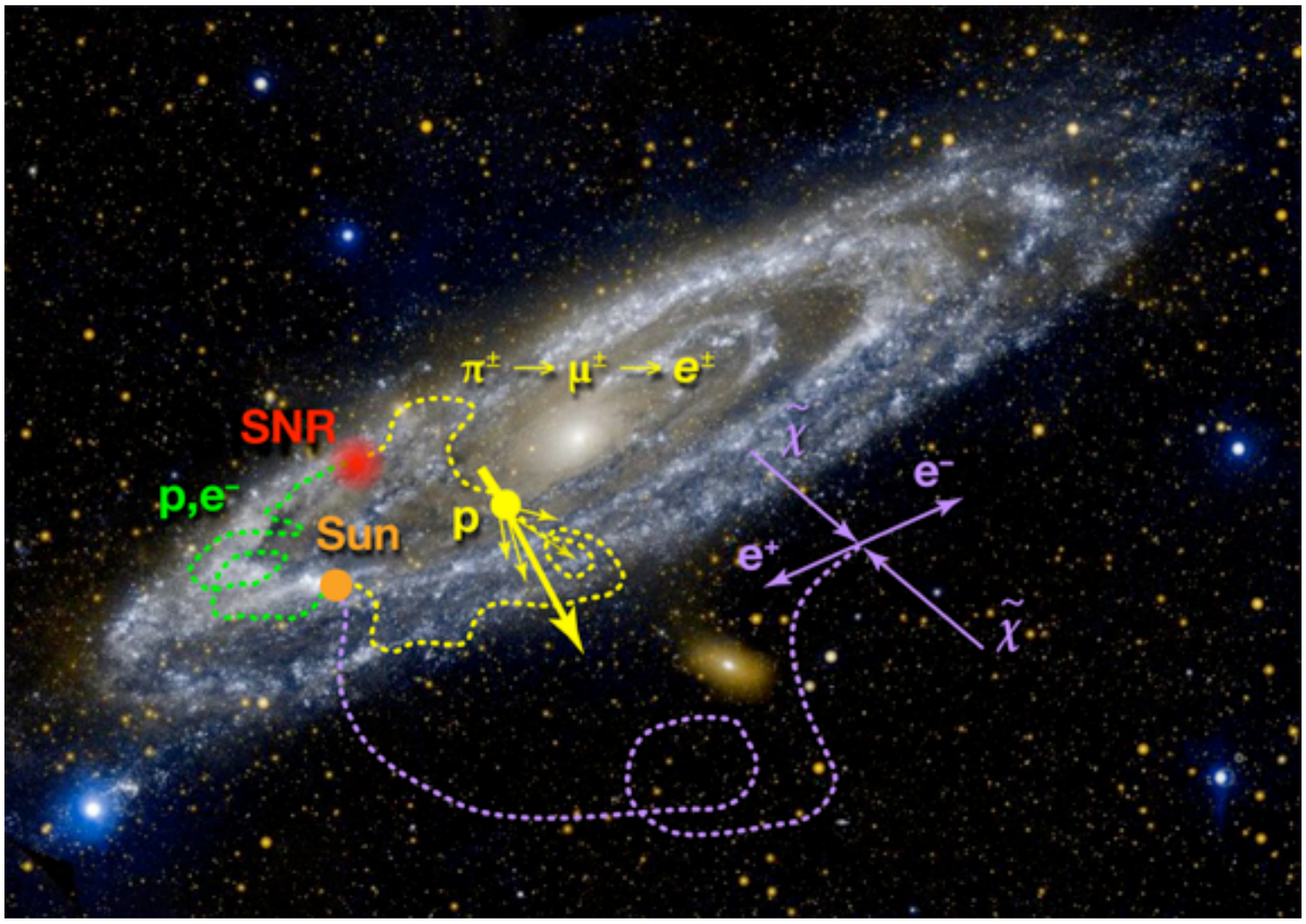

Propagation of electrons and positrons

Current conservation equation:

$$\widehat{\mathcal{D}}\mathcal{N} = \mathcal{Q}(E, \boldsymbol{x}, t)$$

$$\partial_t \mathcal{N} - \boldsymbol{\nabla} \cdot \{K(E)\boldsymbol{\nabla}\mathcal{N}\} + \partial_E \left\{ \frac{dE}{dt}\mathcal{N} \right\} = \mathcal{Q}(E, \boldsymbol{x}, t)$$

- The source term Q is the number of electrons and positrons emitted from the Galactic source (SNRs or PWNe).
- The operator D takes into account the phenomenon of the propagation:
  - energy losses dE/dT=b(E)
  - diffusion K(E) due to the motion of CRs in the irregularities of the Galactic magnetic field.

Deriving propagation parameters

- The propagation zone is modeled as a cylinder of radius Rdisk≃20 kpc, a vertical half-height of L≃1−15 kpc and a disk, which has a vertical extent of zdisk≃0.1 kpc.
- These parameters and the diffusion $K(E) \equiv \beta K_0 \left(\frac{\mathcal{R}}{1\,\mathrm{GV}}\right)^{\delta} \simeq K_0\,\epsilon^{\delta}$ are derived by fitting CR data (e.g., B/C ratio).
- **The diffusion has been derived to be of the order of 10^{28} cm^2/s at 1 GeV and be stronger along the spiral arms.**

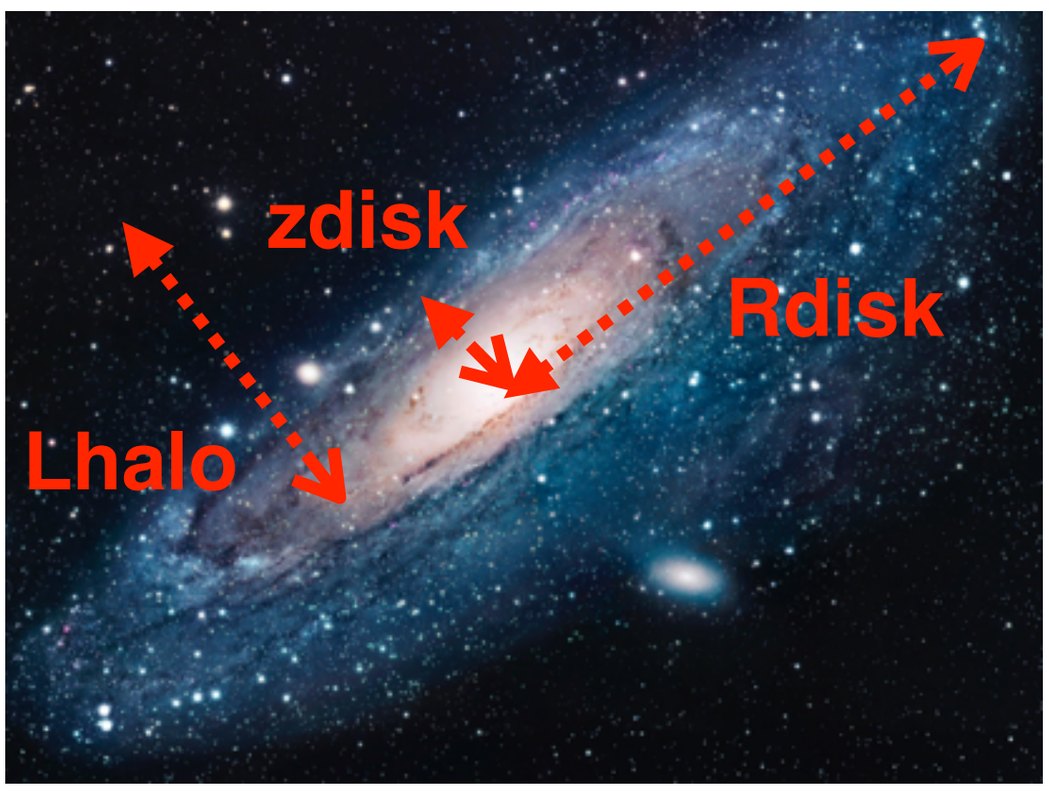

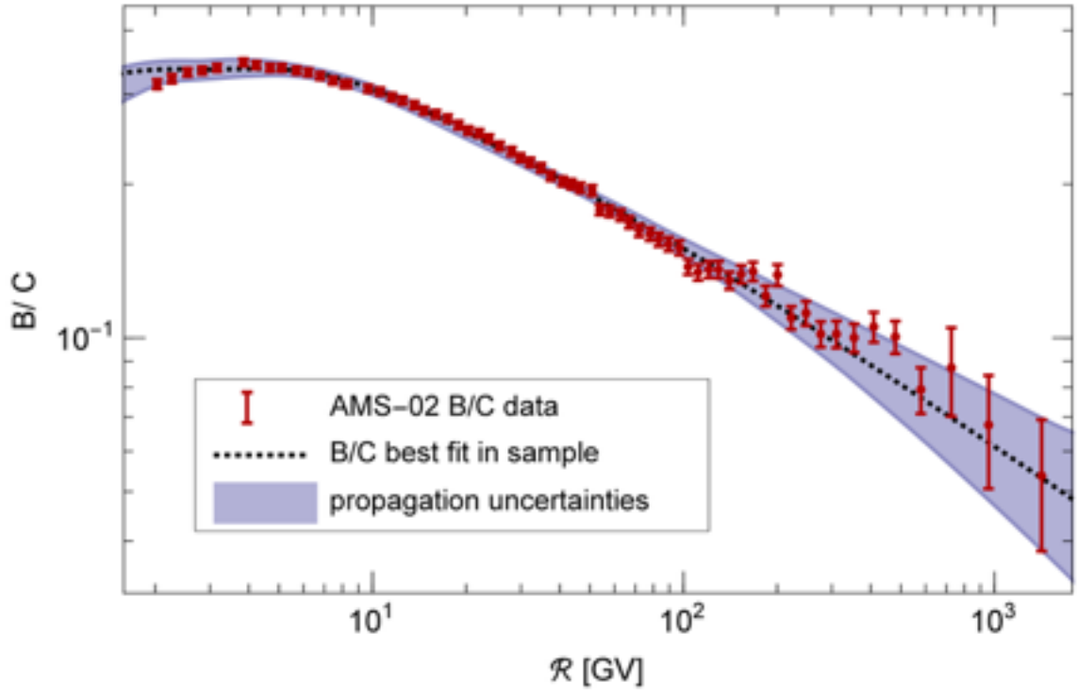

δ	K_0 (kpc^2 Myr^{-1})	L (kpc)	V_c (km s^{-1})	V_a (km s^{-1})
0.408	0.0967	13.7	0.2	31.9

Compton scattering

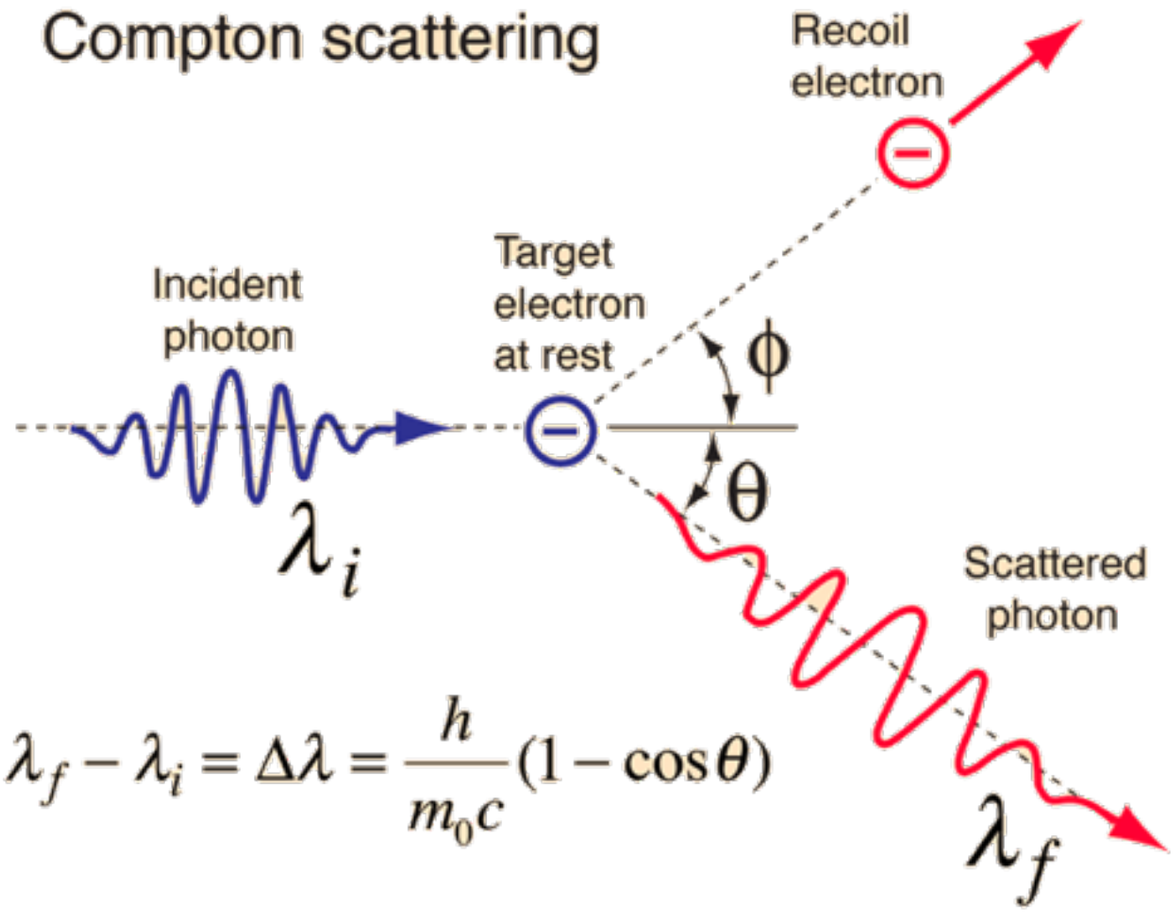

$$\lambda_f - \lambda_i = \Delta\lambda = \frac{h}{m_0 c}(1 - \cos\theta)$$

The ***differential cross section*** for Thomson scattering is:

$$\frac{d\sigma_T}{d\Omega} = \frac{1}{2} r_0^2 (1 + \cos^2\Theta)$$

r_0 = Classical electron radius

$$= \frac{e^2}{4\pi\varepsilon_0 m_e c^2} = 2.818\times10^{-15}\,\text{m}$$

Inverse Compton scattering

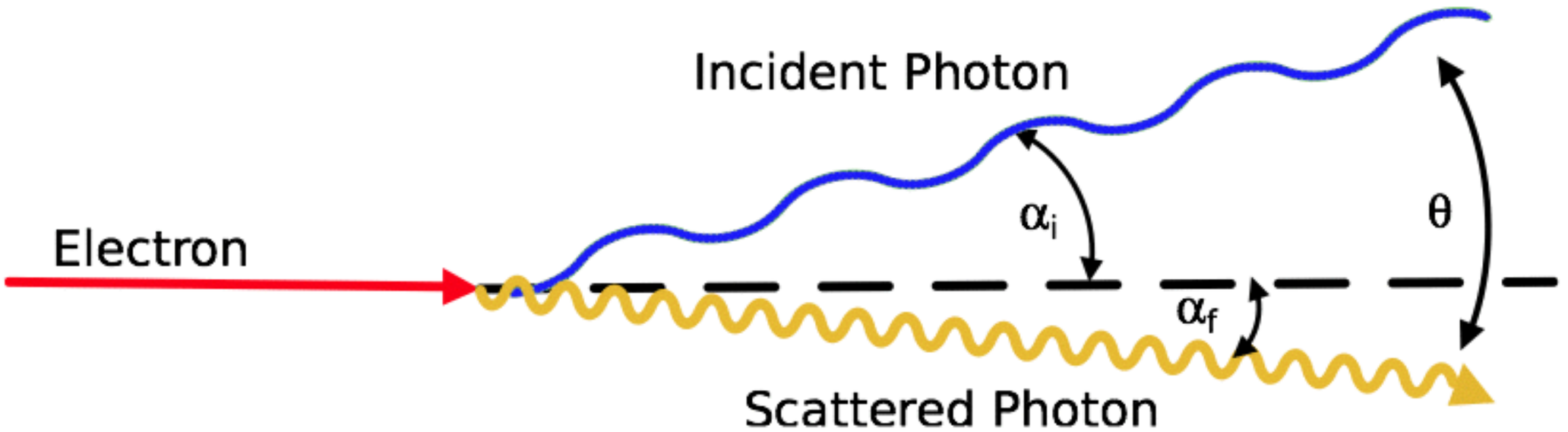

Thomson limit: low photon energy, $\varepsilon \ll mc^2$

$$\epsilon_{1max} = 4\gamma^2\epsilon$$

Electron energy 0.5 GeV

Waveband	*Frequency (Hz)* ν_0	*Scattered Frequency (Hz) and Waveband*
Radio	10^9	$10^{15} =$ UV
Far-infrared	3×10^{12}	$3 \times 10^{18} =$ X-rays
Optical	4×10^{14}	$4 \times 10^{21} \equiv 1.6\text{MeV} = \gamma$-rays

Electron energy loss for ICS

$$-\left(\frac{dE_e}{dt}\right)_{TL} = \frac{4}{3} c\,\sigma_T\,\gamma^2\,\mathcal{E}_{iso} \qquad \mathcal{E}_{iso} = \int \epsilon dn_{iso}$$

$$n(\epsilon)_{BB} = \frac{1}{\pi^2(\hbar c)^3} \frac{\epsilon^2}{\exp\frac{\epsilon}{kT} - 1}$$

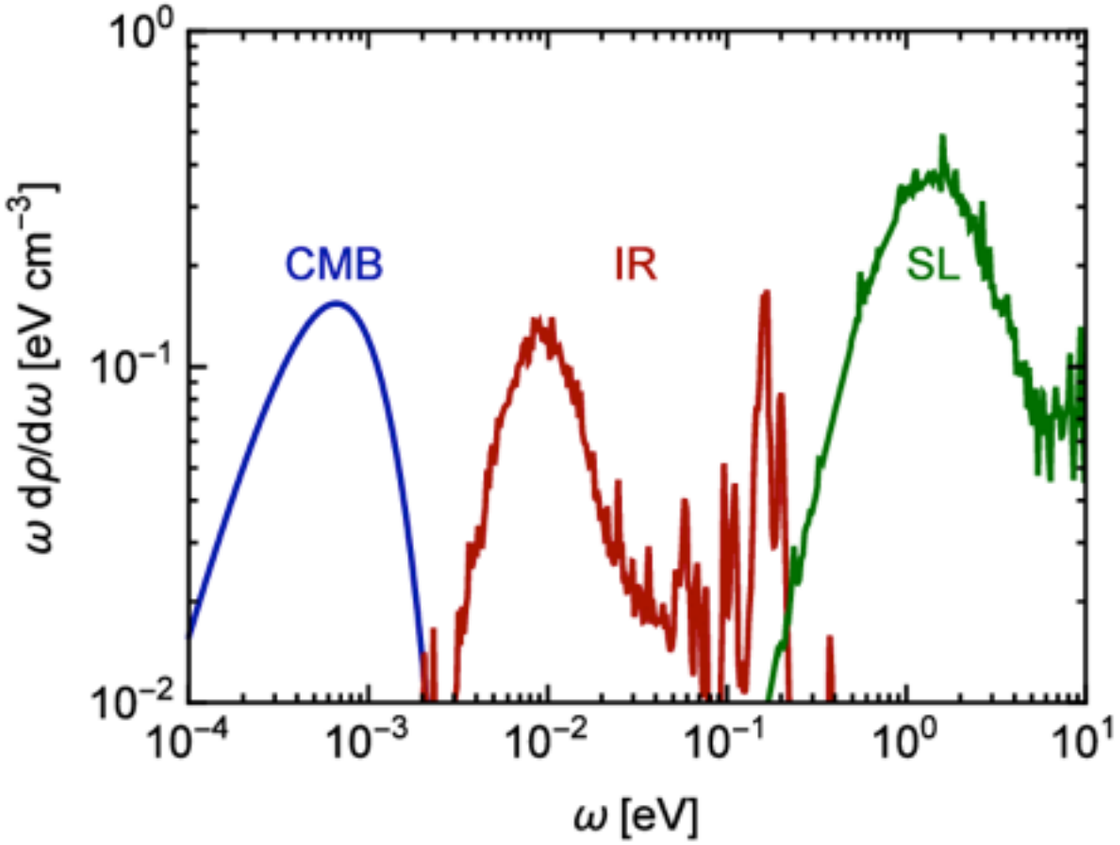

- T_{CMB} = 2.7 K and E_{CMB}= 2.3 10^{-4} eV
- T_{IR} = 20 K and E_{IR}= 2.4 10^{-3} eV
- T_{SL} = 5000 K and E_{SL}= 3.5 10^{-1} eV

Other Electron energy losses

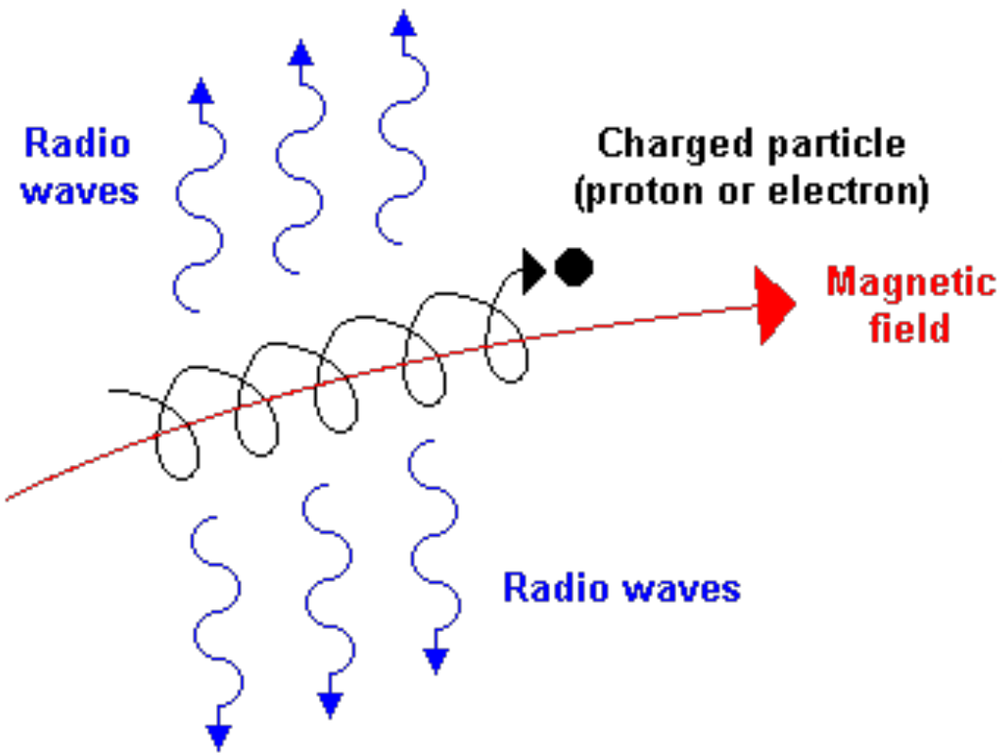

Synchrotron radiation

$$-\left(\frac{dE}{dt}\right) = \frac{4}{3}\sigma_T c U_B \gamma^2 \beta^2 \sim 2.53 \times 10^{-18} \left(\frac{B}{\mu\mathrm{G}}\right)^2 \left(\frac{E}{\mathrm{GeV}}\right)^2 \ \mathrm{GeV\ s^{-1}}$$

nrumiano

- **Bremsstrahlung**: This process, also called braking radiation, occurs when an electron or a positron is accelerated by the electric fields associated with interstellar ions or nuclei.
- **Ionization losses**: Relativistic charged particles moving through a material medium interact with electrons belonging to atoms in that same material: the interaction thus excites or ionises the atoms.
- **Coulomb scattering**: Coulomb collisions in a completely ionised plasma are dominated by scattering off the thermal electrons.

Total electron energy losses

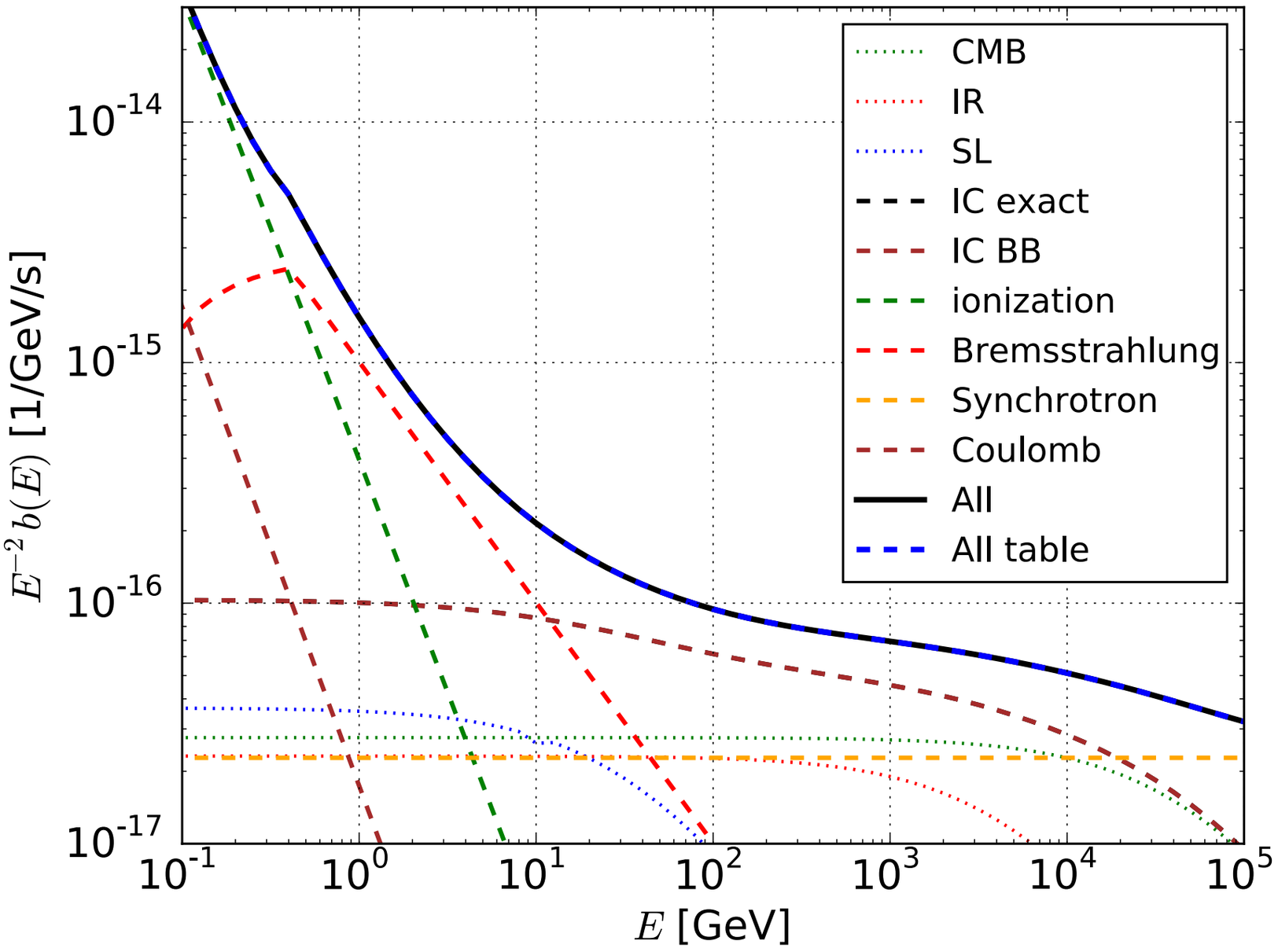

At energy > 100 GeV
$b(E) = 5\ 10^{-17}\ E^2$

Gamma-ray production from CRs

γ-rays = CRs x ISM (or ISRF)

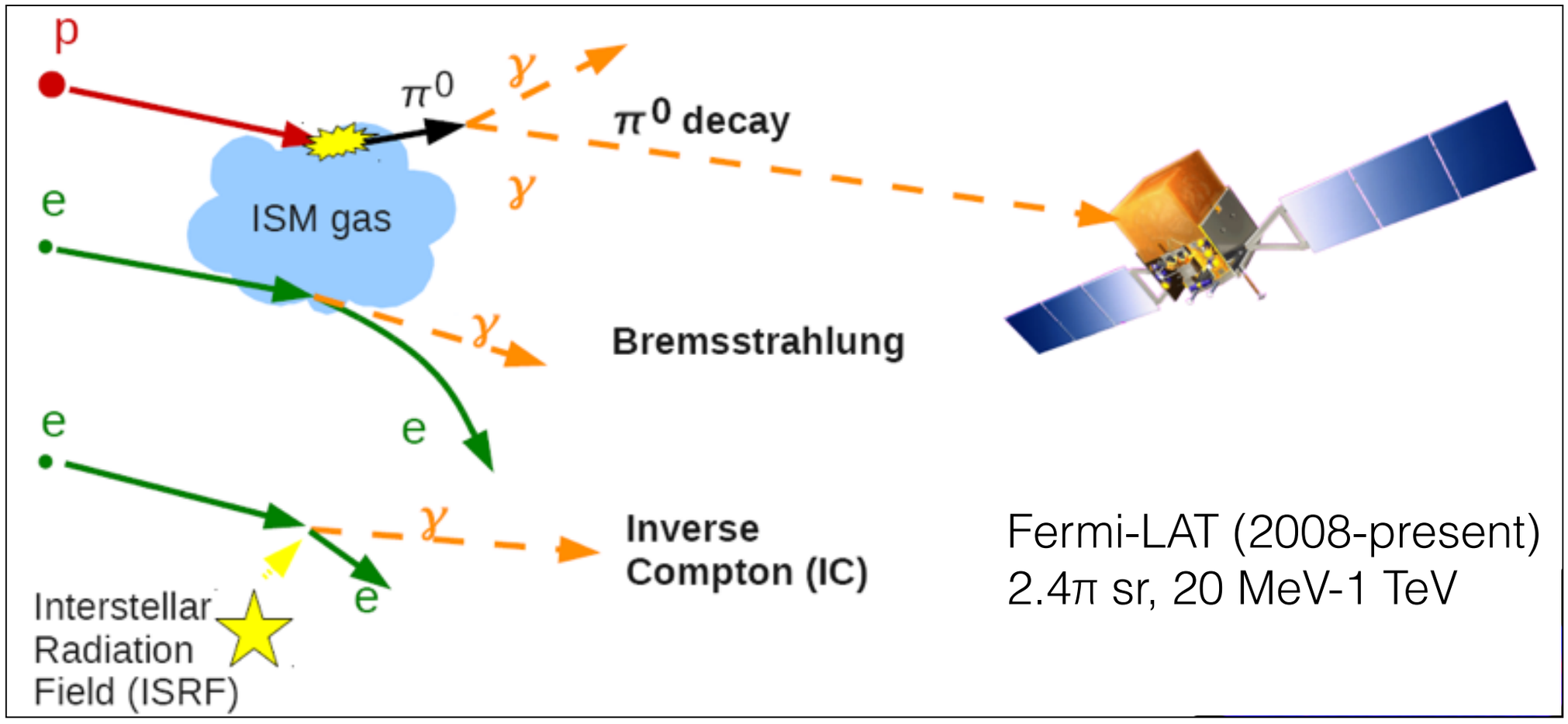

The study of interstellar emission from distant sources is a powerful probe for the CR production and propagation in the Galaxy

SNRs detected by Fermi-LAT

- Fermi-LAT has detected 39 SNRs so far (FL8Y).
- 27 of them have been detected as extended.
- SNRs are thought to be the main accelerators of Galactic CRs.

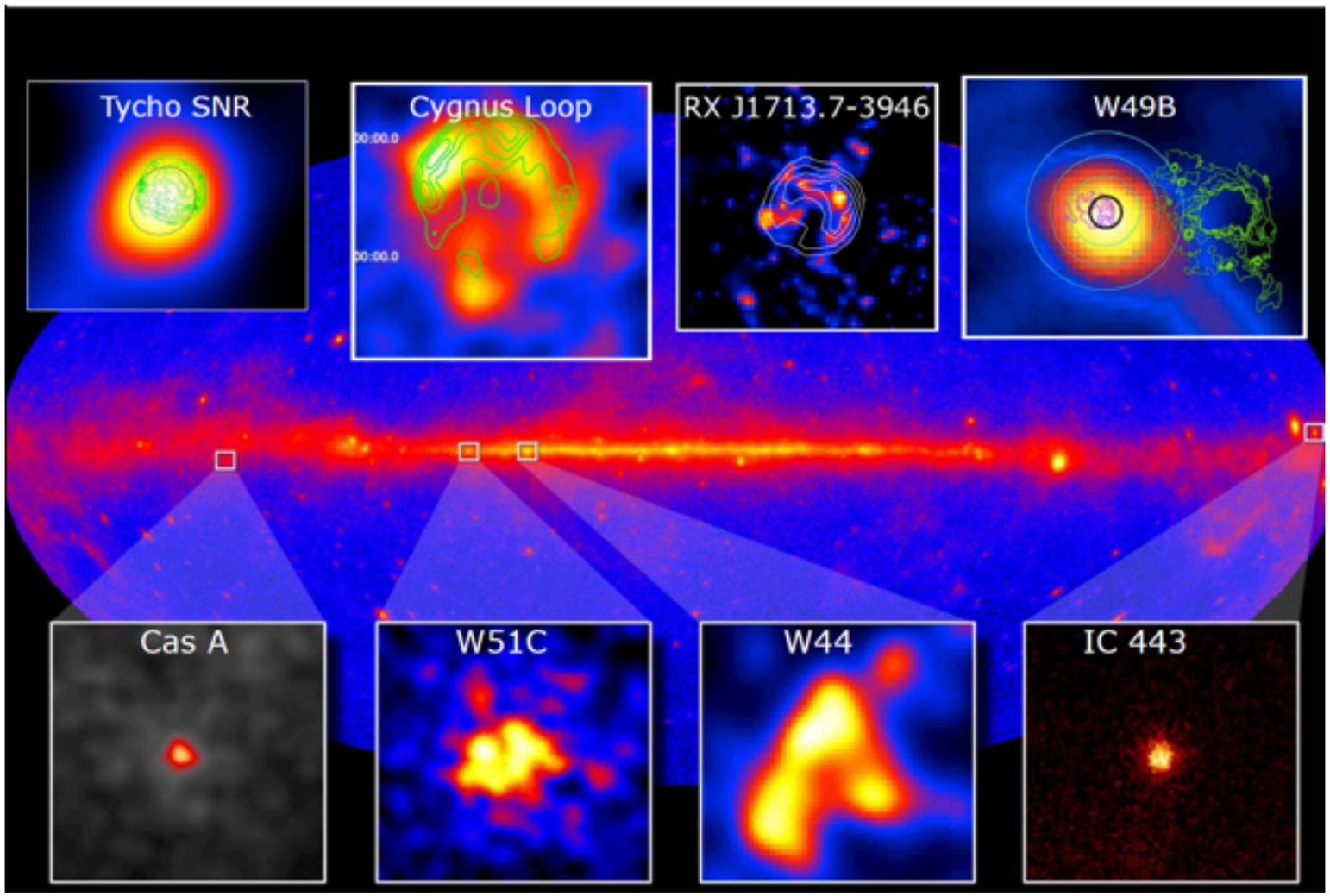

Fermi-LAT ApJs, V. 224, N. 1

Evidence of hadronic acceleration in SNRs

- A direct signature of acceleration of high energy protons from SNRs is provided by gamma rays generated in the decay of neutral pions (π^0)
  - p-p collisions create π^0 mesons which usually quickly decay into 2γ each having an energy of 67.5 MeV.
- The LAT team published evidence for the characteristic pion-decay feature in the gamma-ray spectra of two SNRs, IC 443 and W44.

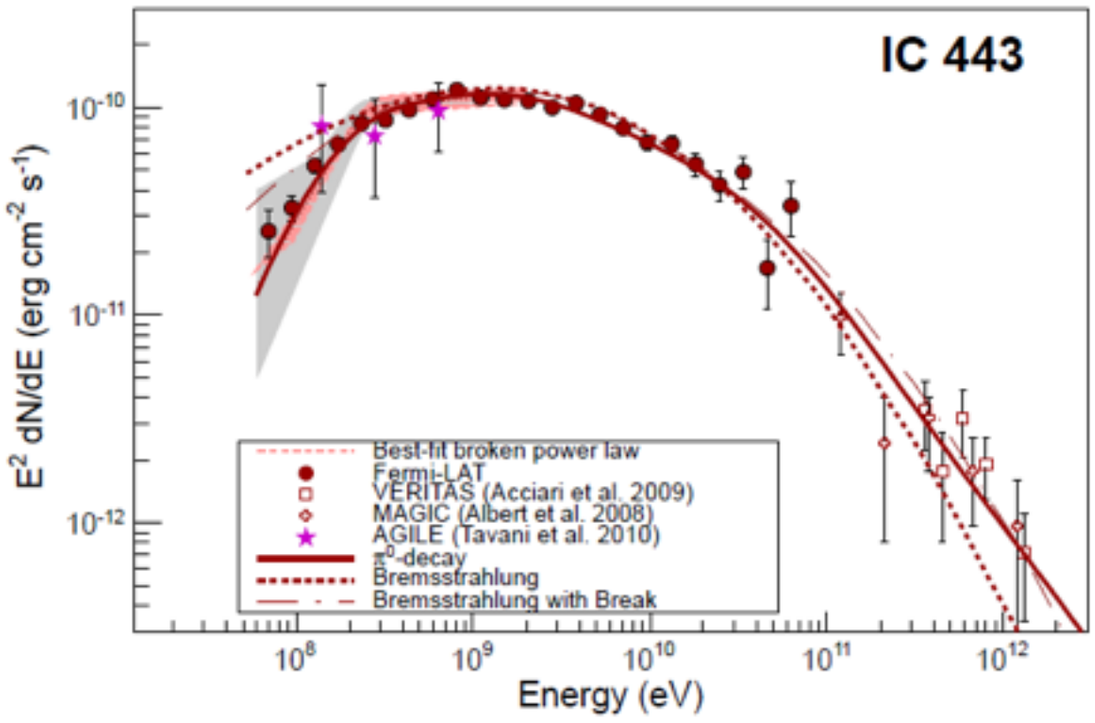

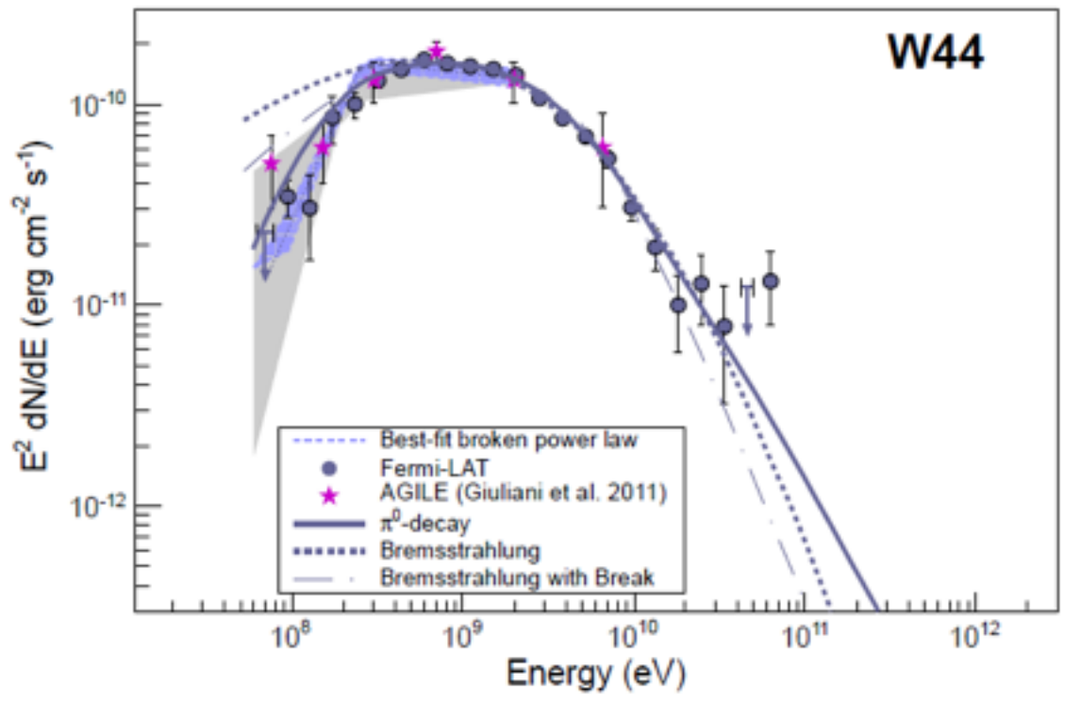

Ackermann+13, Science 339, 807

Hadronic or lepton origin

- For most of the SNRs detected in gamma rays both the hadronic and leptonic mechanism can explain the spectrum.
- It is important to have also X-ray and radio data to try to disentangle between the two mechanisms.

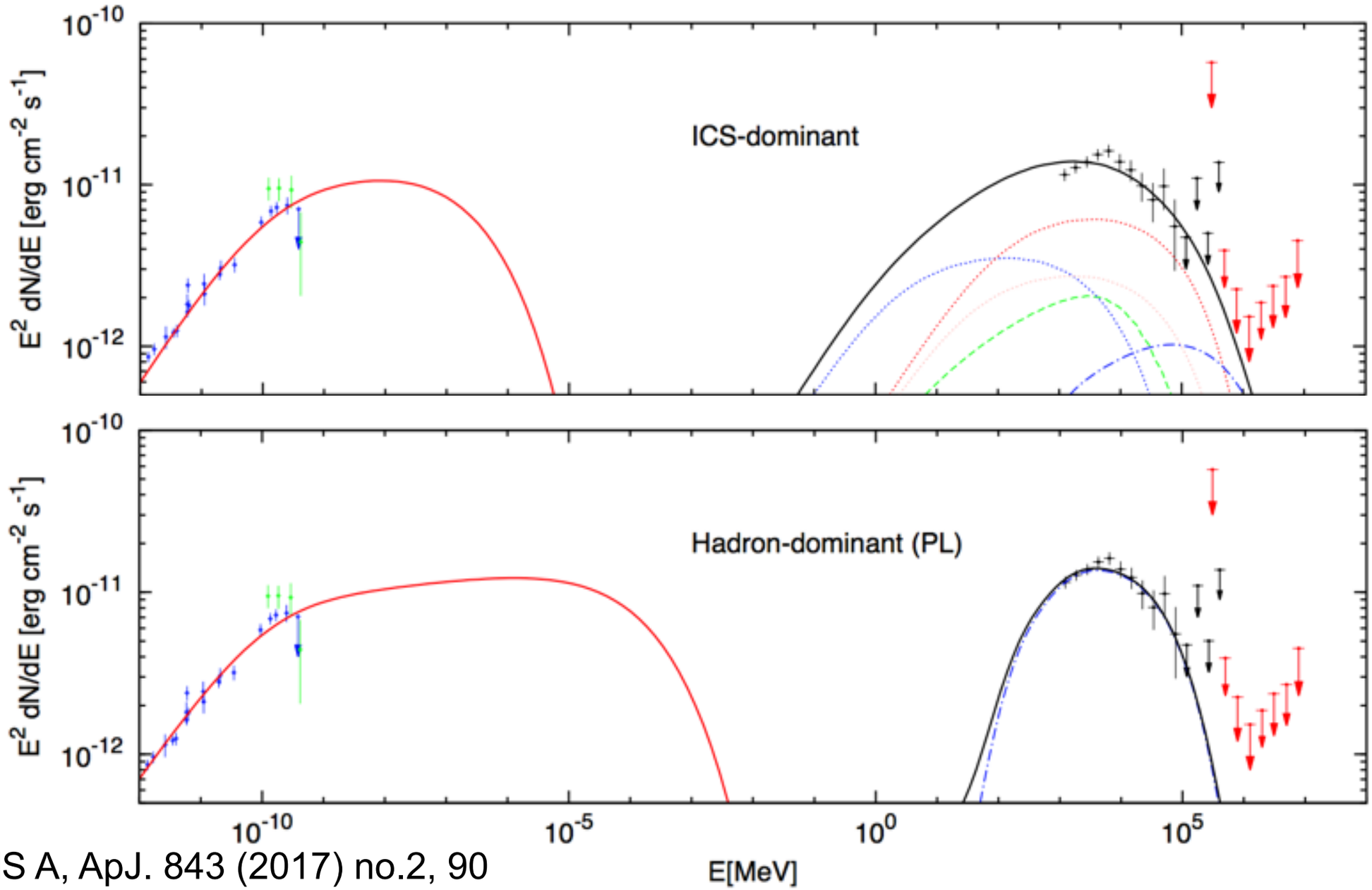

SNR PUPPIS A, ApJ. 843 (2017) no.2, 90

Hadronic or lepton origin

Model	α_p	α_e	$\Delta\alpha_e$	$E_{p,\mathrm{br}}$ (TeV)	$E_{p,\mathrm{cut}}$ (TeV)	$E_{e,\mathrm{br}}$ (GeV)	$E_{e,\mathrm{cut}}$ (TeV)	B (μG)	W_e [a] (10^{49}erg)	$n_{\mathrm{gas}} \times W_p$ [a,b] (10^{49}erg cm^{-3})	ε_p [c] ($eV\ cm^{-3}$)
ICS-dominated	1.80	1.80	1.0	–	10.0	20.0	0.8	6.0	1.7	2.5	46.5
Brems-dominated	1.85	1.85	1.0	–	4.0	18.0	4.0	11.0	0.7	1.4	3.3
Hadron-dominated (PL)	1.90	1.90	1.0	–	0.6	6.0	6.9	72.0	3.2×10^{-2}	30.0	69.8
Hadron-dominated (SBPL)	1.90	1.90	1.0	0.2	> 6.9	6.0	6.9	72.0	3.2×10^{-2}	30.0	69.8

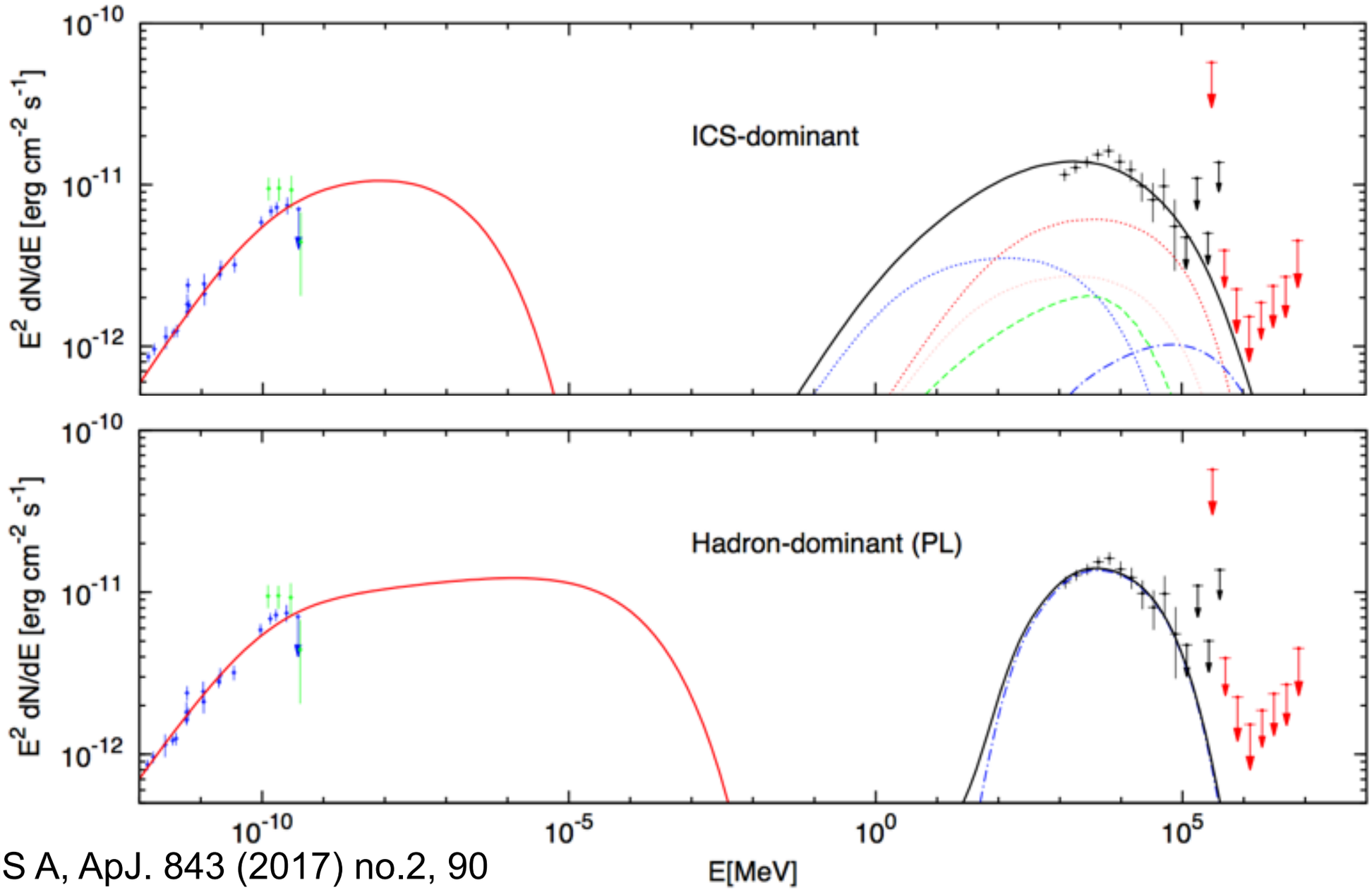

SNR PUPPIS A, ApJ. 843 (2017) no.2, 90

Origin of CR positrons

- Positrons are emitted through the secondary mechanism (CRs ISM —> X e^+).
- An excess of positrons above 10 GeV with respect to the secondary production has been measured by different experiments.
- Annihilation or decay of dark matter particles and emission from PWNe have been suggested as possible interpretations.

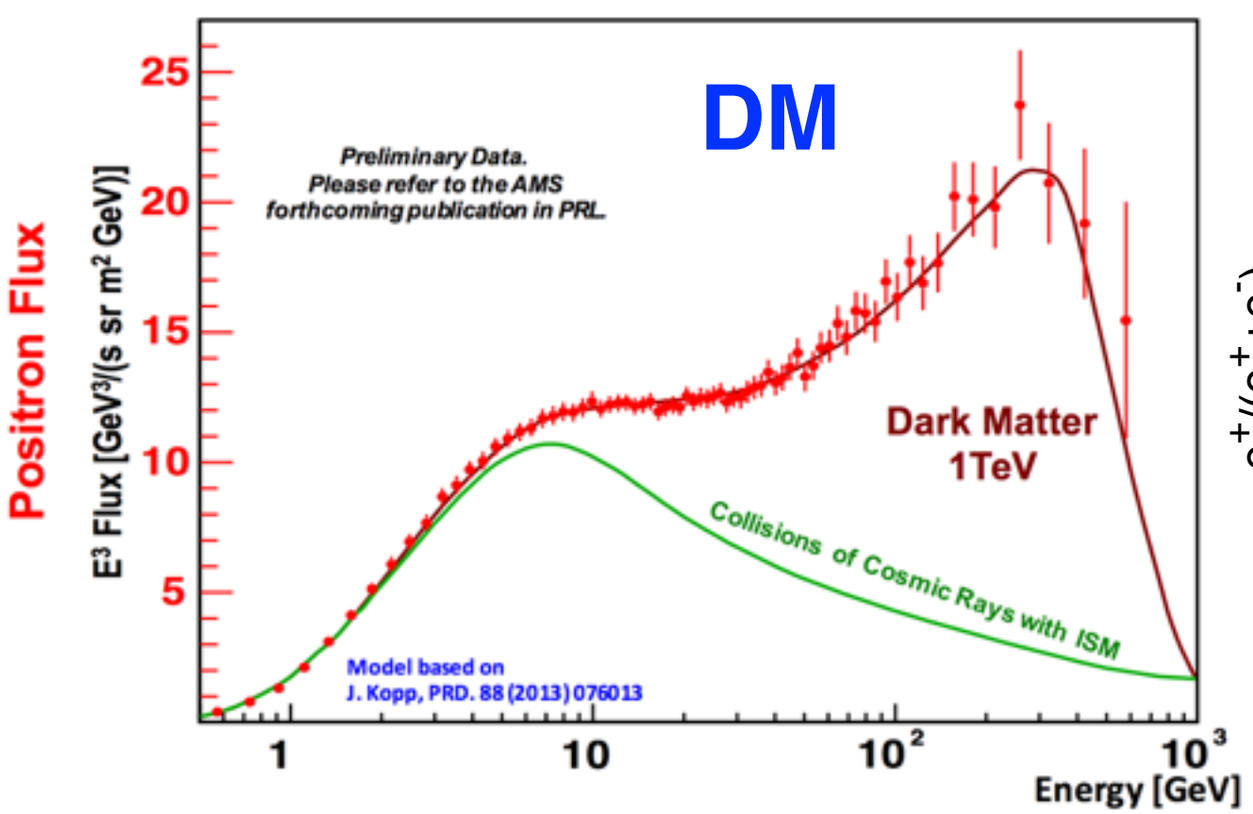

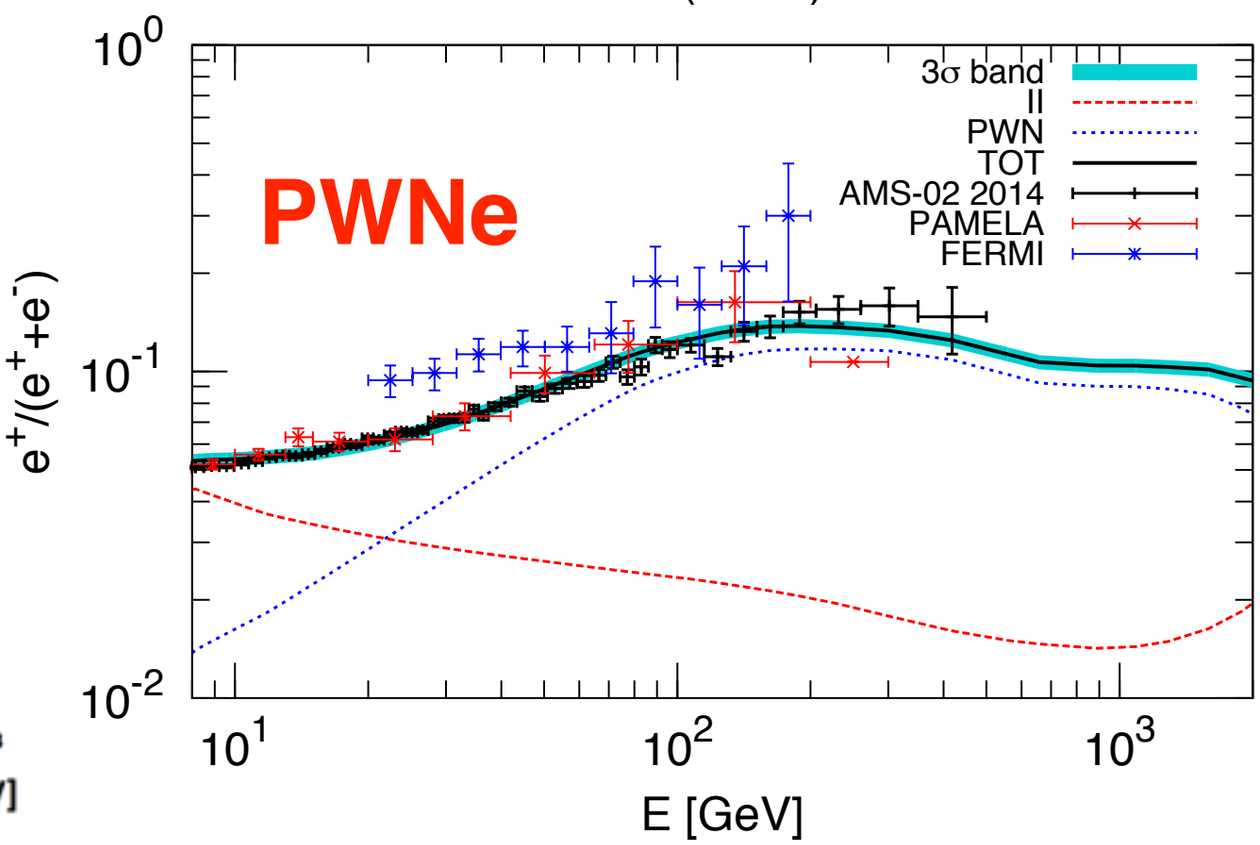

(M. Di Mauro and others. JCAP 1605 (2016) no.05, 031., M. Di Mauro and others. JCAP 04 (2014) 006.)

γ rays produced by ICS

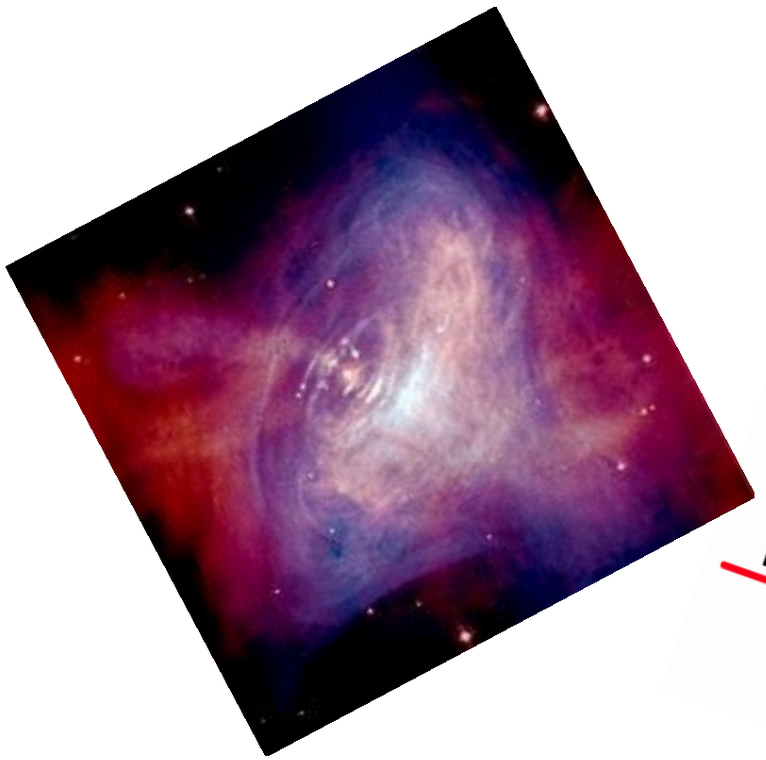

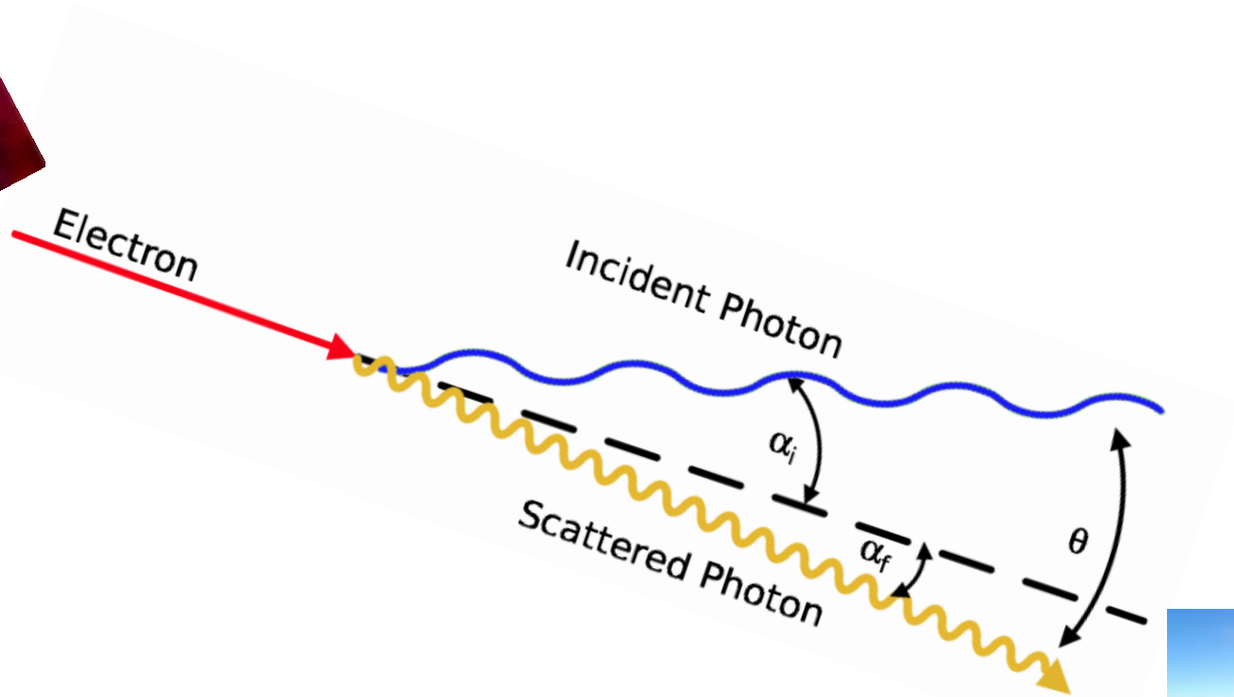

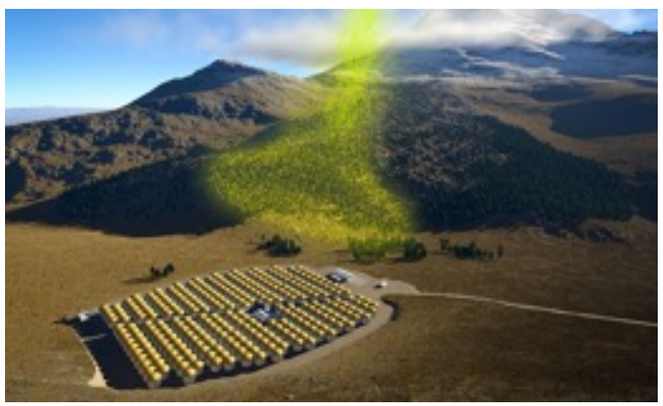

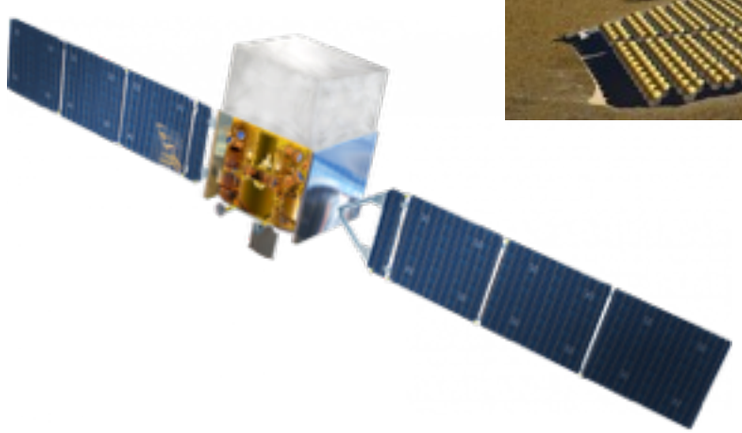

HAWC results for Geminga and Monogem PWNe

- HAWC detected an extended emission from Geminga and Monogem PWNe for **E>5 TeV**.
- Interpreted as ICS emission from e^+ and e^- accelerated from the PWN.
- **In the vicinity of the PWN, the diffusion coefficient D must be about 500 times smaller than the average in the Galaxy.**

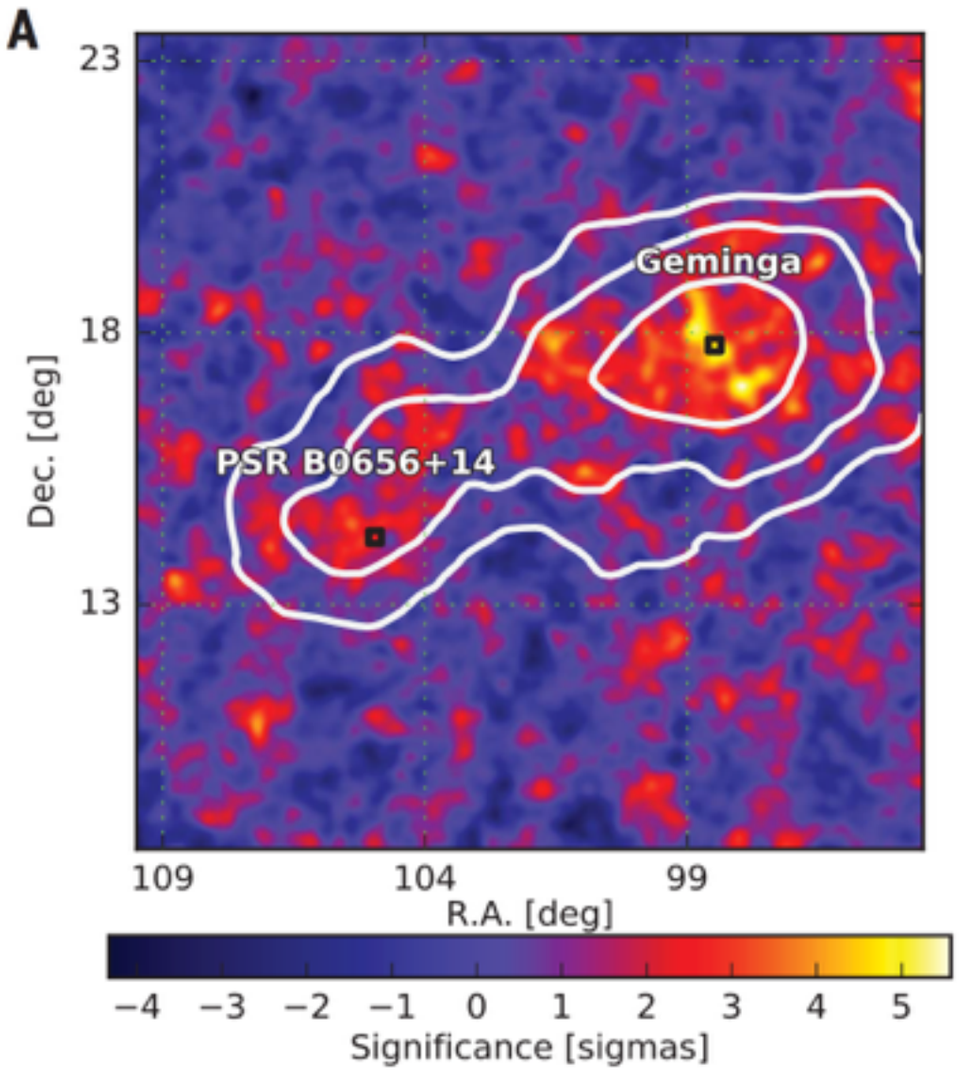

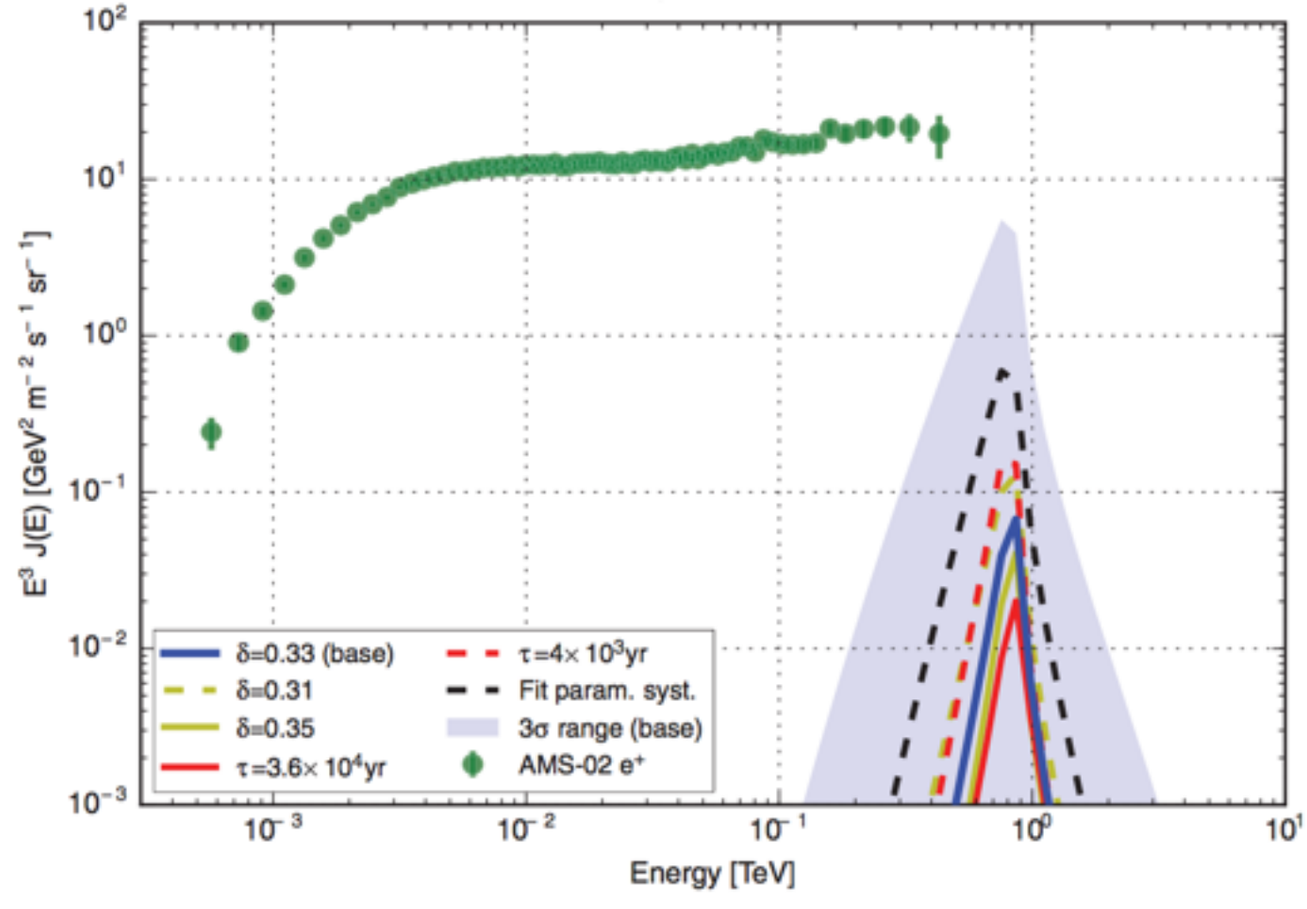

Science 358 (2017) no.6365, 911-914

Geminga and Monogem surface brightness

- HAWC measured the surface brightness, i.e. the flux in different annuli around the source.
- Using the surface brightness data we can find the diffusion coefficient around these two PWNe.
- **In the vicinity of the PWN, the diffusion coefficient D must be about 500 times smaller than the average in the Galaxy.**

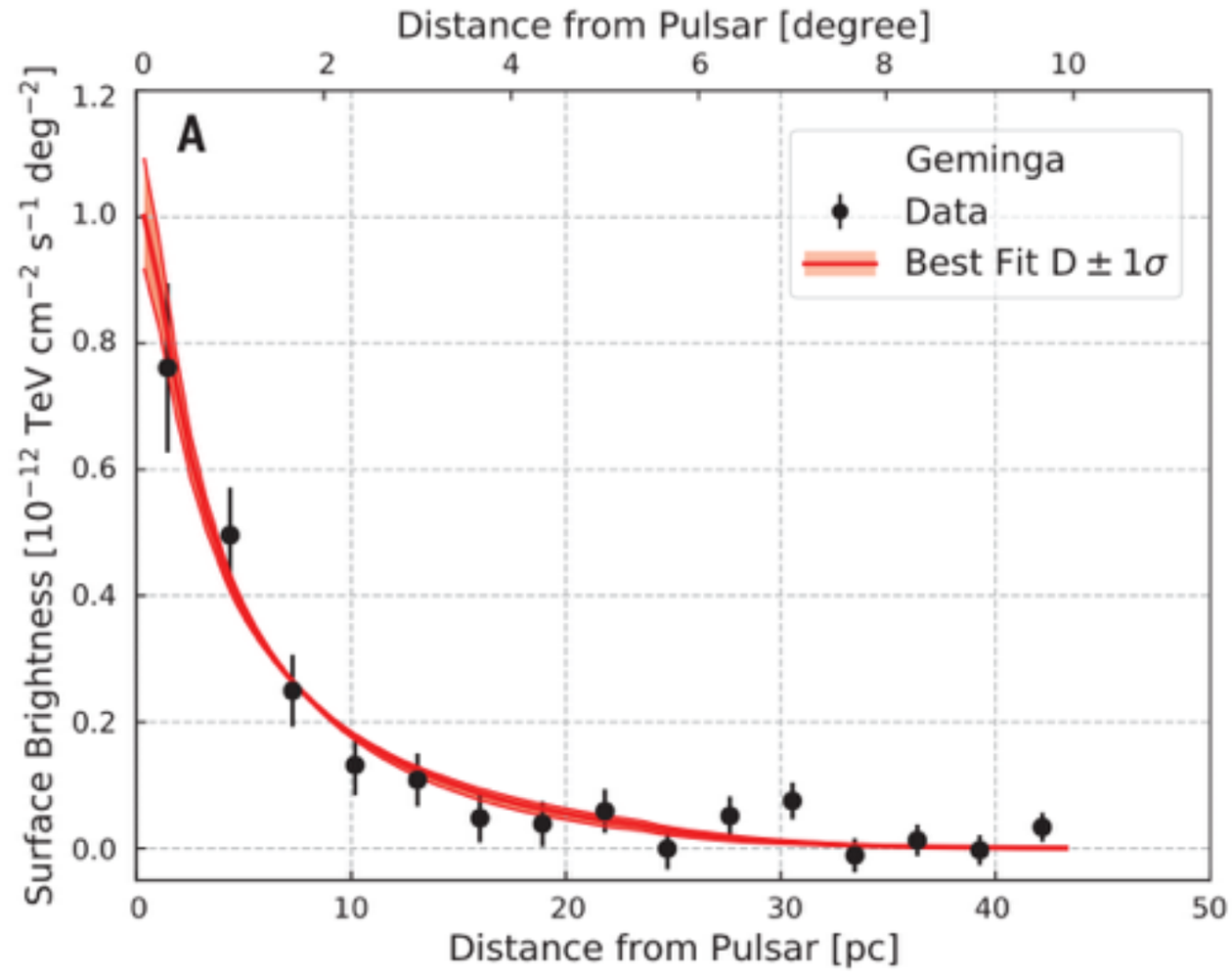

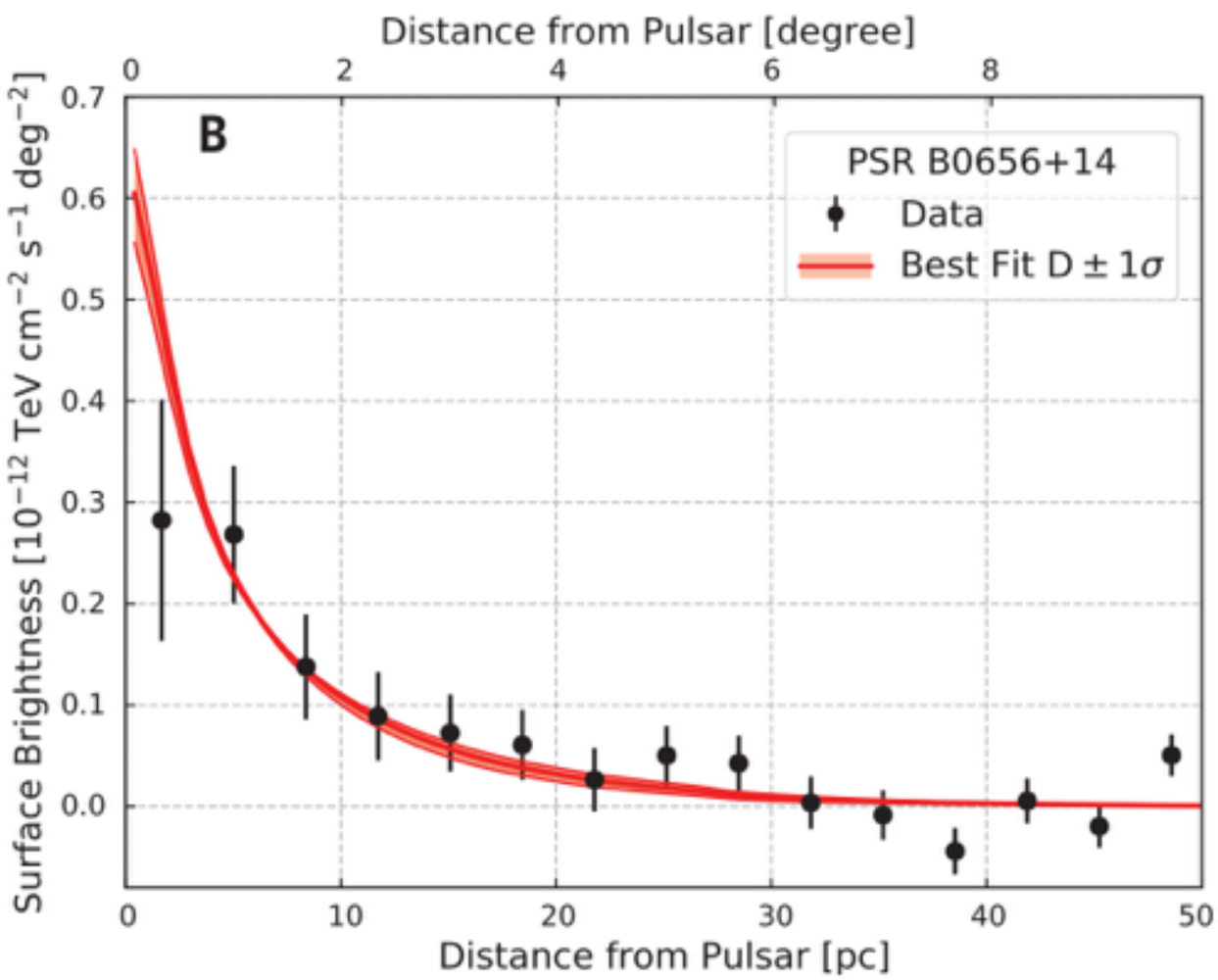

Science 358 (2017) no.6365, 911-914

Geminga and Monogem surface brightness

- HAWC measured the surface brightness, i.e. the flux in different annuli around the source.
- Using the surface brightness data we can find the diffusion coefficient around these two PWNe.
- **In the vicinity of the PWN, the diffusion coefficient D must be about 500 times smaller than the average in the Galaxy.**

		Geminga	PSR B0656+14
Pulsar parameters			
(Right ascension, declination) (J2000 source location)	(degrees)	(98.48, 17.77)	(104.95, 14.24)
τ_c (characteristic age)	(years)	342,000	110,000
T (spin period)	(seconds)	0.237	0.385
d (distance)	(parsecs)	250^{+120}_{-62}	288^{+33}_{-27}
dE/dt (energy loss rate due to pulsar's spin slowing)	($\times 10^{34}$ ergs per second)	3.26	3.8
Model values			
θ_0 (θ_d for 20-TeV gamma ray)	(degrees)	5.5 ± 0.7	4.8 ± 0.6
N_0	($\times 10^{-15}$ photons per tera–electron volt per square centimeter per second)	$13.6^{+2.0}_{-1.7}$	$5.6^{+2.5}_{-1.7}$
α		2.34 ± 0.07	2.14 ± 0.23
D_{100} (diffusion coefficient of 100-TeV electrons from joint fit of two PWNe)	($\times 10^{27}$ square centimeters per second)	4.5 ± 1.2	4.5 ± 1.2
D_{100} (diffusion coefficient of 100-TeV electrons from individual fit of PWN)	($\times 10^{27}$ square centimeters per second)	$3.2^{+1.4}_{-1.0}$	15^{+49}_{-9}
Energy range	(tera–electron volt)	8 to 40	8 to 40
Luminosity in gamma rays over this energy range	($\times 10^{31}$ ergs per second)	11 × $(d/250\ \text{pc})^2$	4.5 × $(d/288\ \text{pc})^2$
Assumed parameters			
L_0 (initial spin-down power)	($\times 10^{36}$ ergs per second)	27.8	4.0
W_e (total energy released since pulsar's birth)	($\times 10^{48}$ ergs)	11.0	1.5

10^{26} cm²/s at 1 GeV

Science 358 (2017) no.6365, 911-914

Predictions for the e^+ flux from Geminga using HAWC data

- Tuning the model with HAWC data (above 10 TeV) is not possible to have a precise prediction for the AMS-02 positron excess.
- We should use γ-ray data between 10 GeV to 1 TeV.
- *Fermi*-LAT is ideal for this scope:
  - It detects γ rays between 100 MeV to TeV.
  - It covers the entire sky every 3 hours
  - It is observing the sky since more than 10 years.

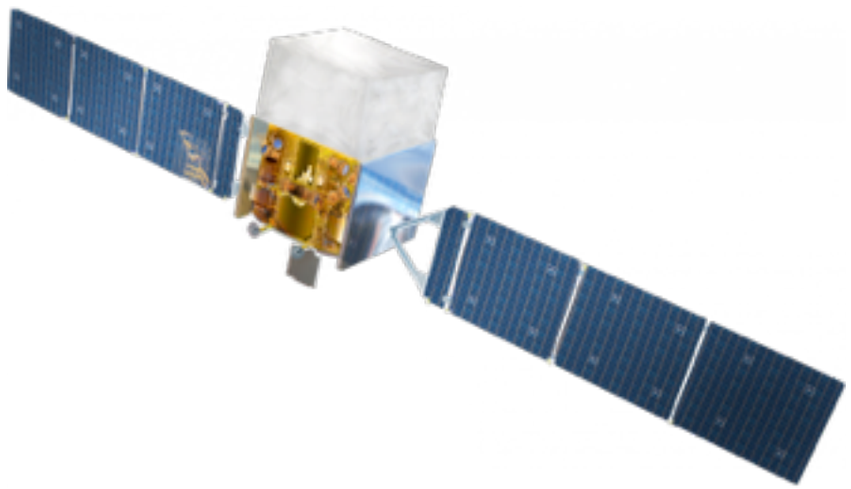

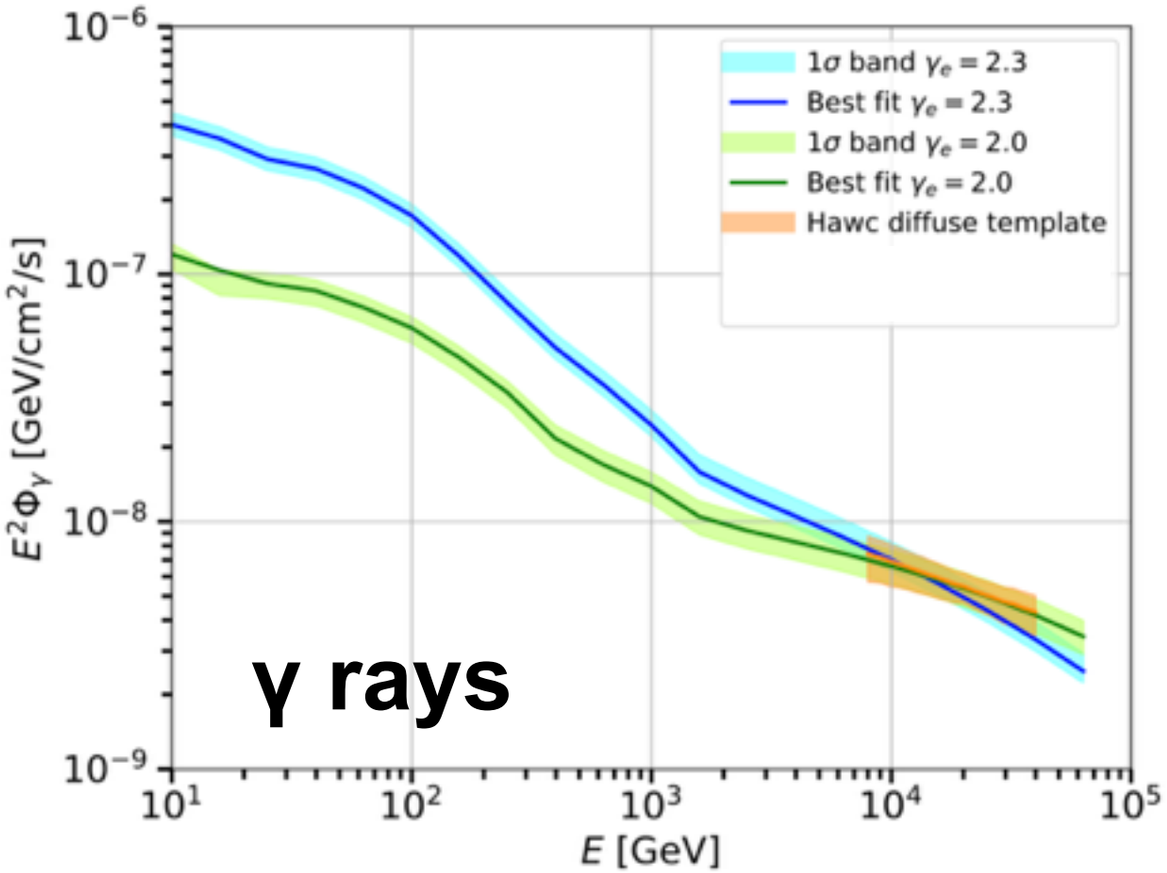

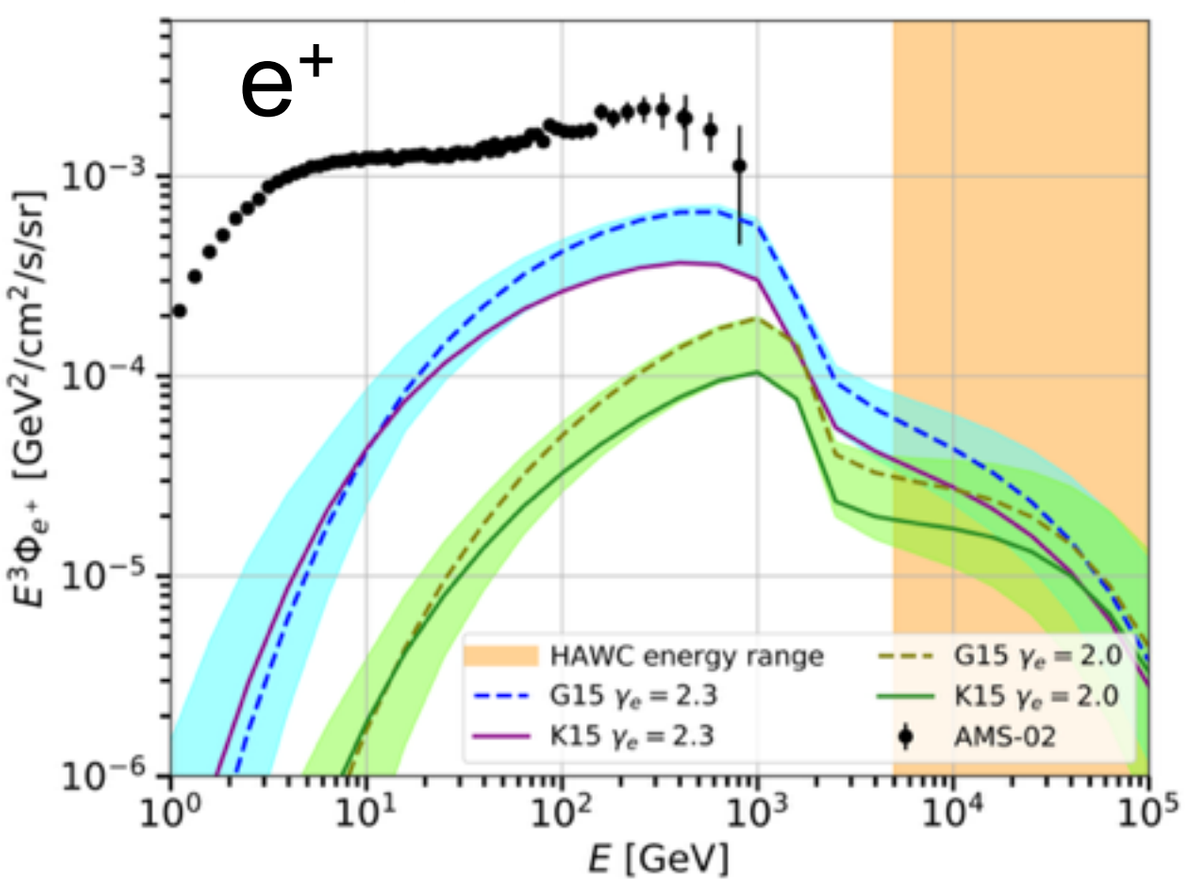

Di Mauro et al. arXiv:1903.05647

Geminga proper motion

- Geminga has a proper motion of **211 km/s** which implies this pulsar moved about **70 pc** across its age.
- We have implemented this effect in our model.
- Our analysis is unique in γ-ray astronomy because we search for a source that is moving across the sky in γ rays.

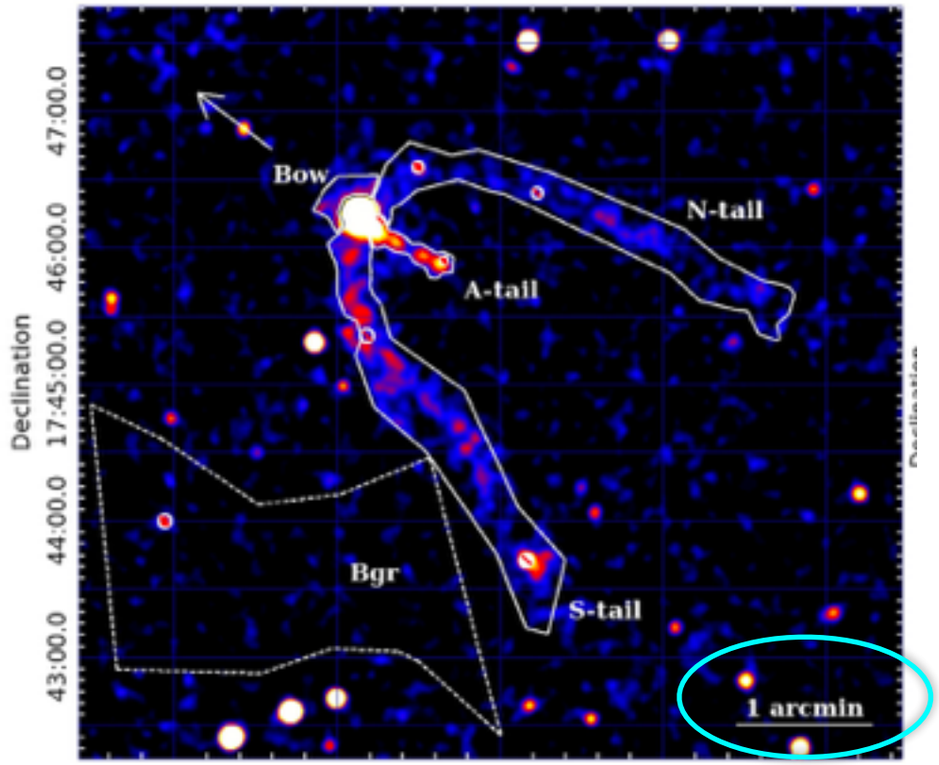

Posselt et al. 2008

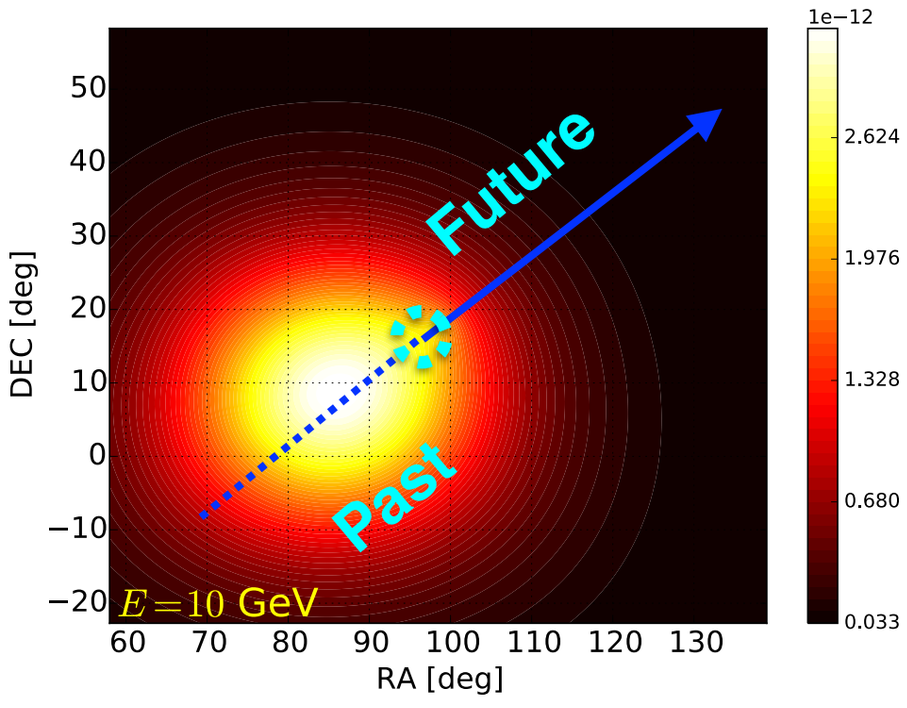

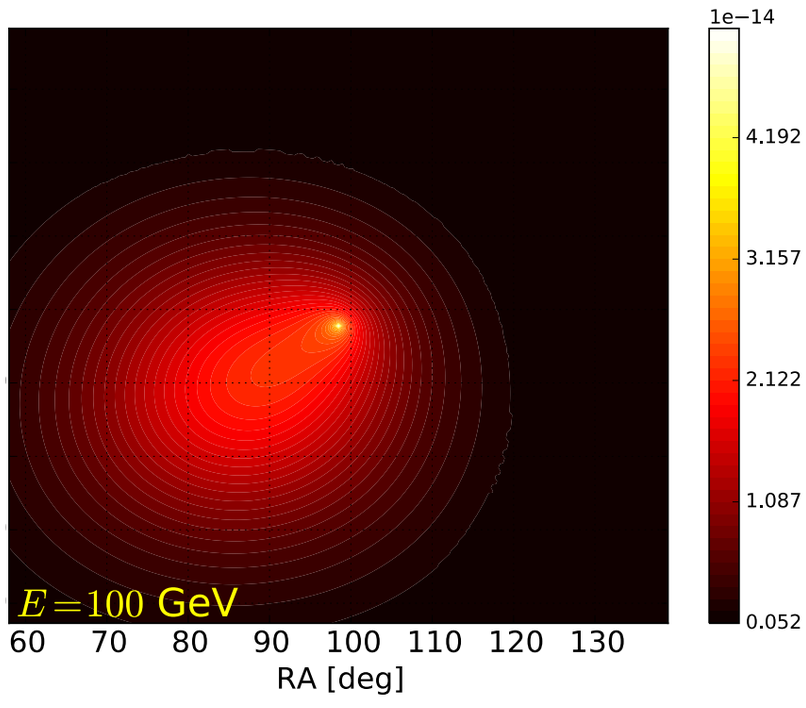

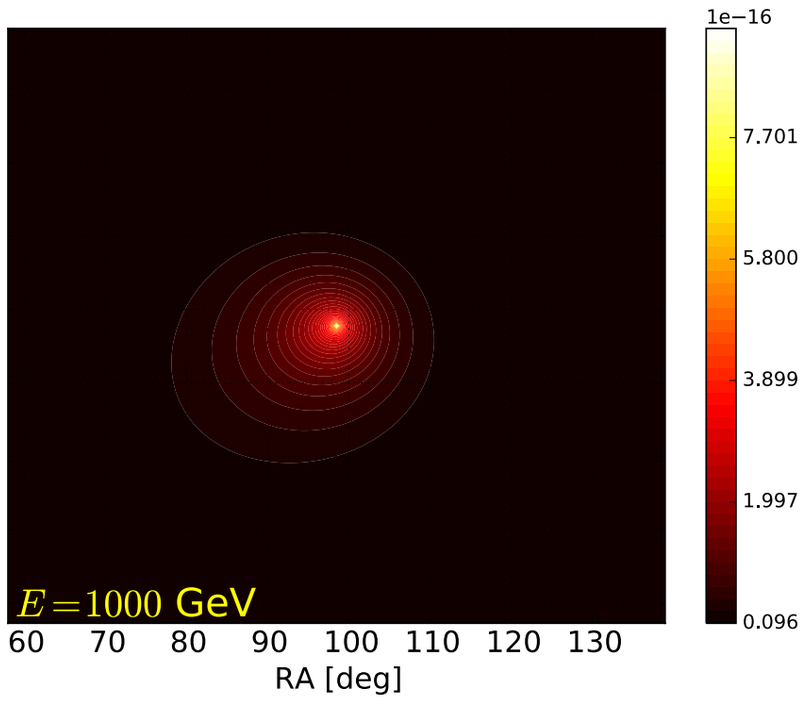

Di Mauro et al. arXiv:1903.05647

Analysis of Fermi-LAT data

- We have performed an analysis of 115 months of Fermi-LAT data for **E>8 GeV**.
- Our model with the pulsar proper motion is preferred at least at **4σ significance**.
- We find a **7.8-11.8 σ significance emission from Geminga with a diffusion D(1 GeV)= 2.3 10^{26} cm^2/s with δ=0.33.**

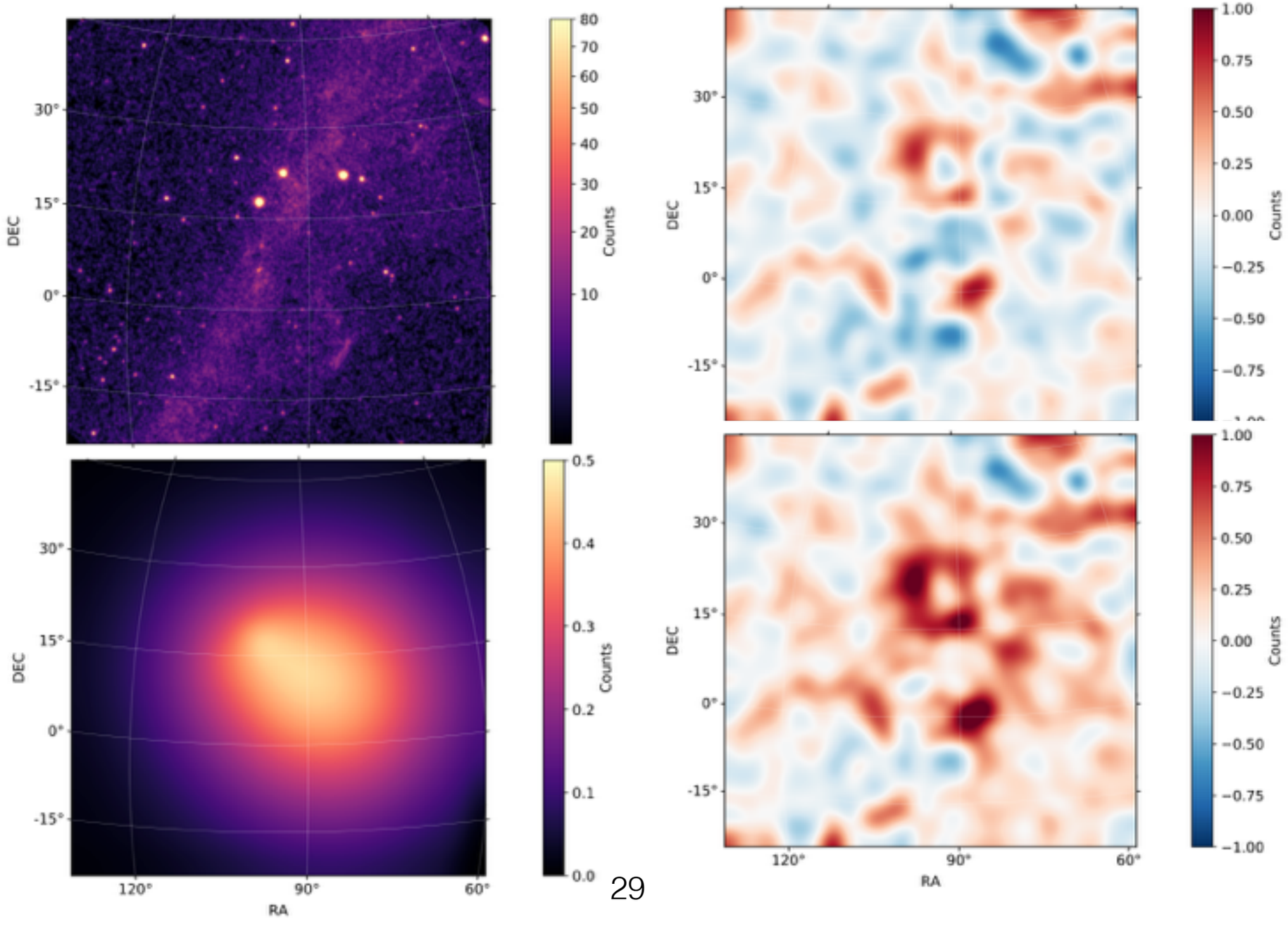

Analysis of Fermi-LAT data

- We have performed an analysis of 115 months of Fermi-LAT data for **E>8 GeV**.
- Our model with the pulsar proper motion is preferred at least at **4σ significance**.
- We find a **7.8-11.8 σ significance emission from Geminga with a diffusion D(1 GeV)= 2.3 10^{26} cm^2/s with δ=0.33.**

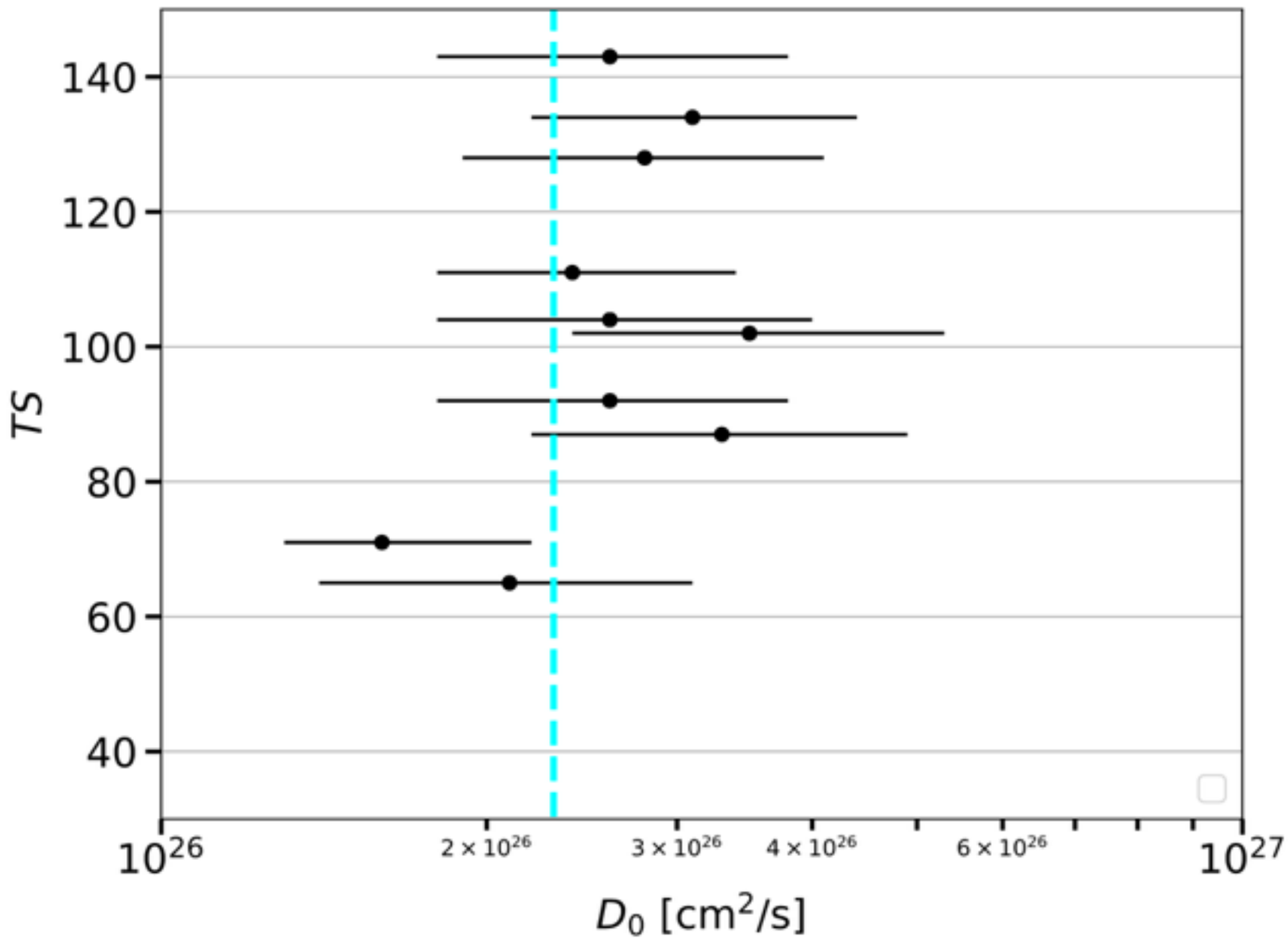

Di Mauro et al. arXiv:1903.05647

ICS γ-ray and positron flux

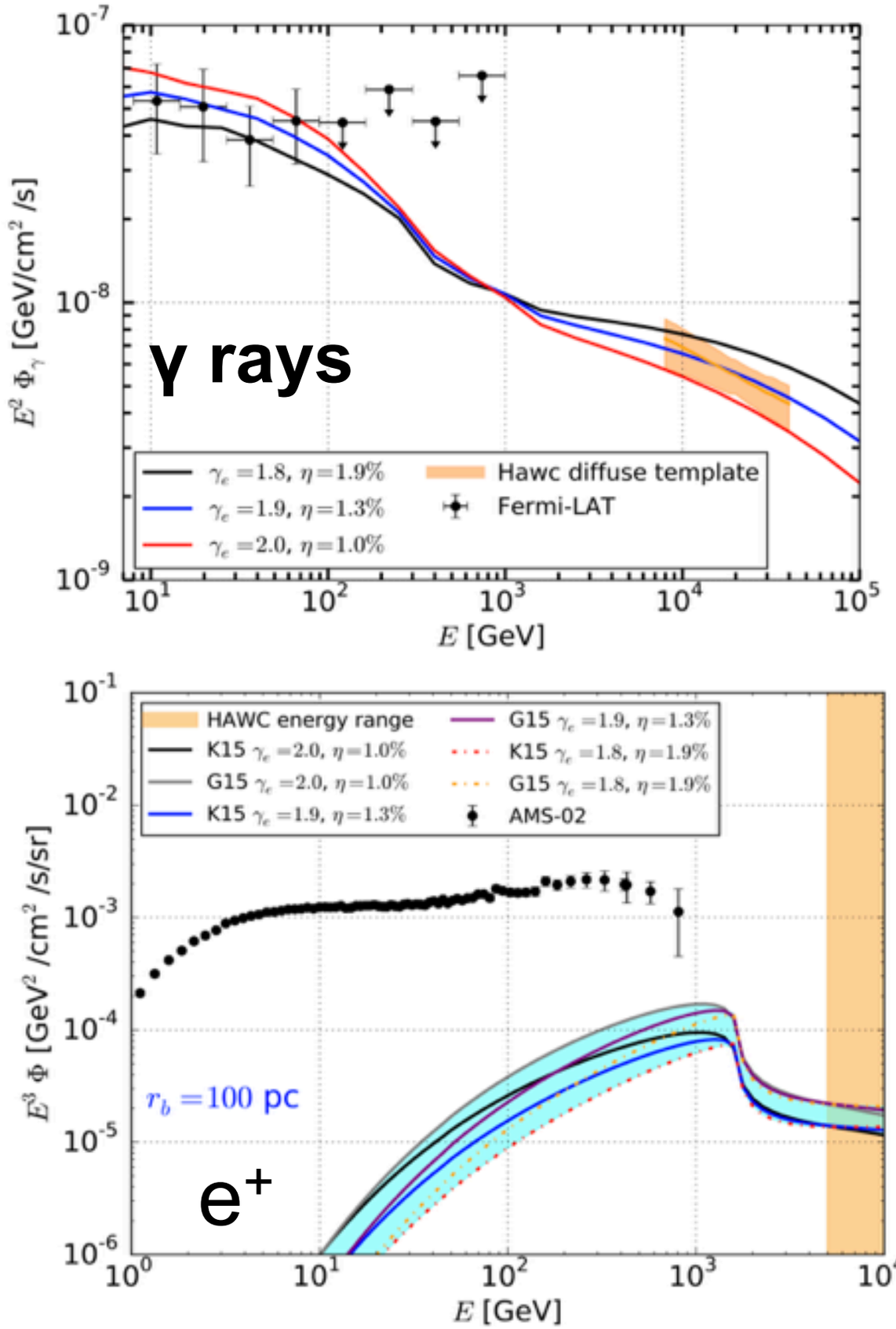

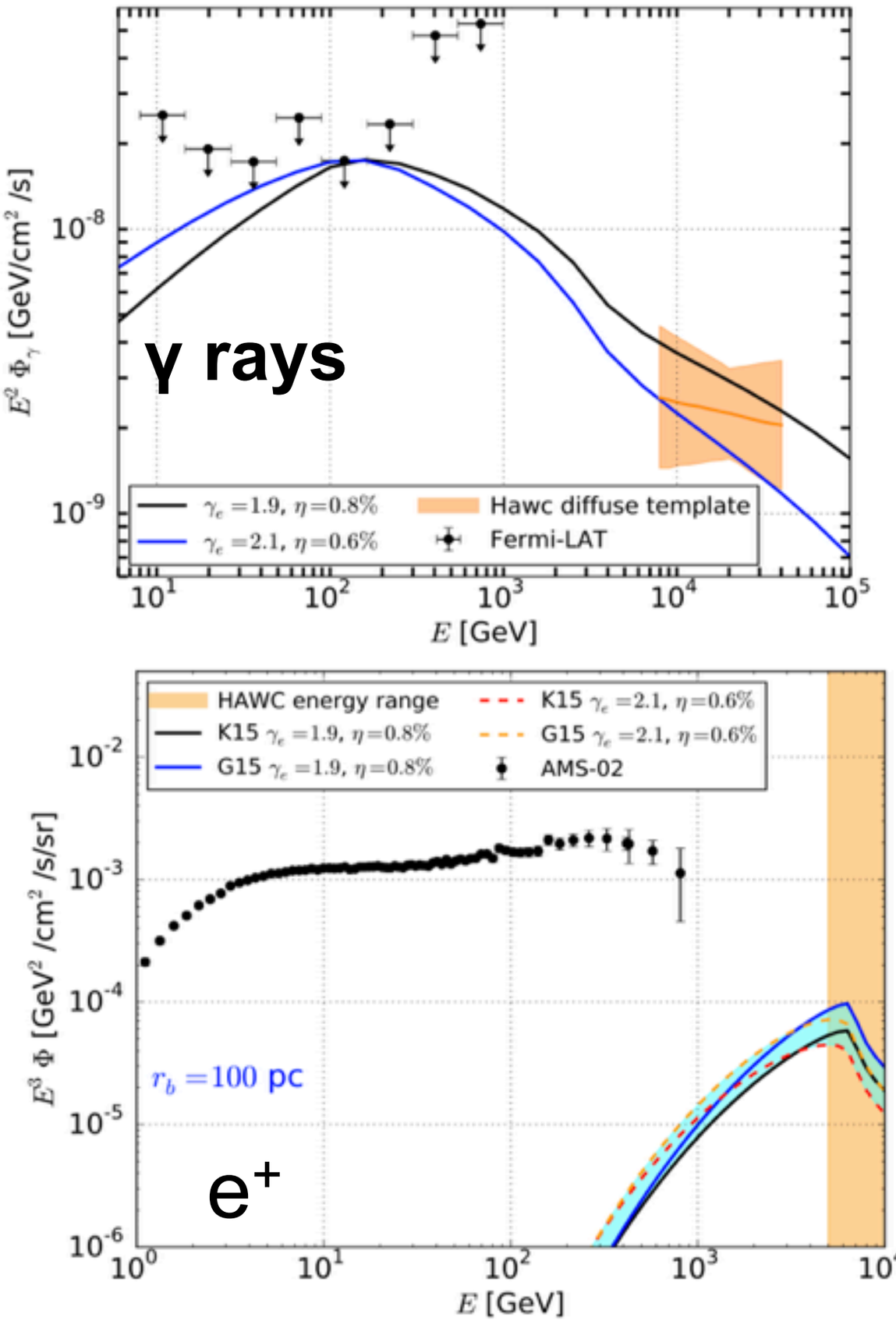

Conclusions and open questions

- Conclusions:
  - SNRs accelerate CRs.
  - Geminga (and Monogem) are confirmed to produce e^+ and e^- and so they contribute to the e^+ excess.
  - The diffusion around Geminga and Monogem is two orders of magnitude smaller than the average of the Galaxy.
- Open questions:
  - It is still not clear what is the dominant mechanism that produces gamma rays in CRs.
  - Do all PWNe produce e^+ and e^- and at which efficiency?
  - Are all PWNe embedded in a low-diffusion bubble?
  - How large is the low-diffusion bubble?
  - Should we include in the propagation of CRs the presence of these bubbles?
  - …….

What's next?

- In order to answer the open questions, we need to find more ICS halos.
- We have to find a promising list of pulsars to analyze.
  - We can inspect the gamma-ray energy and pulsar characteristics (distance, age) that are more promising to detect ICS halos.
  - We calculate the extension and the flux of ICS halos around Galactic pulsars.

$$\Phi_\gamma^{68\%} = 2\pi \int_0^{\theta_{\rm EXT}} \frac{d\Phi_\gamma}{d\theta} \sin\theta d\theta$$

ICS halo extension

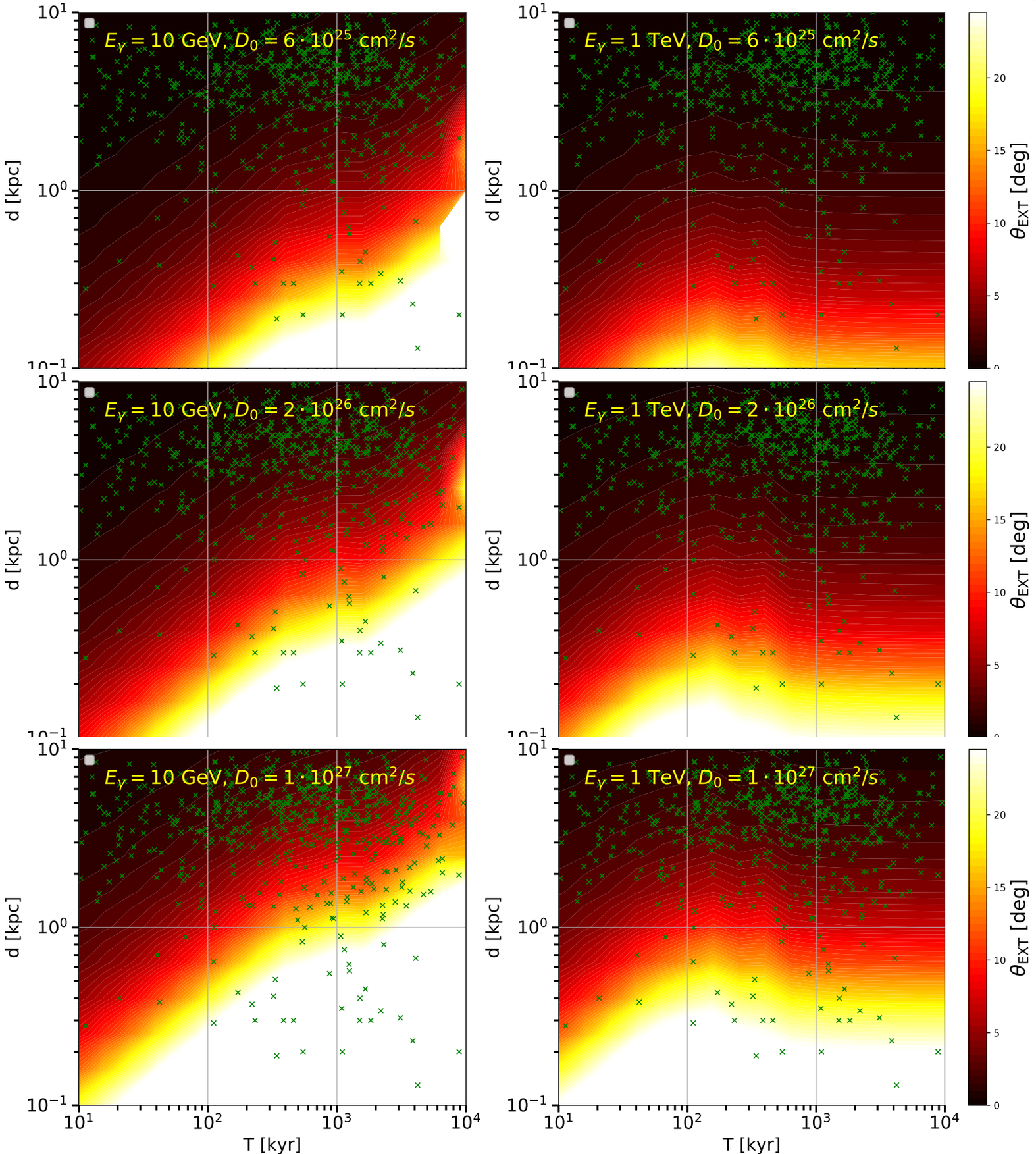

If D is larger than 10^{27} cm^2/s most of ICS halos would be undetectable by IACTs and HAWC.

In the Fermi-LAT energy range even with a low D, most of the pulsars would have a very extended ICS halo.

If we will find an extension for the halos of the order the degree at TeV energies D must be of the order of 10^{26} cm^2/s.

$$\Phi_\gamma^{68\%} = 2\pi \int_0^{\theta_{\rm EXT}} \frac{d\Phi_\gamma}{d\theta} \sin\theta d\theta$$

Number of detectable ICS halos

- An other interesting question is: how many ICS halos current and future gamma-ray experiments could detect?
- We took the pulsars in the ATNF catalog and we calculate the predicted gamma-ray flux.
- We focused the results on HESS, HAWC and CTA.

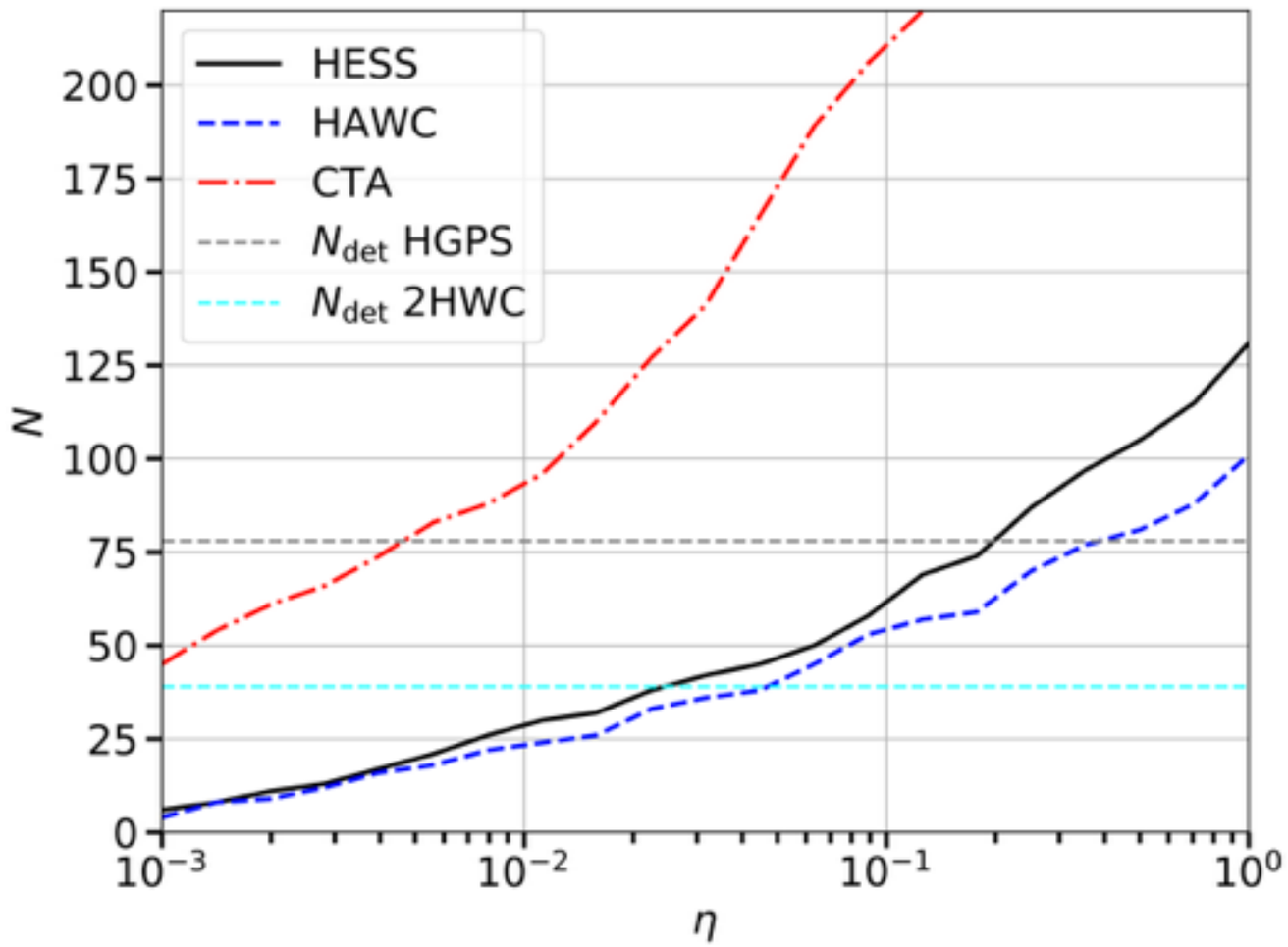

Effect of the size of the low-diffusion bubble on the ICS halo extension

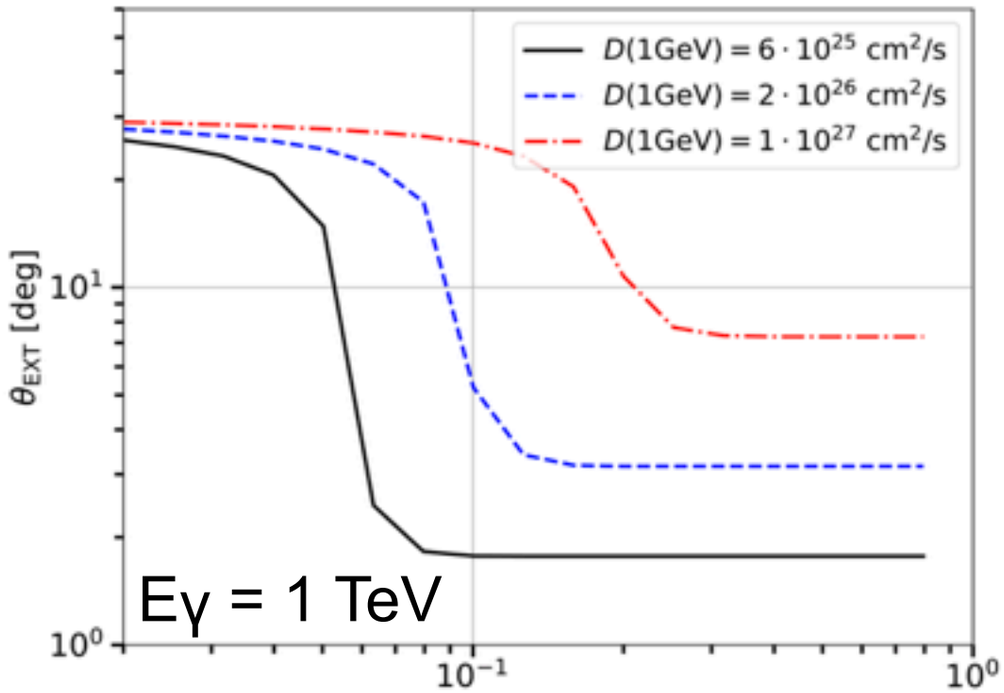

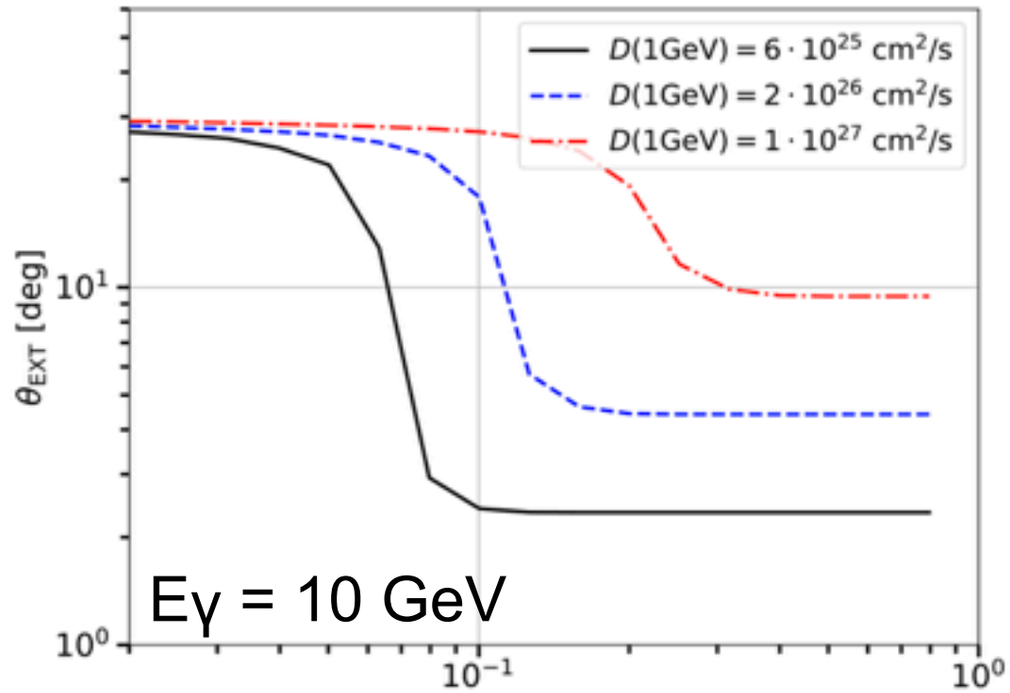

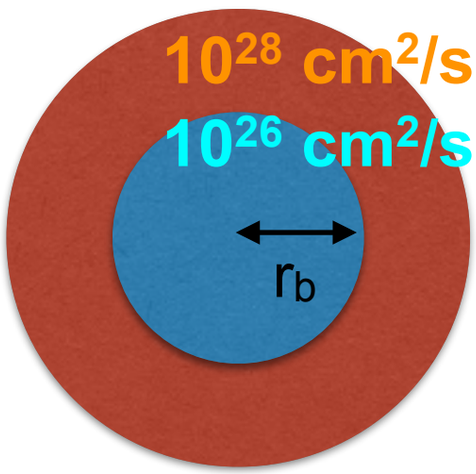

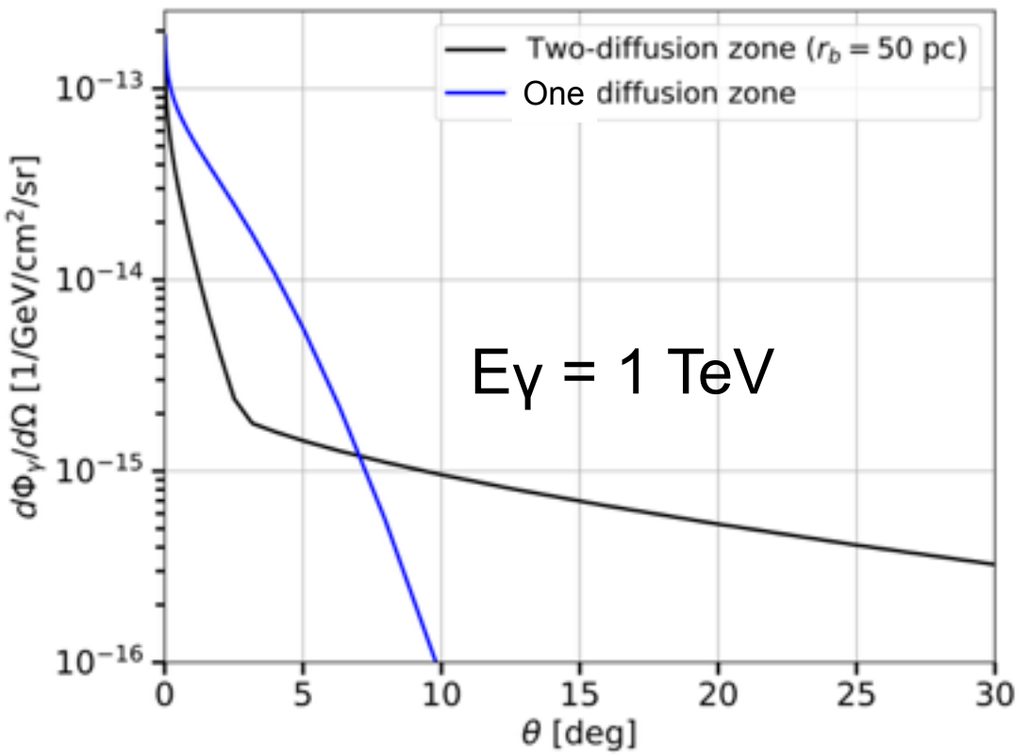

d = 1 kpc and T = 100kyr

Effect of pulsar proper motion on the ICS halo extension

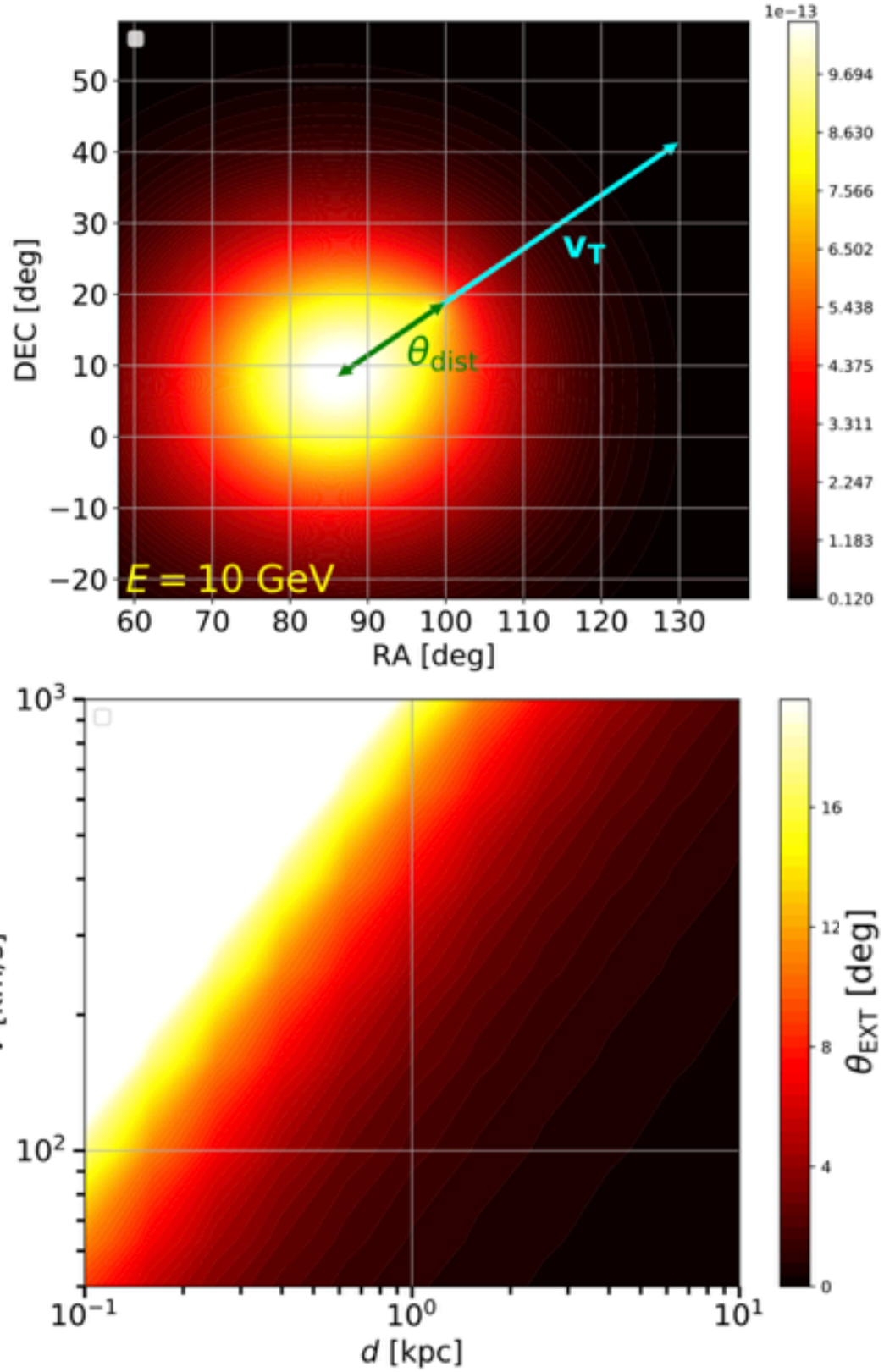

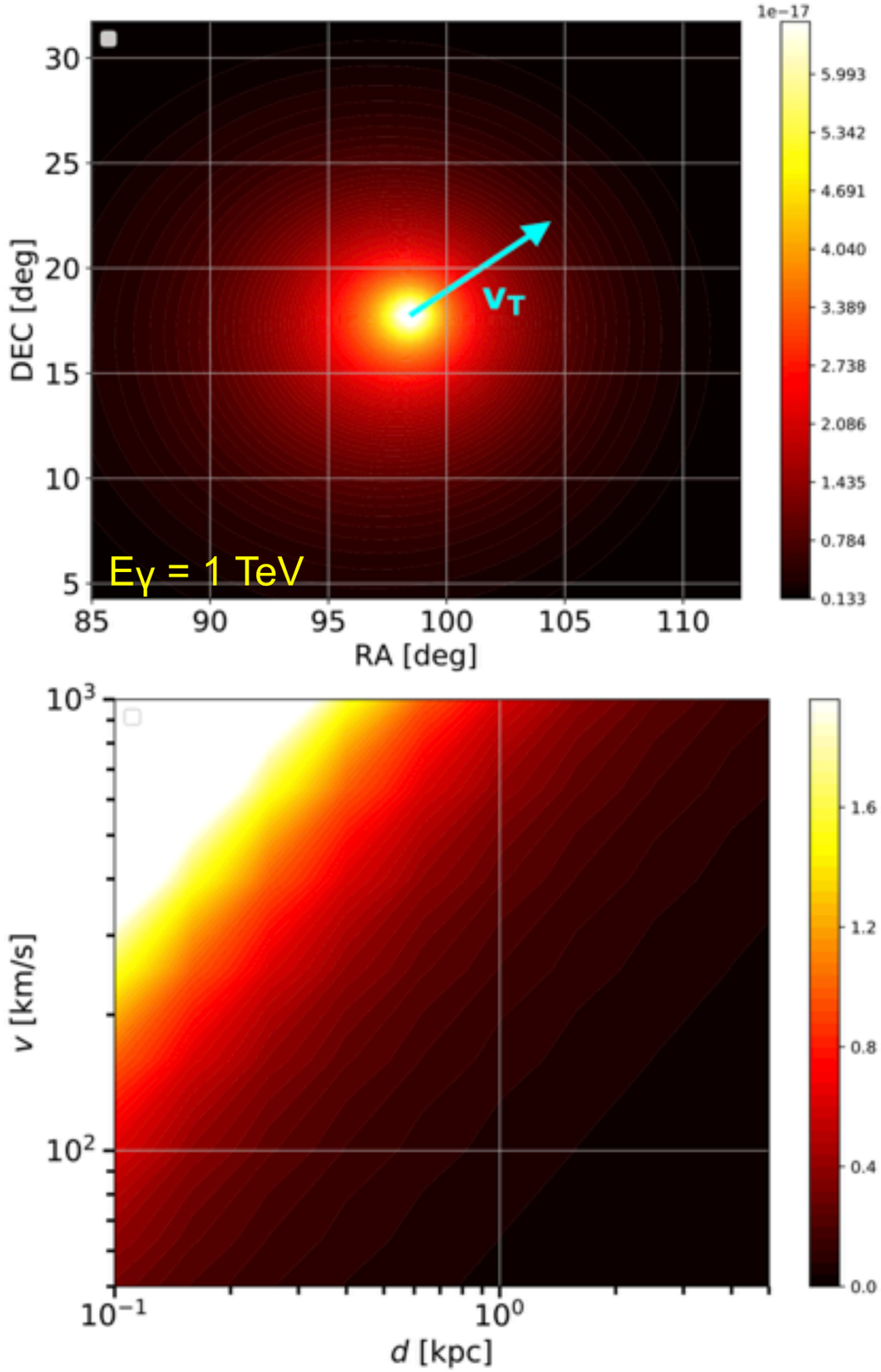

Contribution of PWNe to the positron excess

- We can now use the results for D and the constraints for the size of the low-diffusion bubble to provide predictions for the PWNe contribution to the positron excess.
- We calculate this with different values of r_b.
- Increasing r_b lowers the high-energy part of the flux.
- With an efficiency of 10% and a spectrum index of 1.9 PWNe can explain entirely the positron excess.

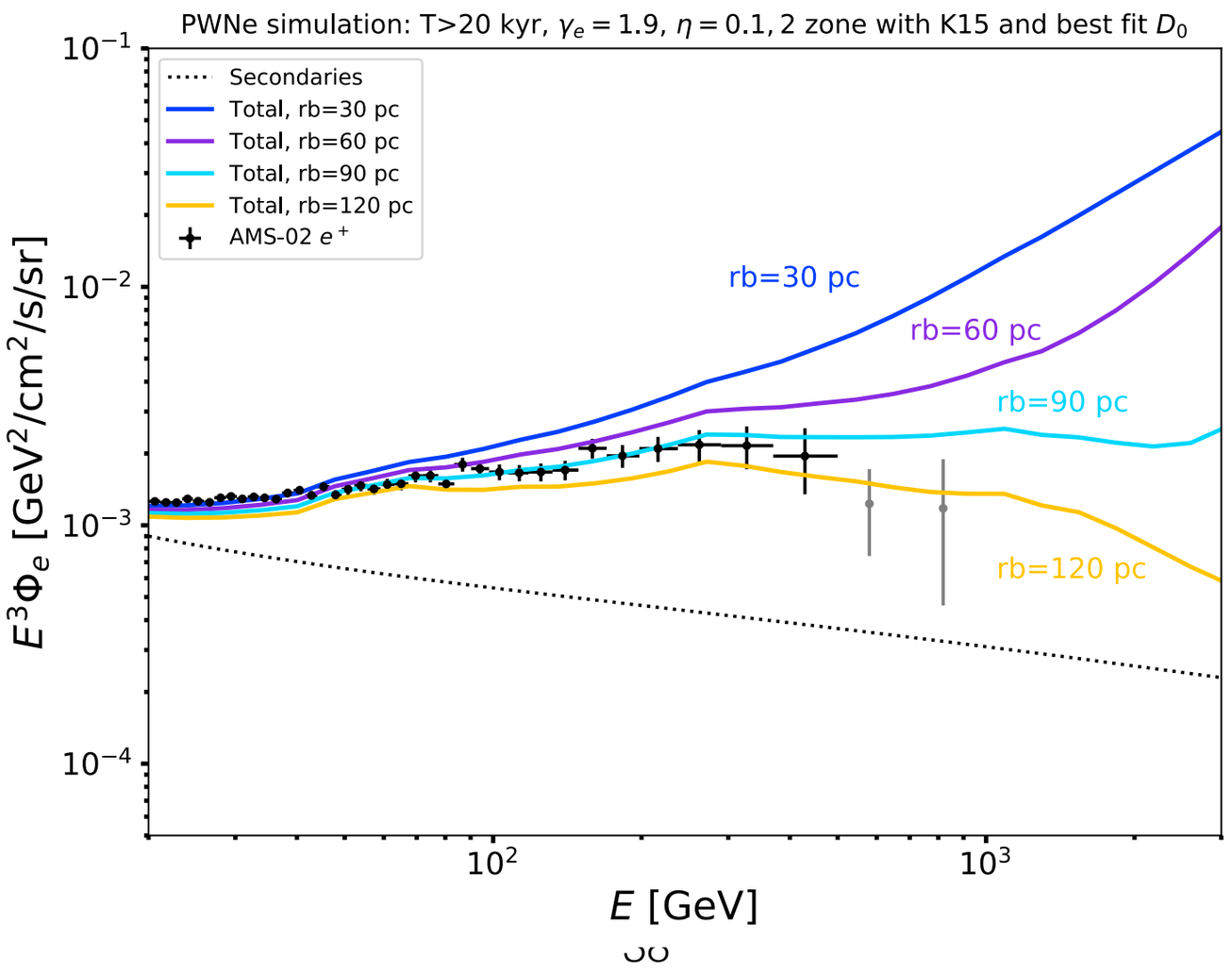

Conclusions

- PWNe are among the major acceleration of CRs in the Galaxy.
- An excess of positron is present above 10 GeV.
- Analyzing HAWC and Fermi-LAT data we found that Geminga is probably one of the major contributor of the positron excess.
- Around PWNe there could be low-diffusion bubbles with $D=10^{27}$ cm^2/s at 1 TeV and a size of at least 35 pc.
- PWNe can explain entirely the positron excess with an efficiency of about 10%.
- In order to confirm this hypothesis we need to analysis Fermi-LAT, HESS and HAWC data.
- More will hopefully come in the future….

Backup slide

Gamma rays produced by IC: calculation

γ rays from IC:

$$\Phi_\gamma(E_\gamma,\Omega)=\int_{E_\gamma}^{\infty}dE_e\int_0^\infty dr\int_0^\infty\int_{\Delta\Omega}d\Omega\,d\epsilon\,\mathcal{N}_e(E_e,r,\Theta)\frac{dN_\epsilon}{d\epsilon dt}(\epsilon,E_e,E_\gamma)$$

Electrons and positrons emitted by a PWN

$$\mathcal{N}_e(\mathbf{x},E,t)=\int_0^T dt_0\frac{b(E(t_0))}{b(E)}\frac{1}{(\pi\lambda^2(t_0,t,E))^{\frac{3}{2}}}\exp\left(-\frac{|\mathbf{x}-\mathbf{x_s}|^2}{\lambda(t_0,t,E)^2}\right)Q(E(t_0))$$

$$Q(E,t)=L(t)\left(\frac{E(t)}{E_0}\right)^{-\gamma}\exp\left(-\frac{E(t)}{E_c}\right)$$

Spectrum of IC γ rays produced by an electron.

$$\frac{dN_\epsilon}{d\epsilon dt}(\epsilon,E_e,E_\gamma)=\frac{3\sigma_T c\,m_e^2c^4}{4{E_e}^2\epsilon}\frac{d\mathcal{N}}{d\epsilon}\left[2q\log q+q+1-2q^2+\frac{1}{2}\frac{(\Gamma_\epsilon q)^2}{1+\Gamma_\epsilon q}(1-q)\right]$$

Systematic studies

- We calculated the flux for burst-like and continuous and for different values for τ_0 (0.1, 1.0, 12 kyr).
- We tested Genolini et al. 2017 propagation mode.
- Magnetic field of 5 μG.
- ISRF models from Porter 2006 and Genolini 2016.

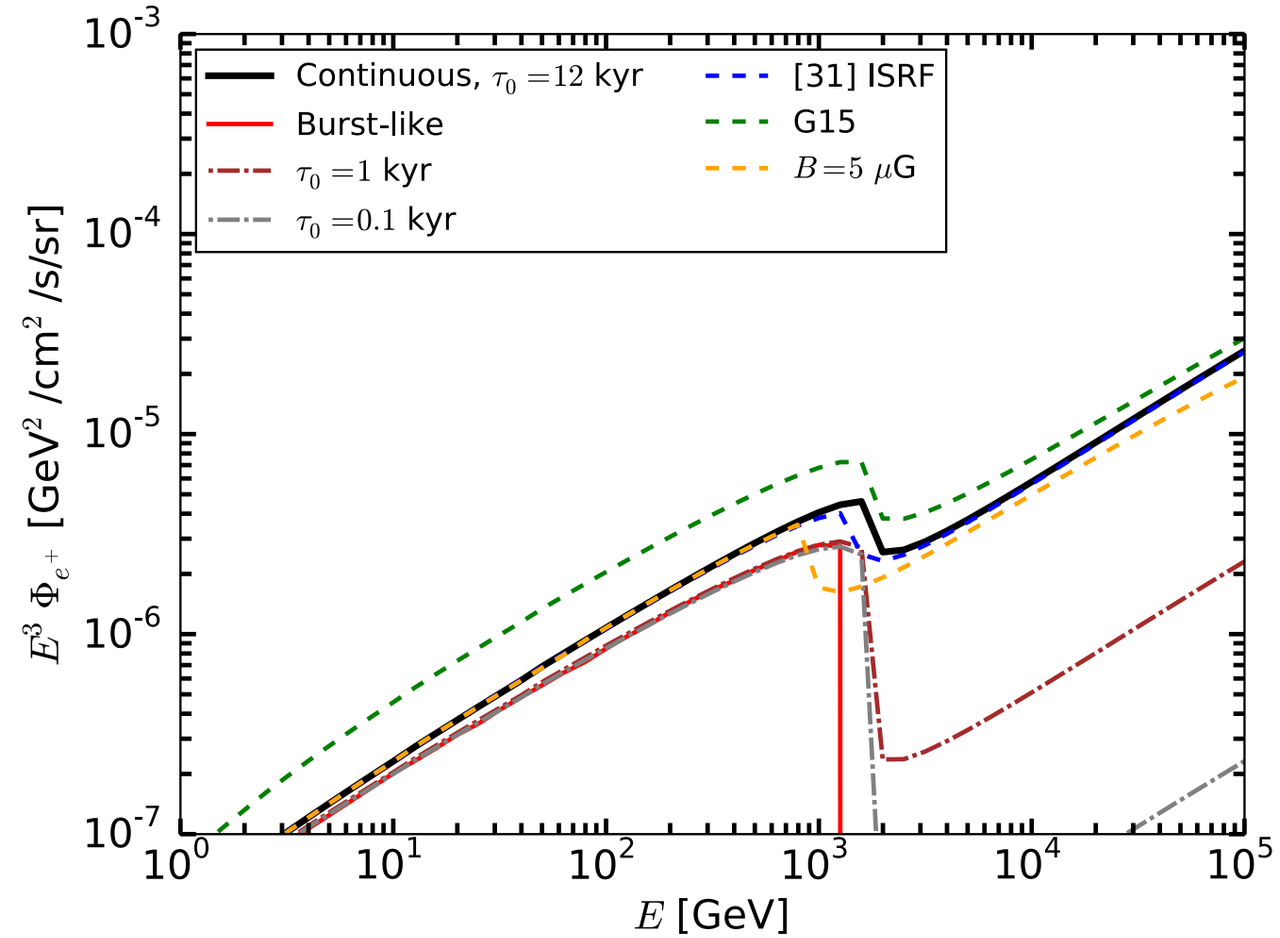

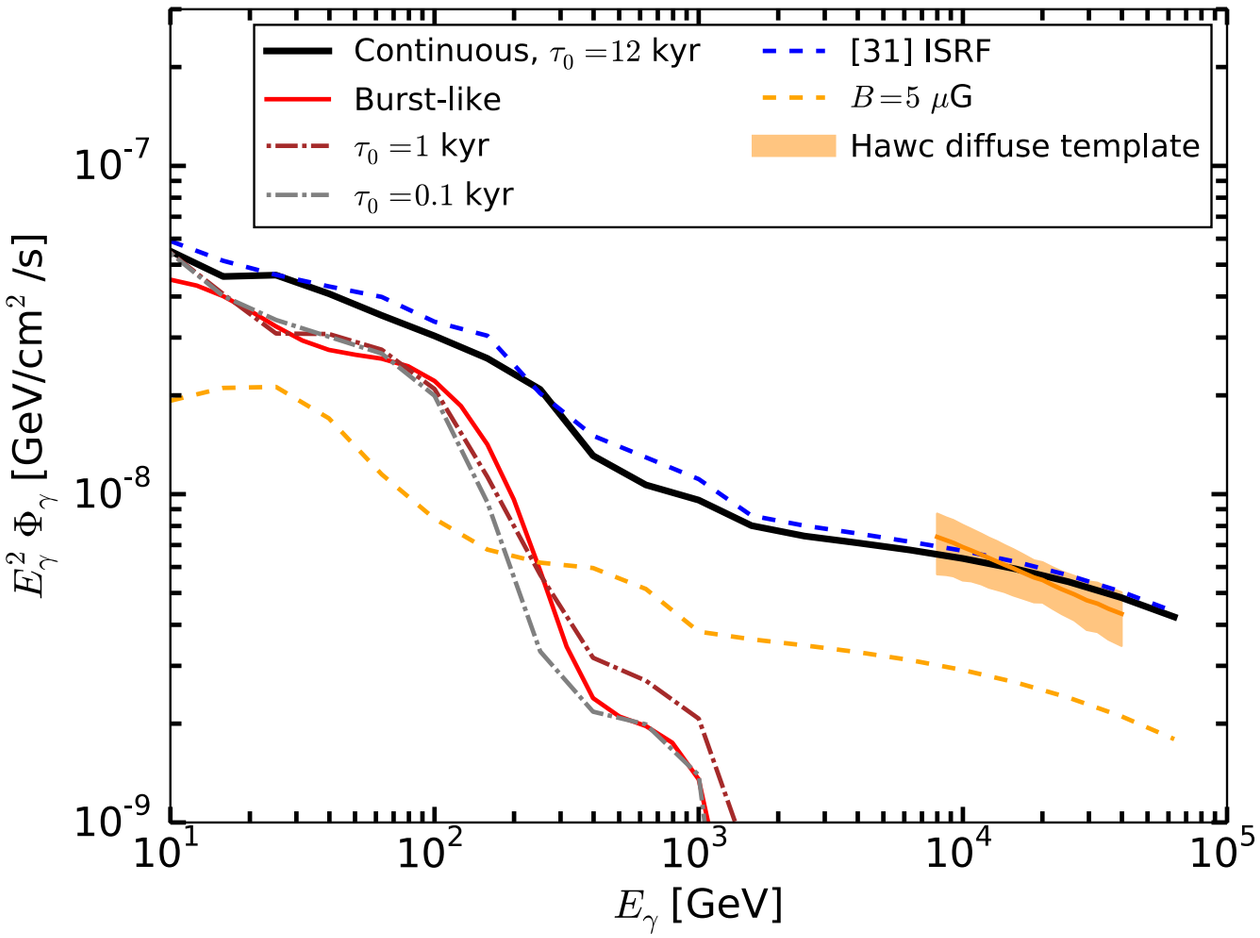

Null hypothesis TS distribution

- We took our ROI and simulated the model (without the Geminga and Monogem ICS templates).
- We ran 1000 simulations with Fermipy and re-launched our analysis.
- The TS distribution of the two ICS are compatible with the chi-square distribution.

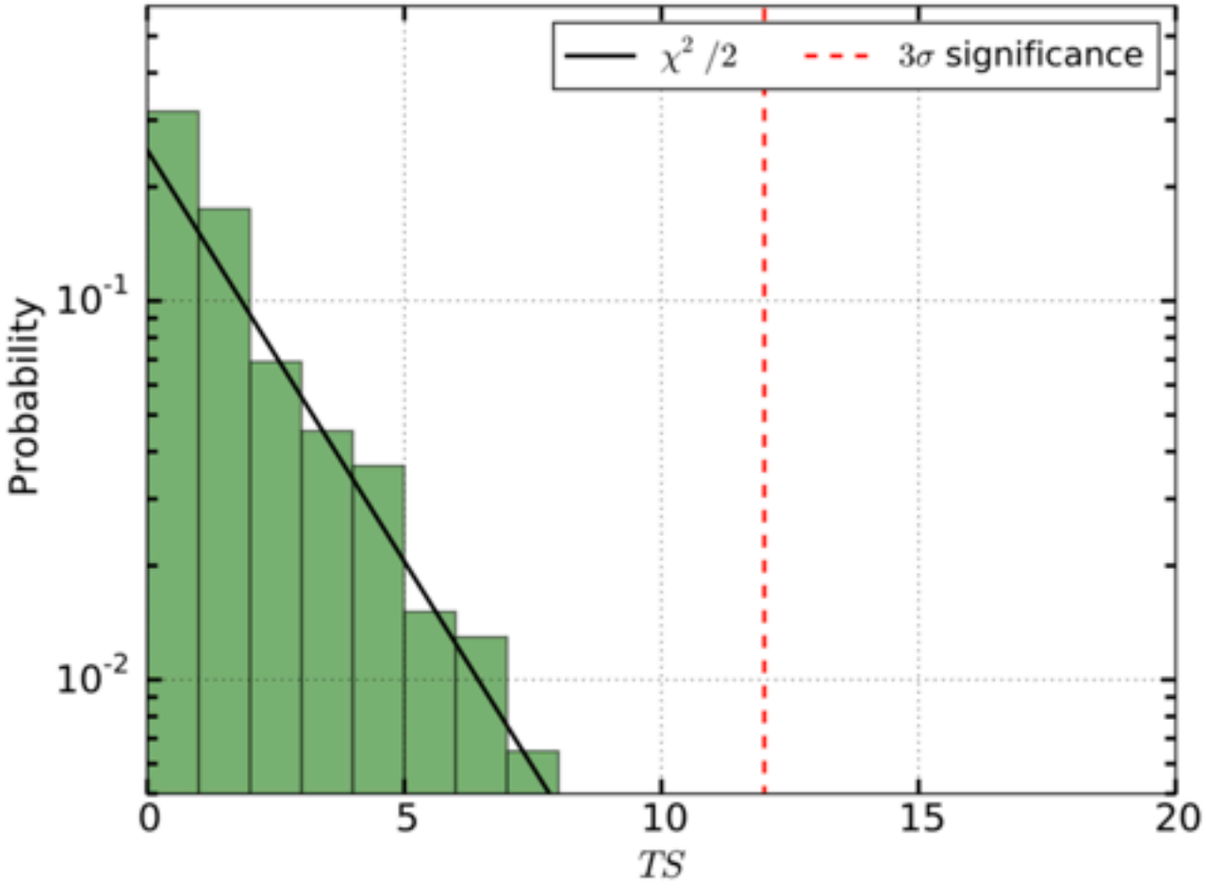

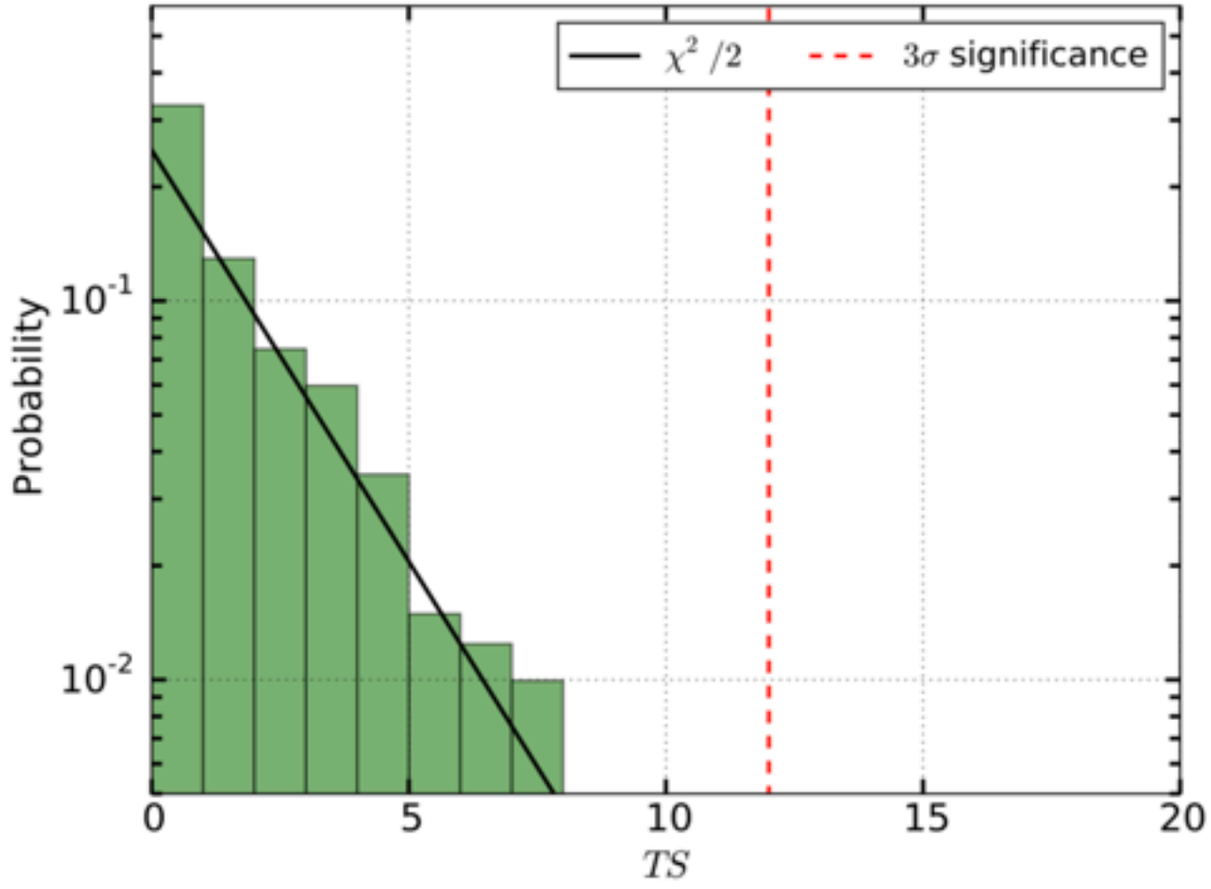

Template for the ICS from Geminga

- We made previously an analysis with templates for the ICS that are spherically symmetric.

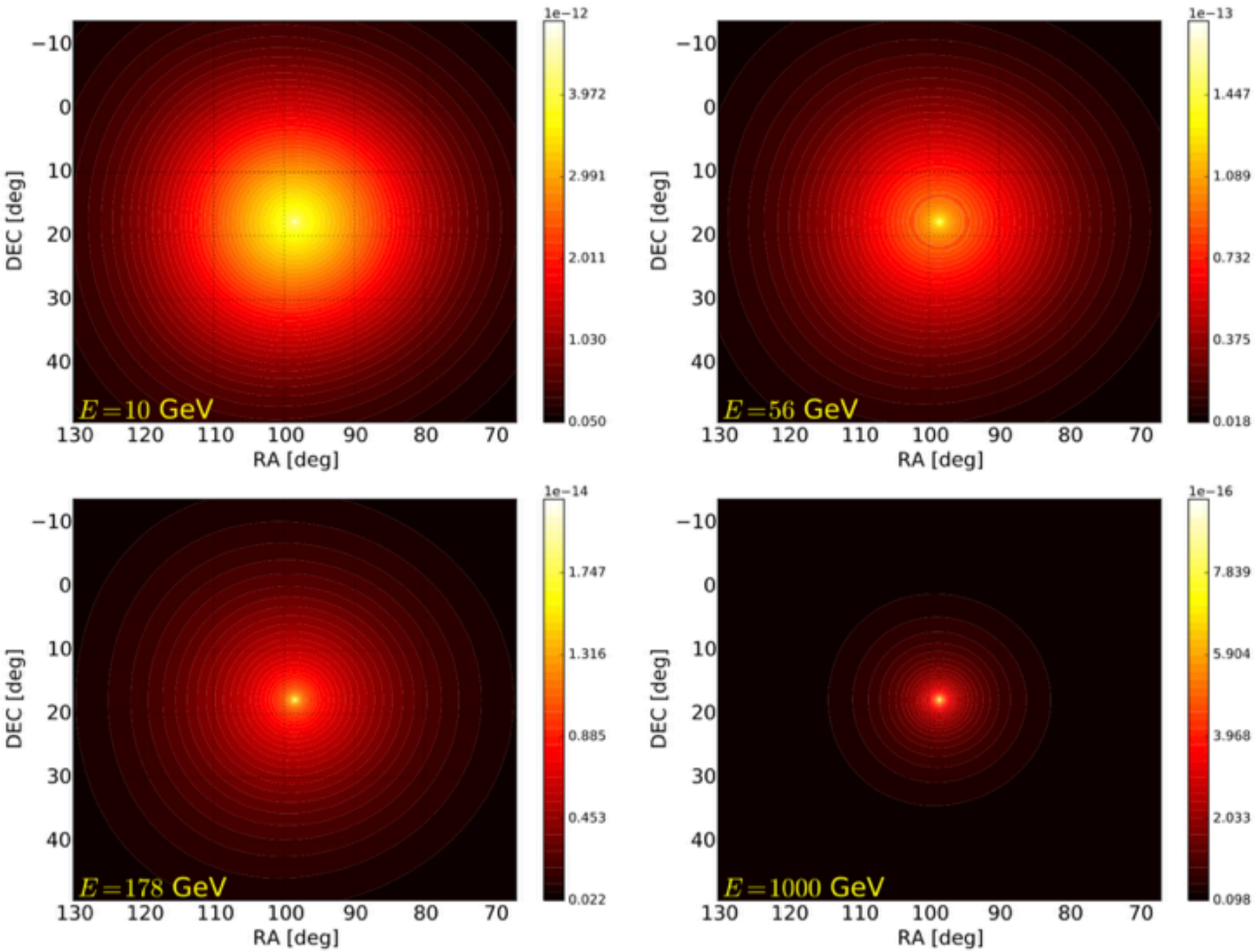

Gemings pulsar proper motion

- Geminga has a proper motion of 211 km/s which implies this pulsar moves about 70 pc across its age.

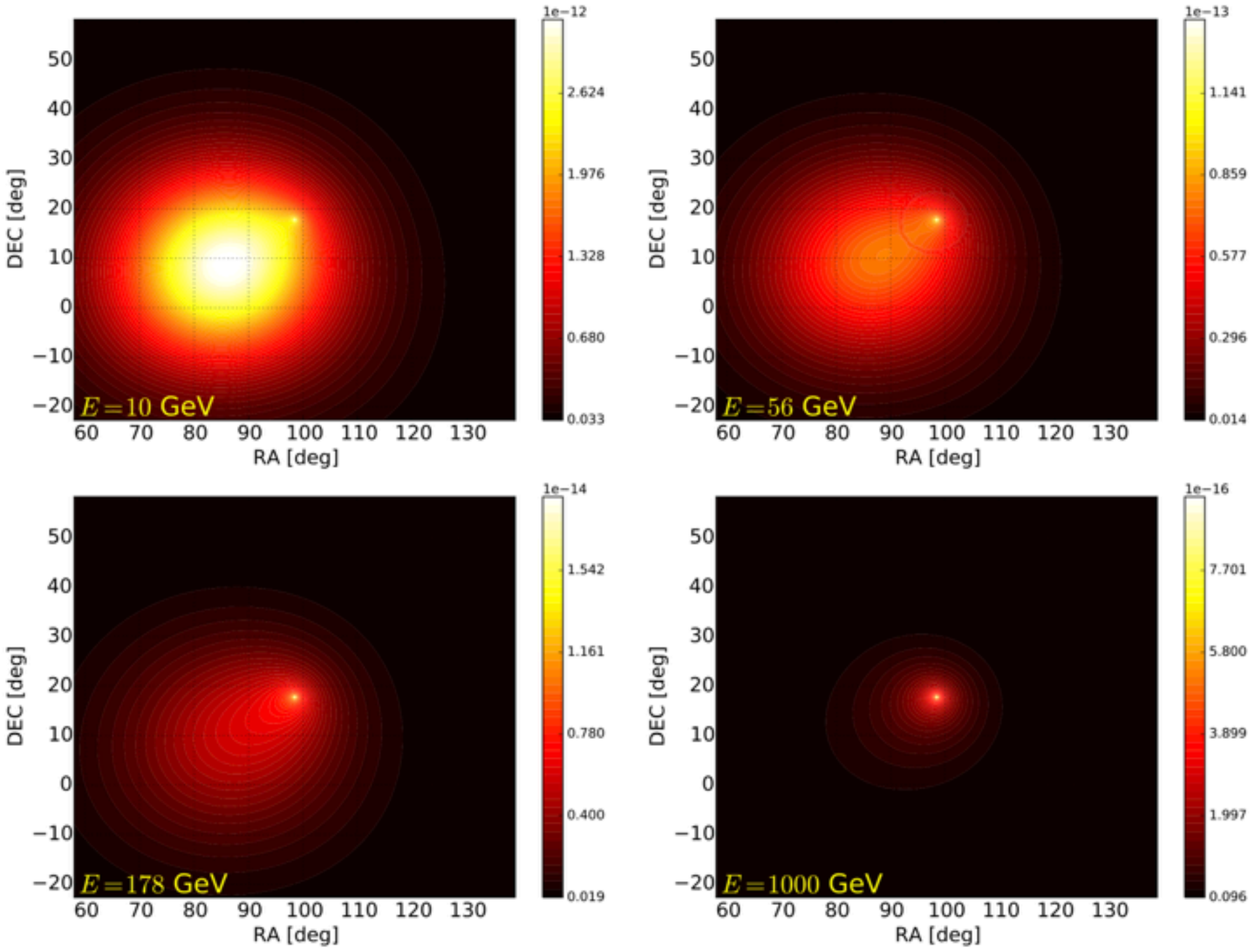

Effect of proper motion for Geminga and Monogem

- Monogem on the other hand is much younger and has a proper motion of 50 km/s.
- We implemented the Geminga pulsar proper motion in our calculation by changing its position $\mathbf{r_s}$ with $\mathbf{v}_T t_0$ where $\mathbf{v}_T$ is the pulsar transverse velocity

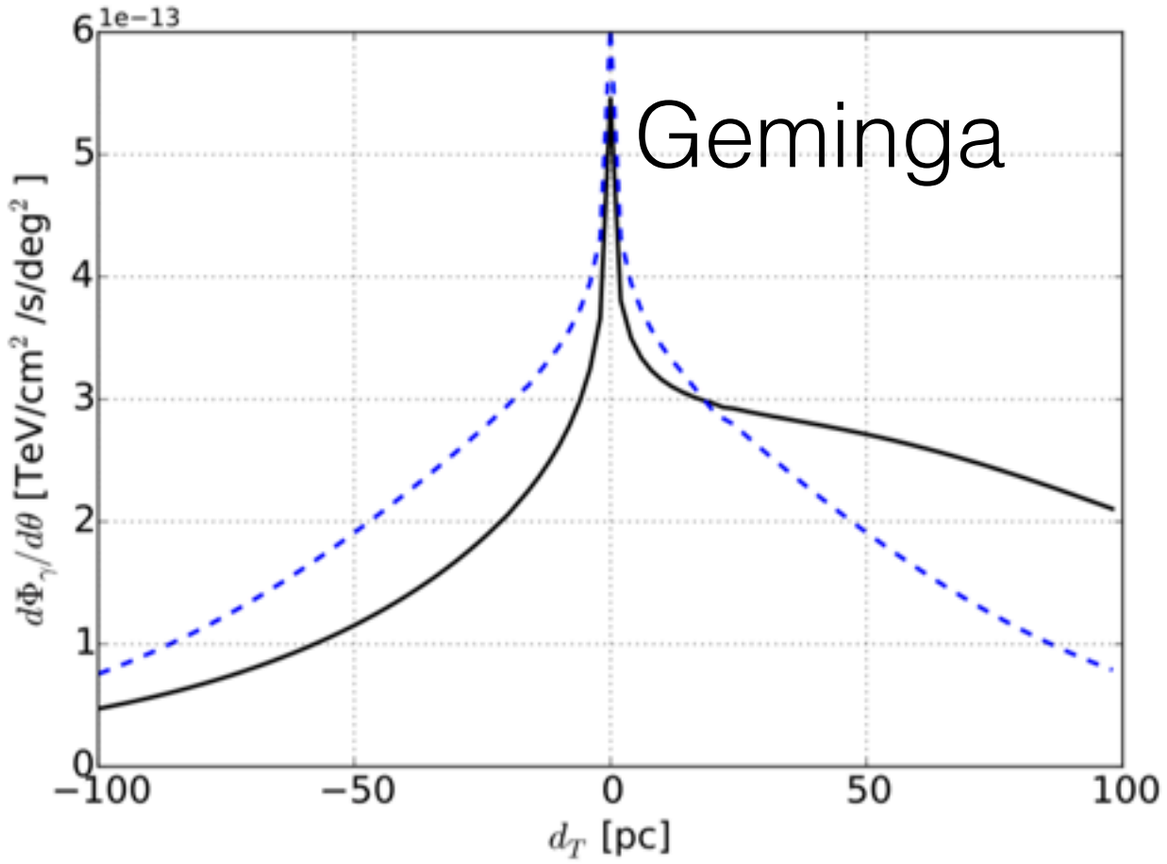

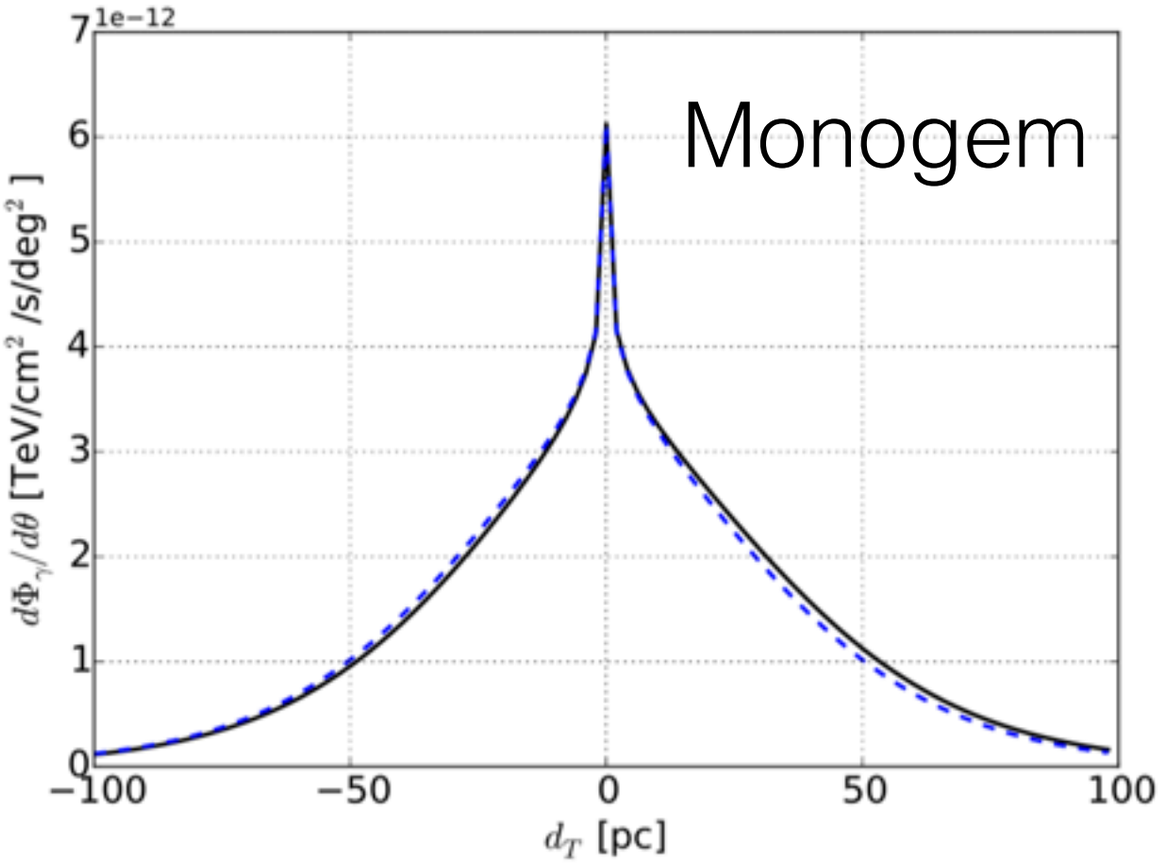

Results

IEM	TS^{Geminga}	D_0^{Geminga} $[10^{26}\ \text{cm}^2/\text{s}]$	TS^{motion} *	TS^{Monogem}	D_0^{Monogem} $[10^{26}\ \text{cm}^2/\text{s}]$
Off.	65	$2.1^{+1.0}_{-0.7}$	28	25	> 2
Alt. 1	104	$2.6^{+1.4}_{-0.8}$	30	3	> 1
Alt. 2	92	$2.6^{+1.2}_{-0.8}$	22	14	> 3
Alt. 3	87	$3.3^{+1.6}_{-1.1}$	24	16	> 4
Alt. 4	102	$3.5^{+1.8}_{-1.1}$	20	26	> 3
Alt. 5	111	$2.4^{+1.0}_{-0.6}$	51	12	> 2
Alt. 6	143	$2.6^{+1.2}_{-0.8}$	43	10	> 3
Alt. 7	128	$2.8^{+1.3}_{-0.9}$	41	12	> 10
Alt. 8	134	$3.1^{+1.3}_{-0.9}$	39	25	> 8
GC	71	$1.6^{+0.6}_{-0.4}$	35	8	> 1

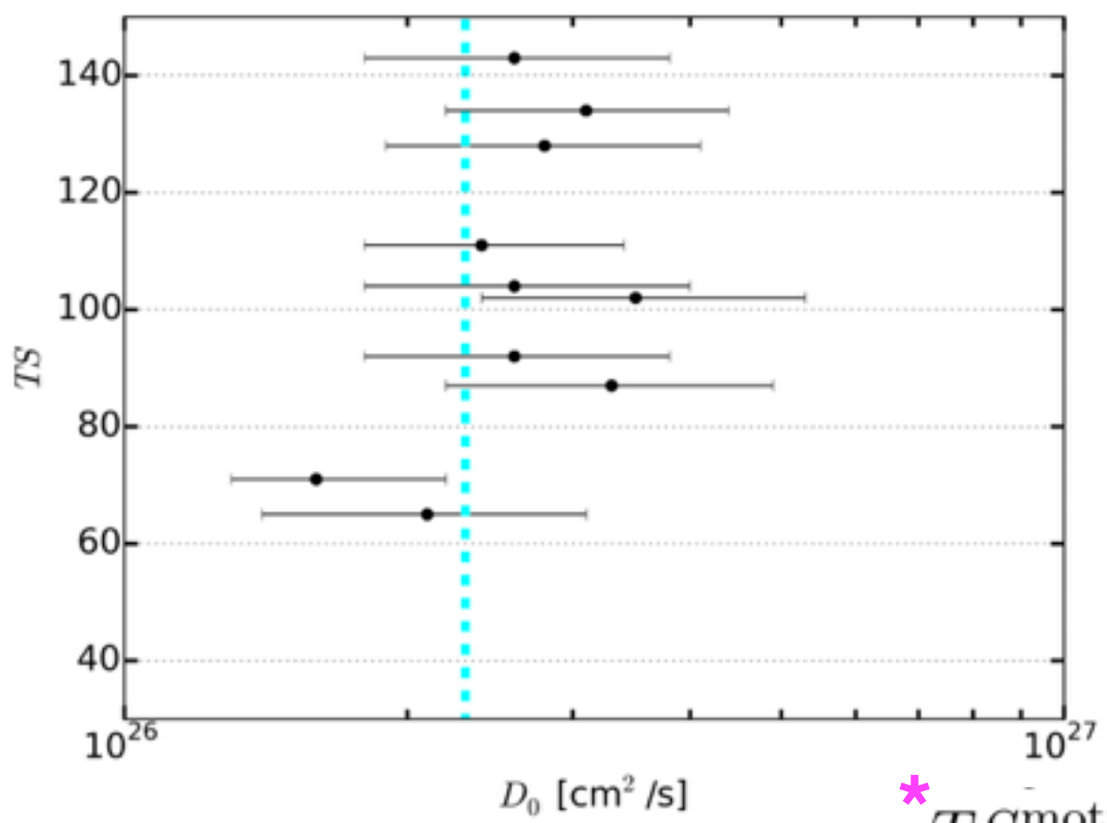

Off: FSSC IEM
Alt: IEM used in the first SNR catalog
GC: IEM model of the Fermi-LAT analysis of the GC

* $TS^{\text{motion}} = -2\log\left(\mathcal{L}_{\text{motion}} - \mathcal{L}_0\right)$

Other tests

- We performed other two tests.
  - **Systematics of the PSF** (5% at 10 GeV) can generate residuals in the directions of extremely bright sources.
    - We ran the analysis using Geminga halo templates (with efficiency and D free to vary) in the direction of the following sources:
      - Vela PSR, 3C454.3, PSR J1836+5925, PSR J1709-4429 (>100 MeV)
      - PG 1553+113 and Mkn 421 (>10 GeV).
    - **We find a TS of at most 2**.
  - We run the analysis with a **50x50 deg^2** ROI finding results for TS and D that are perfectly compatible with the one reported before.
- In addition to those checks the **correlation coefficient** between the isotropic template and the Geminga ICS halo that is **-0.28** meaning that there is a weak anti correlation between them.

HESS flux maps

- We selected sources detected mainly by HESS because they released flux maps.
- The flux is provided for a correlation radius of 0.1 and 0.2 deg and in maps with a pixel size of 0.02 deg.
- We removed sources close to our sources of interests.

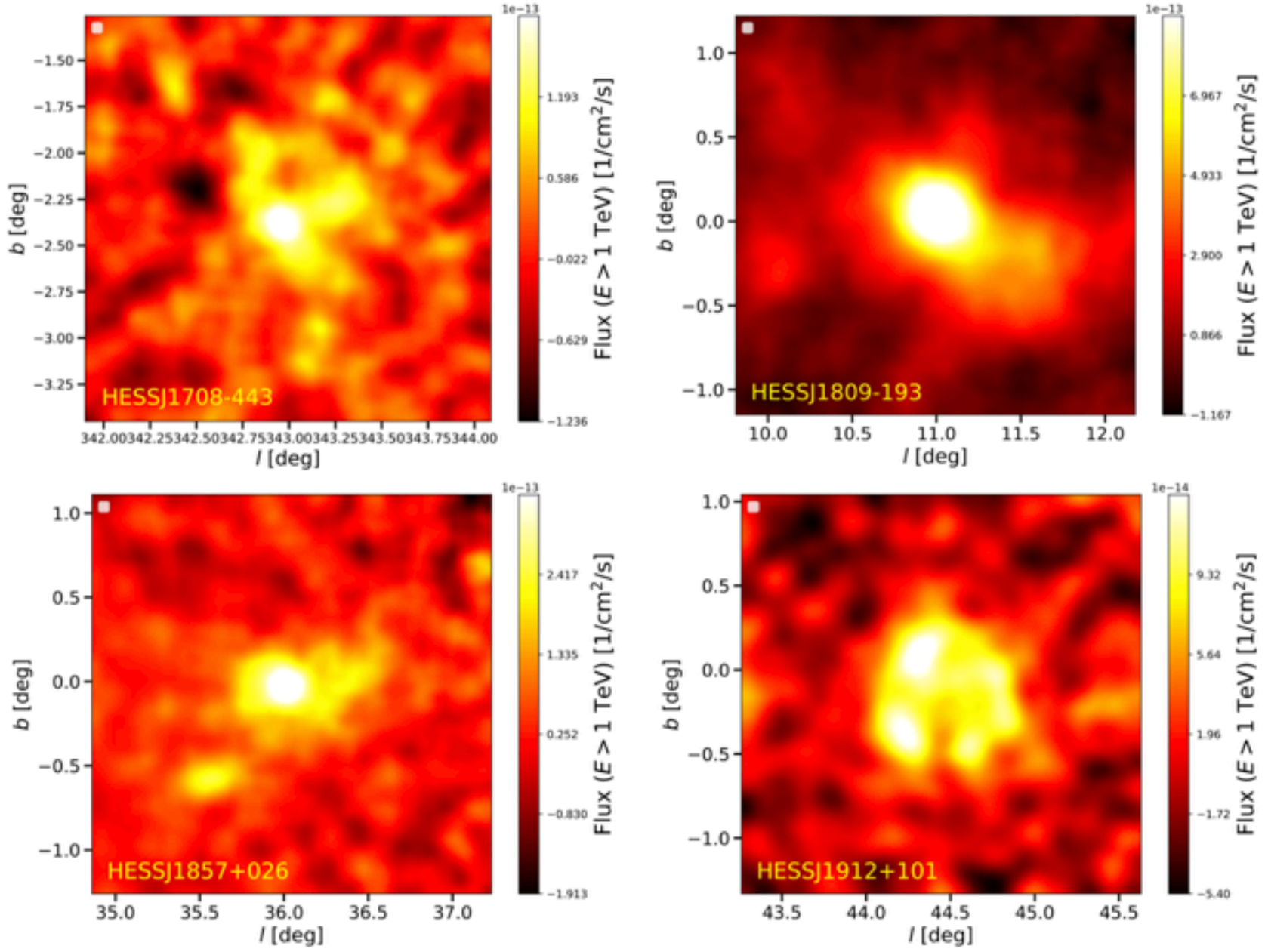

Testing the flux maps

- Since the maps contain redundant information for the flux, we need to demonstrate they can be reliably used for spatial source extension analysis.
- We calculate the extension using a gaussian shape and compare it with HESS catalog.
- Most of the our results are compatible within 1σ.

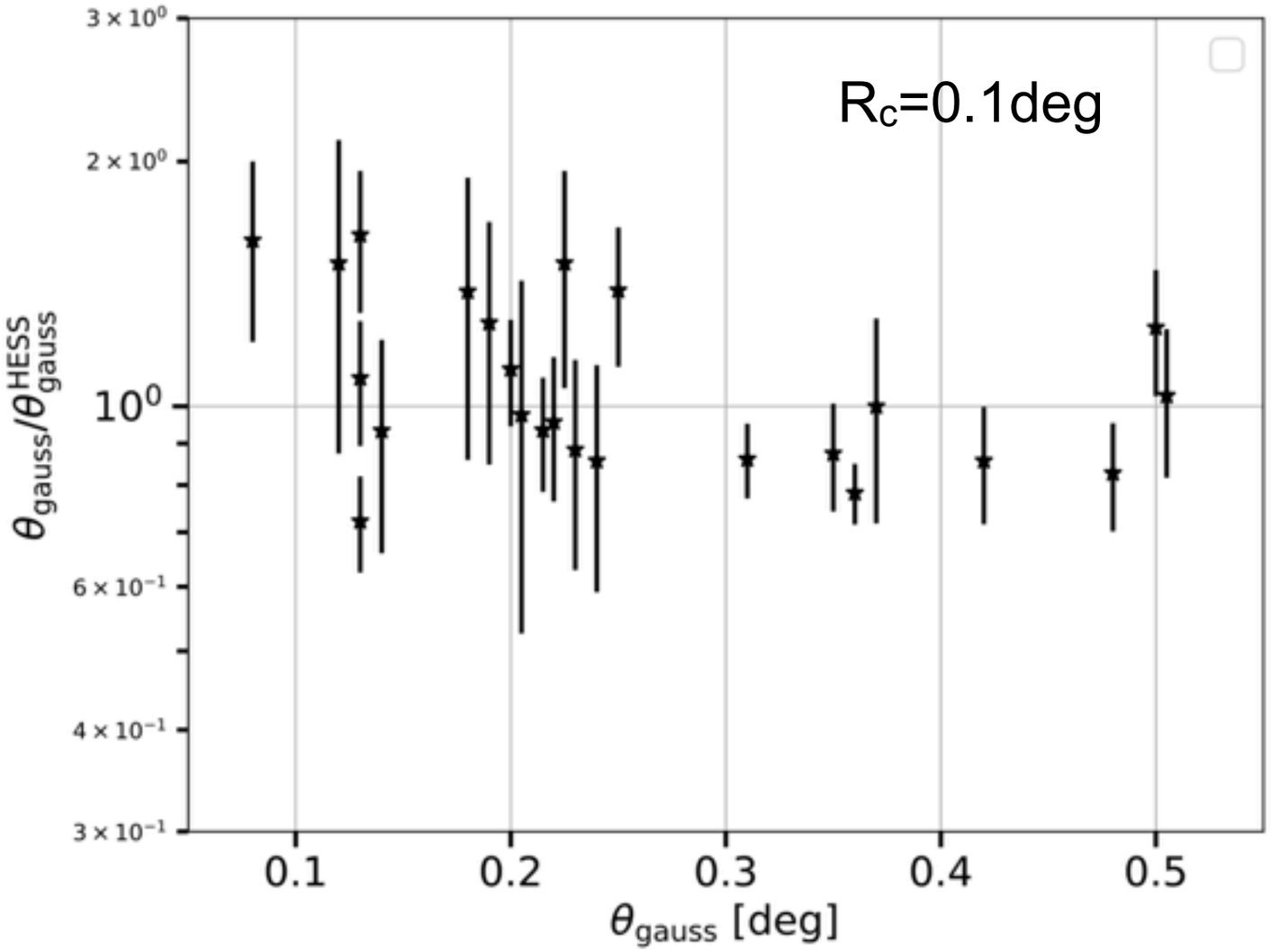

Surface brightness data

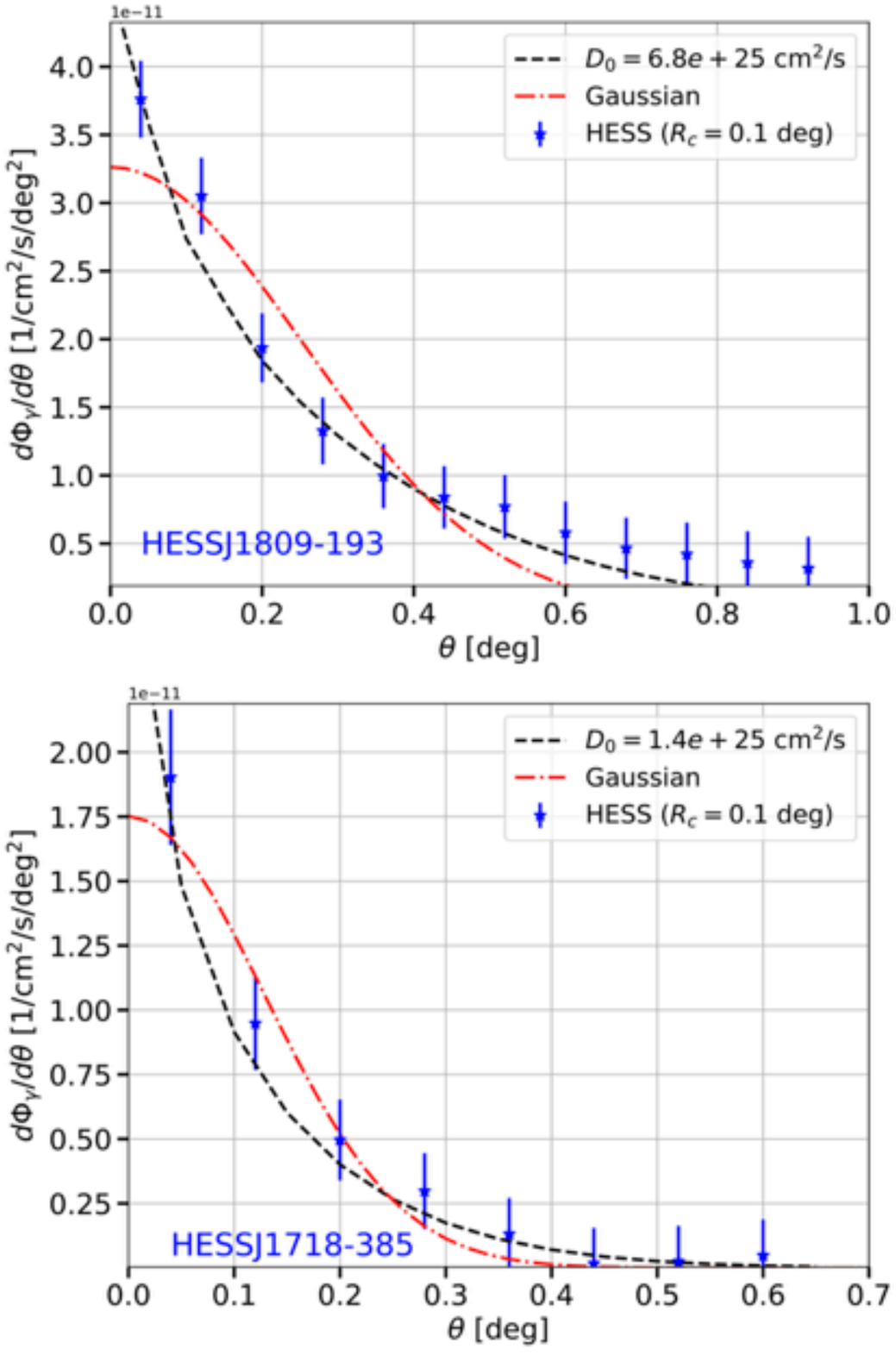

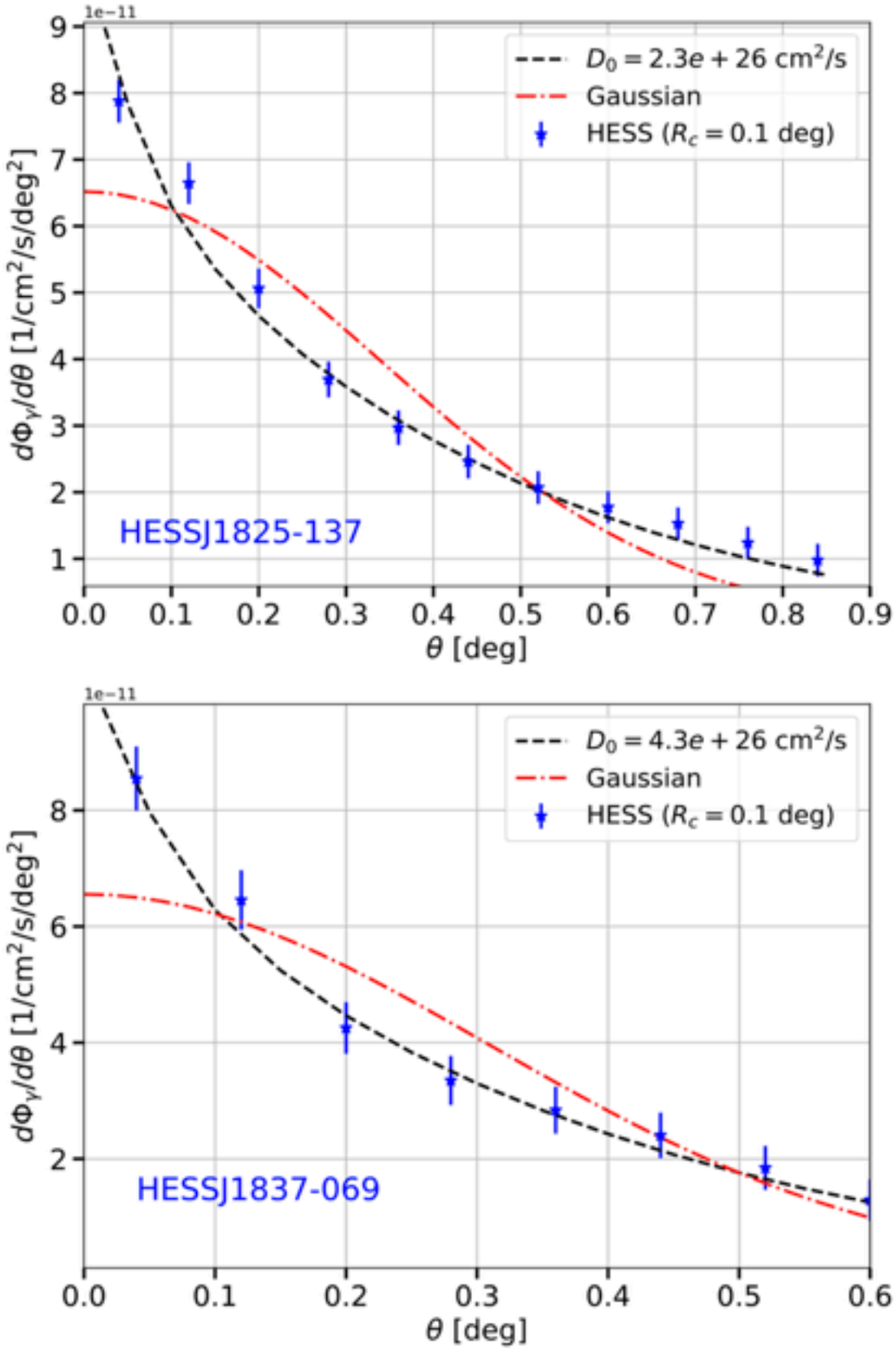

Results for the diffusion coefficient around PWNe

- We find a diffusion coefficient around the PWNe of our sample of **8 10^{26} cm^2/s at 1 TeV**.
- There is no clear difference between ‘old’ and ‘young’ pulsars.
- The diffusion coefficient around PWNe is about 2 orders of magnitude lower than the value found from CR data.

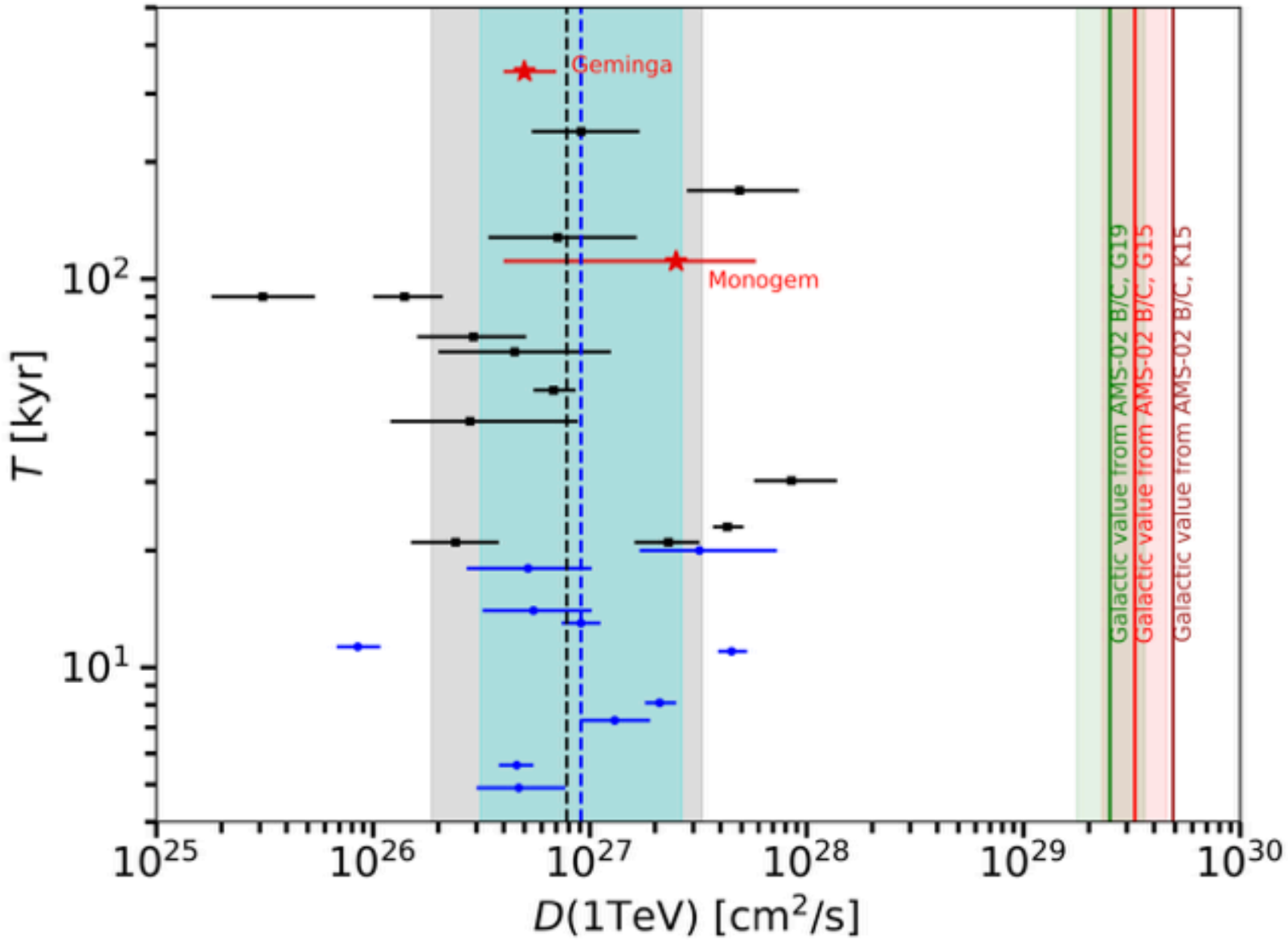

Results for the size of the ICS halos

- We find that the size of the ICS halo is on average **35 pc**.
- The trend with the age is compatible with models of PWN evolution.
- The size of the low diffusion bubble should be larger than that.

$$\frac{d\Phi_\gamma}{d\theta} \sim \frac{1}{\theta_{\rm ICS}(\theta + 0.06 \cdot \theta_{\rm ICS})} e^{-\left(\frac{\theta}{\theta_{\rm ICS}}\right)^2}$$

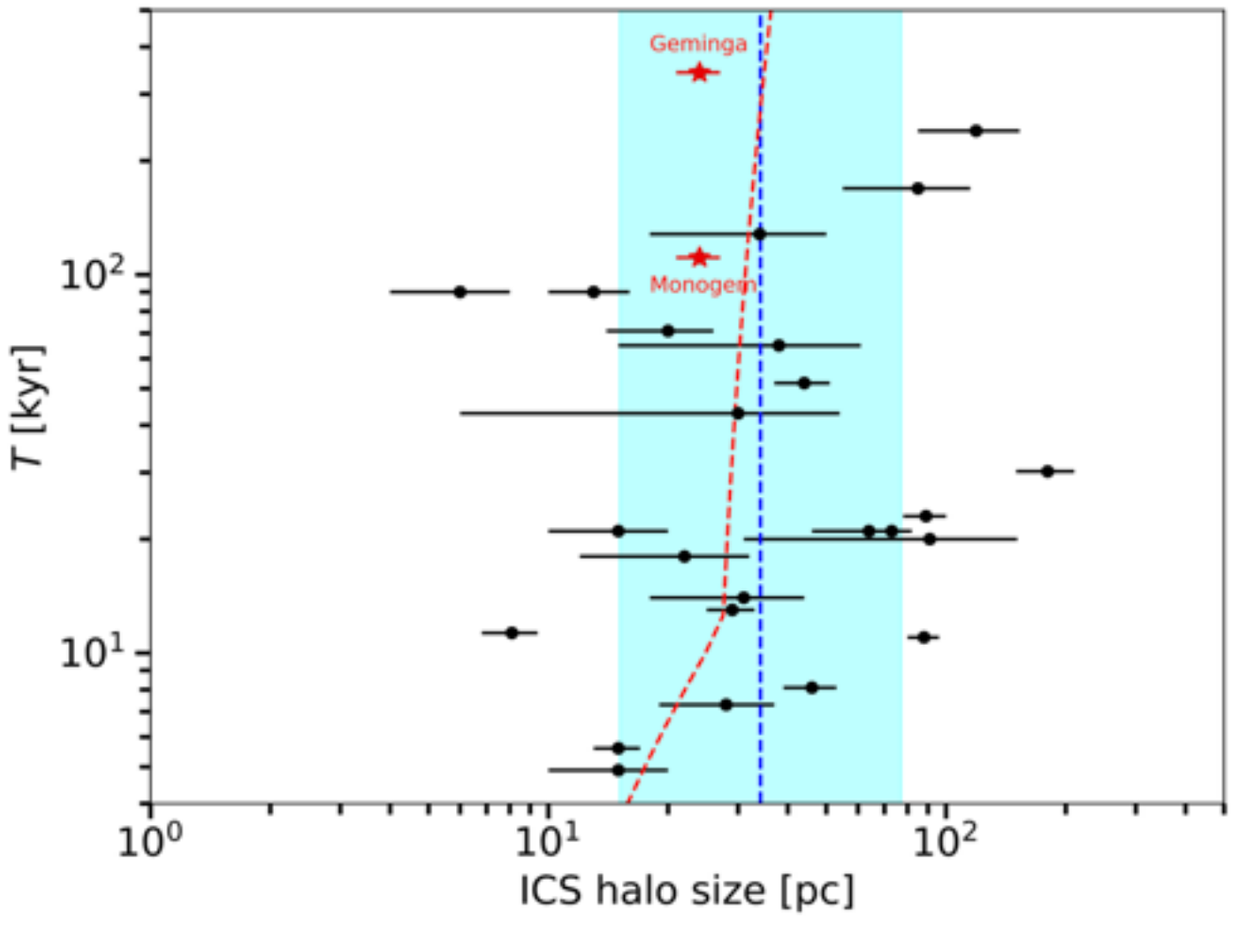

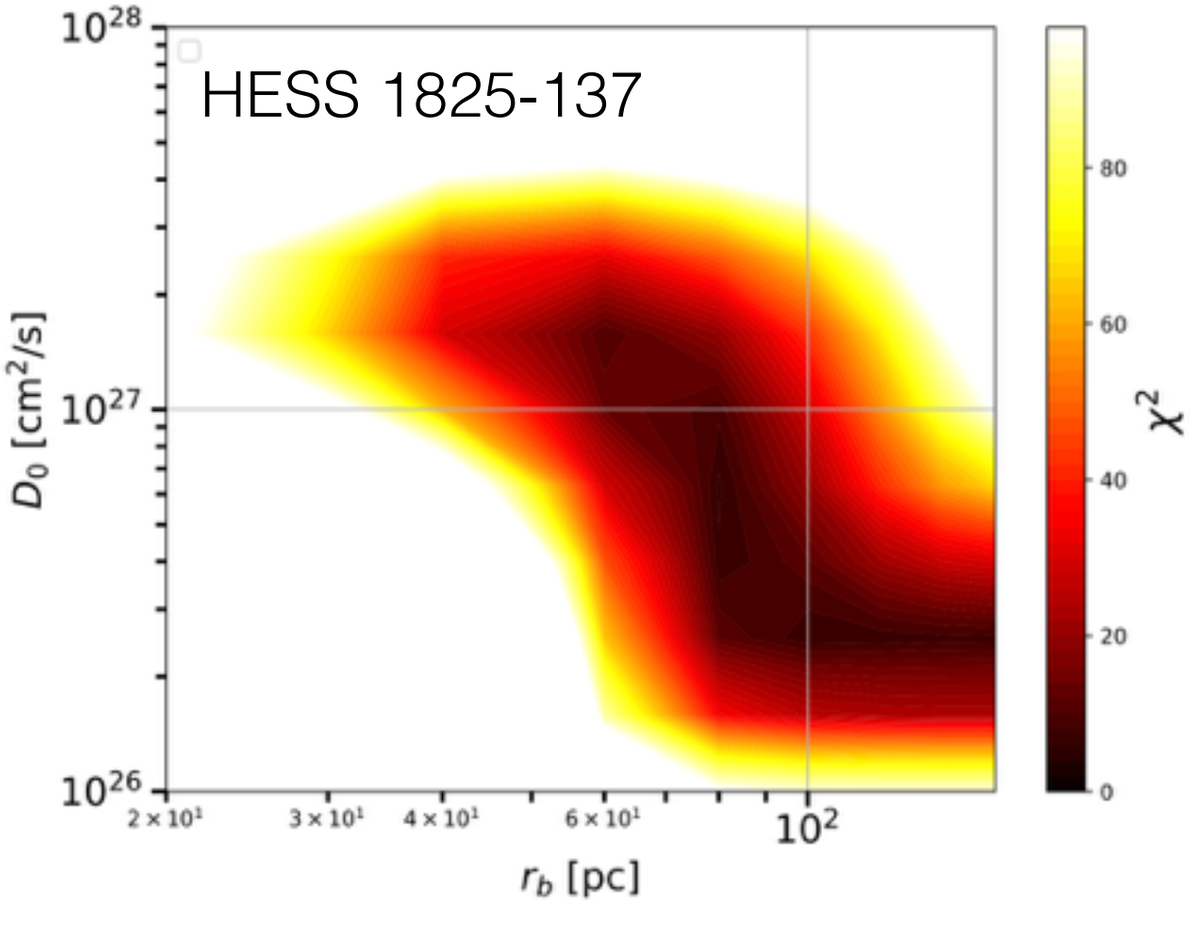

Results for the efficiency

- We also tried to use the results for the flux released in the HESS catalog to find the efficiency.
- However, gamma-ray data above hundreds of GeV are produced by electrons and positrons spectrum above 1 TeV.
- The efficiency values we find are heavily affect by extrapolations.
- We need to analysis Fermi-LAT data to constrain more effectively the efficiency.

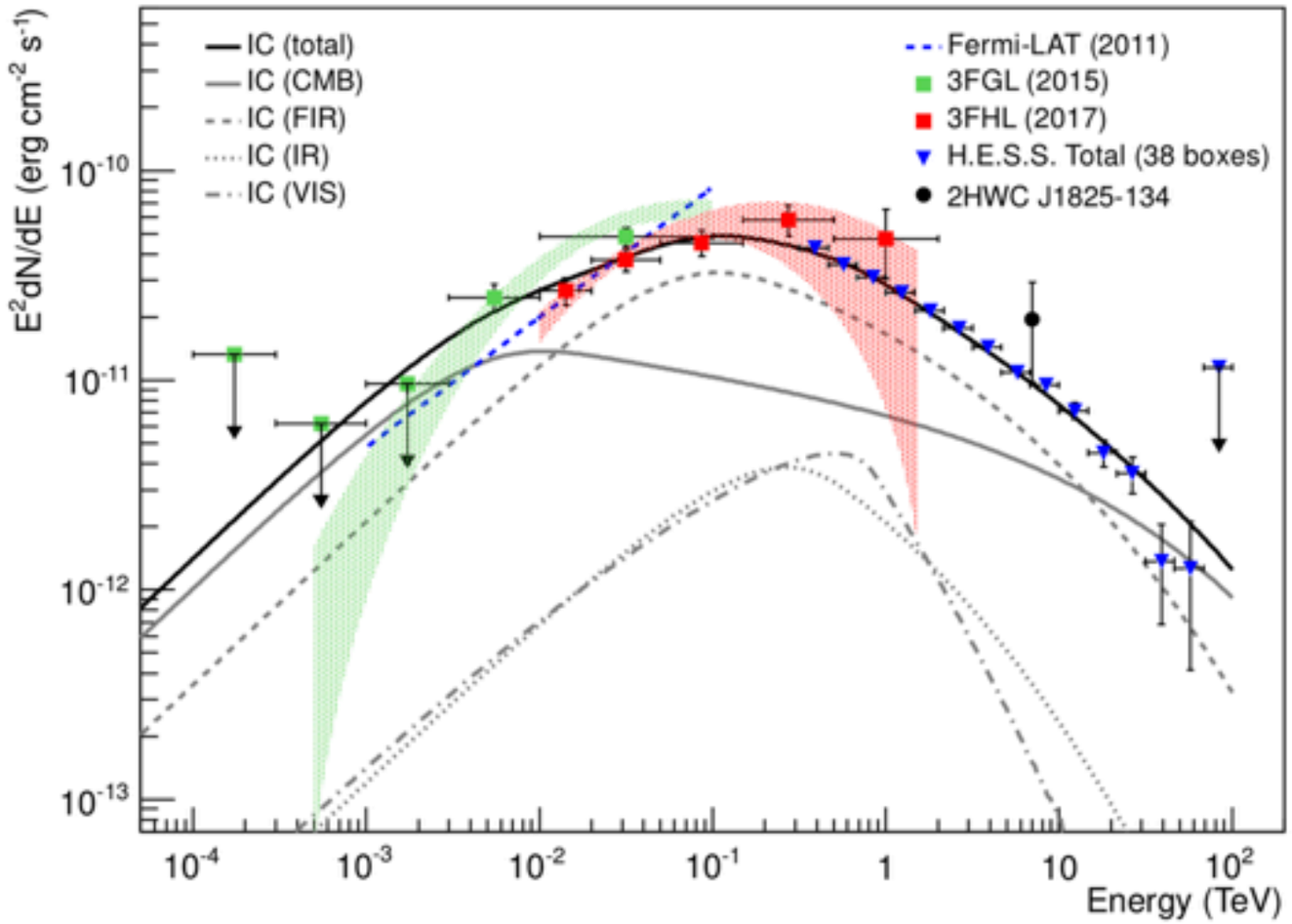

Consequences for the propagation of CR electrons

- The presence of a low-diffusion bubble might affect significantly the propagation of electrons in the Galaxy.
- A size r_b>100 pc makes the total volume of low-diffusion bubble around Galactic pulsars to be at least few % of the total propagation volume.

$$f \sim \frac{N_{\rm region} \times \frac{4\pi}{3} r^3_{\rm region}}{\pi R^2_{\rm MW} \times 2 z_{\rm MW}}$$
$$\sim 0.25 \times \left(\frac{r_{\rm region}}{100\,{\rm pc}}\right)^3 \left(\frac{\dot{N}_{\rm SN}}{0.03\,{\rm yr}^{-1}}\right) \left(\frac{\tau_{\rm region}}{10^6\,{\rm yr}}\right) \left(\frac{20\,{\rm kpc}}{R_{\rm MW}}\right)^2 \left(\frac{200\,{\rm pc}}{z_{\rm MW}}\right)$$